

## ABSTRACT

LAVOIE, JOSEPH HENRY. Approaches for Surface Energy Control of Nonwoven Fibers for Alcohol Repellency and Electret Charge Protection (Under the direction of Saad Khan, Orlando Rojas, and Eunkyong Shim).

Bulk polymer additives are commonly used in the nonwovens manufacturing industry for a variety of applications. One such application is the modification of surface properties for controlled repellency of solvents. This is particularly relevant in the field of electret air filtration materials, which have been shown to be rapidly discharged in the presence of oil and alcohol vapors or aerosols. Increased resistance to wetting by these low surface tension fluids can be challenging, but the use of additives to create nonwoven fabrics capable of repelling oils and alcohols allows these products to be manufactured cheaply and easily. While the use of melt additives is established in the prior art, there are many factors in the efficacy of the additives on the resultant properties of the final product, not all of which are well understood. Chief among these is the impact of additive migration on surface properties of manufactured fibers. In this work we seek to explore the effects of melt additive migration on meltblown nonwoven fibers as well as the kinetics and resultant microstructure of additive migration in the polymer matrix.

Fibers containing fluorochemical melt additive compounds were characterized by several different analytical techniques. Scanning Electron Microscopy (SEM) images of nonwoven fiber mats allow for the quantitative evaluation of median fiber diameter. By monitoring changes in fiber diameter with respect to additive concentration and fiber manufacturing parameters, we are able to elucidate the correlation between these critical parameters. X-ray Photoelectron Spectroscopy (XPS) was used to characterize the kinetics of the changing

surface composition of the fiber mat, as migration of the additive to the surface occurs over time. In an effort to gain a more thorough understanding of the migration process, Time-of-Flight Secondary Ion Mass Spectroscopy (TOF-SIMS) was used to generate compositional maps of fiber cross-sections. These 2D maps of fluorine content throughout the core and surface of fibers offer a unique view of additive migration and allow for additional understanding of the role of fiber diameter and nonwoven manufacturing methods on the resultant surface properties of the material.

Migration of additives was monitored over several months, allowing for the evaluation of compositional changes over multiple timescales. This changing composition was then related to repellency of alcohol solutions via contact angle data. By collecting composition and contact angle data in tandem, thresholds in surface fluorine content for repellency were identified, as well as protection of charge against isopropanol vapor discharging methods.

In addition to bulk polymer melt additive approaches, we also utilized novel surface modification methods for the creation of extremely low surface energy nonwoven webs. In this study, we utilized the non-specific binding of unfolded natural polymers to highly inert hydrophobic surfaces like polypropylene to generate an activated surface capable of further functionalization. Through the use of sequentially deposited charged moieties, an extremely conformal, rough, and densely decorated silica surface was created on fiber surfaces. After functionalization of the silica surface with a highly fluorinated silane molecule through a simple vapor phase silane reaction, the multi-scale roughness of the coated nonwoven web in combination with the low surface energy of the fluorinated surface enabled extremely high water contact angles ( $>160^\circ$ ) and significant improved repellency of low surface tension oils and alcohols.

© Copyright 2018 Joseph Henry Lavoie

All Rights Reserved

Approaches for Surface Energy Control of Nonwoven Fibers for Alcohol Repellency and  
Electret Charge Protection

by  
Joseph Henry Lavoie

A dissertation submitted to the Graduate Faculty of  
North Carolina State University  
in partial fulfillment of the  
requirements for the degree of  
Doctor of Philosophy

Chemical Engineering

Raleigh, North Carolina

2018

APPROVED BY:

---

Dr. Saad Khan  
Committee Co-Chair

---

Dr. Orlando Rojas  
Committee Co-Chair

---

Dr. Eunkyong Shim  
Committee Co-Chair

---

Dr. Behnam Pourdeyhimi

## **DEDICATION**

*To my family, who have always loved and believed in me,*

*to my friends, whom I consider family,*

*and to my wife, who is my best friend, and my everything.*

## BIOGRAPHY

Joseph Lavoie grew up in Underhill, Vermont, with his sister Nicole and parents Mark and Lois. He attended Mount Mansfield Union High School and graduated 2004 before moving to Boston, Massachusetts. There he enrolled in the Chemical Engineering program at Northeastern University. After several co-op experiences, he graduated *magna cum laude* with his Bachelor's Degree in 2009 and began working at the US Army Natick Soldier Research, Development and Engineering Center in Natick, MA. In the fall of 2012, Joseph was accepted into the Ph.D. program in the Department of Chemical and Biomolecular Engineering at North Carolina State University. During his first semester at NC State, Joseph returned to Boston to marry his wife Ashton. In the spring of 2013 Joseph joined the research groups of Dr. Saad Khan and Dr. Orlando Rojas, and later became an advisee of Dr. Eunkyong Shim in the College of Textiles. Following completion of his graduate studies in the spring of 2018, Joseph plans to remain in the Raleigh, NC area, with his amazing wife, and two dogs.

## ACKNOWLEDGMENTS

First and foremost, I would like to recognize my advisors, Dr. Saad Khan, Dr. Orlando Rojas, and Dr. Eunkyong Shim, without whom none of this would have been possible. Their kind advice, technical mentorship, and advocacy on my behalf throughout all of my endeavors during my Ph.D. experience have been essential to my success. I also would like to thank Dr. Behnam Pourdeyhimi for his support and for the Nonwovens Institute, which has funded the large majority of this work and provided me with many opportunities for which I am extremely grateful.

I would also like to thank my wife, Ashton Bradley Lavoie, for all of her patience, support, and love throughout my graduate education and always. Her enduring belief in my abilities, and my potential, gave me the motivation I so desperately needed at many times throughout this experience, and without her I would not have achieved a fraction of the work displayed in this dissertation. She has always pushed me to greater excellence, through my desire to make her proud, and through striving follow the example of drive, passion, and excellence as an engineer that she exemplifies.

To all of my friends and colleagues, thank you for your support and comradery. I cherish the bond I share with all those students who enriched my time at NC State, in particular those who entered the program with me in 2012. I would also like to thank all of the group members with whom I've worked these past five years. Graduate students, post-docs and undergrads from Khan Research Group, CIG/BiCMat, and NWI, I am grateful for your support and advice, especially my classmates Zach Mundy and Prajesh Adhikari. To the family dinner crew – Kevin, Brittany, Craig, Erinn, Daniel, Jenna, Joe and Deepti – our frequent dinners and other

activities over the past five years have been the highlight of so many weeks, and I cannot imagine having gone through this process without you all. To the Northeastern gang, our all too infrequent visits never cease to buoy my spirits and your constant support and encouragement have helped me more than I could ever properly articulate. And to all my friends, old and new, near and far, know that I appreciate your kind words and shared laughter. Thank you all.

Last and certainly not least, I want to thank my family for their love and support. I am eternally grateful for your never ending belief in me, and your understanding as work and distance has kept me from visiting and spending time with those I love the most. I look forward to making up for lost time for many years to come. None of this would have been possible without you!

## TABLE OF CONTENTS

LIST OF TABLES .....	x
LIST OF FIGURES .....	xi
CHAPTER 1. Introduction.....	1
1.1 Motivation and Goals.....	1
1.2 Background.....	2
1.2.1 Nonwovens Manufacturing.....	2
1.2.2 Air Filtration .....	6
1.2.3 Electrets.....	7
1.2.4 Charge Protection.....	9
1.2.5 Repellency.....	11
1.2.6 Surface Modification of Polymers by Sequential Deposition.....	12
1.2.7 Surface Active Bulk Polymer Melt Additives .....	13
1.3 Organization of Dissertation.....	14
1.4 Works Cited .....	15
CHAPTER 2. Omniphobic polypropylene nonwovens by surface modification with bio-hybrid and conformable coatings followed by chemical vapor deposition .....	19
2.1 Abstract.....	19
2.2 Introduction.....	20
2.3 Experimental .....	24
2.3.1 Materials & Methods. ....	24
2.3.2 Preparation of Polypropylene Thin Films.....	24
2.3.3 Preparation of Coating layers.....	25

2.3.4	Scanning Electron Microscopy .....	29
2.3.5	Fluorescence Microscopy .....	29
2.3.6	X-Ray Photoelectron Spectroscopy .....	29
2.3.7	Contact Angle Goniometry .....	30
2.4	Results and Discussion .....	30
2.4.1	Surface Morphology of Coating Layers .....	30
2.4.2	Surface chemical composition .....	37
2.4.3	Wetting with fluids of different surface tensions.....	39
2.5	Conclusions.....	45
2.6	Works Cited .....	47
2.7	Appendix – Supplementary Material .....	50
CHAPTER 3. Characterization of Fluorochemical Melt Additive Migration for		
Alcohol Repellency in Electret Filter Materials .....		
		51
3.1	Abstract.....	51
3.2	Introduction.....	52
3.3	Experimental .....	54
3.3.1	Materials & Methods. ....	54
3.3.2	Meltblown Nonwoven Manufacturing.....	54
3.3.3	X-Ray Photoelectron Spectroscopy .....	59
3.3.4	Contact Angle Goniometry .....	59
3.3.5	ToF-SIMS .....	60
3.3.6	Scanning Electron Microscopy .....	60
3.4	Results and Discussion .....	60

3.4.1	Fiber Size Analysis .....	60
3.4.2	Additive surface migration characterization.....	63
3.4.3	Dependence of Repellency Performance on Surface Composition.....	66
3.4.4.....	High-resolution investigation of cross-sectional composition by ToF- SIMS .....	68
3.4.5	Effects of processing parameters on migration.....	72
3.4.5.1	Die-to-collector distance .....	72
3.4.5.2	Molecular weight .....	74
3.4.5.3	Air flow rate .....	76
3.4.6	Repellency of resulting fiber mats .....	80
3.5	Conclusions.....	82
3.6	Works Cited .....	83
 CHAPTER 4. Charge protection and additive migration in electret air filtration		
	materials.....	85
4.1	Abstract.....	85
4.2	Introduction.....	86
4.3	Experimental.....	88
4.3.1	Materials & Methods. ....	88
4.3.2	Meltblown Nonwoven Manufacturing.....	88
4.3.3	X-Ray Photoelectron Spectroscopy .....	90
4.3.4	Contact Angle Goniometry .....	90
4.3.5	Scanning Electron Microscopy .....	91

4.3.6	Charge State Preparation.....	91
4.3.7	Fractional Filter Testing.....	91
4.4	Results and Discussion .....	92
4.4.1.1	Characterization of Nonwoven Fiber Web Structure.....	92
4.4.2	Additive surface migration characterization.....	95
4.4.3	Discharging & Filter Performance of Repellent Nonwovens .....	101
4.5	Conclusions.....	108
4.6	Works Cited .....	110
CHAPTER 5.	Conclusions & Future Work.....	112
5.1	CHAPTER 2. Omniphobic Polypropylene Nonwovens By Surface Modification With Bio-Hybrid And Conformable Coatings Followed By Chemical Vapor Deposition.....	112
5.2	CHAPTER 3. Characterization Of Fluorochemical Melt Additive Migration For Alcohol Repellency In Electret Filter Materials.....	113
5.3	CHAPTER 4. Charge Protection And Additive Migration In Electret Air Filtration Materials .....	114
5.4	Future Work .....	115
APPENDICES	.....	117
APPENDIX A.	Thermal Analysis .....	118
A.1	Thermal Gravimetric Analysis.....	118
A.2	Differential Scanning Calorimetry.....	119
APPENDIX B.	Compositional Analysis.....	121
B.1	Fourier Transform Infrared Spectroscopy .....	121

## LIST OF TABLES

Table 2.1: Atomic composition values of coating after each processing step as measured by XPS .....	38
Table 3.1: Biax Research Line Conditions .....	57
Table 3.2: Reicofil Pilot Line 500 MFR Run Conditions .....	57
Table 3.3: Reicofil Pilot Line 1200 MFR Run Conditions .....	58
Table 4.1: Reicofil Pilot Line DoE and Run Conditions .....	89

## LIST OF FIGURES

Figure 1.1: Reicofil pilot scale meltblown nonwoven manufacturing line at The Nonwovens Institute.....	5
Figure 1.2: Contributions of filtration mechanisms to overall filtration efficiency.....	8
Figure 1.3: Effect of ethanol exposure on particle collection efficiency in electret filter materials (Choi et al, 2015). .....	10
Figure 2.1: Coating schematic for both flat and fiber substrate geometries, showing the development of self-assembled layers on polypropylene. Sequential adsorption of unfolded soy protein isolate (green), polyDADMAC (yellow) and fumed silica (blue) from solutions, results in a dense coating of fumed silica for further functionalization by CVD approaches. ....	23
Figure 2.2: The reactor chamber used for the CVD functionalization process (A) was composed of a sealed glass jar with a small volume of FOTS contained in a vial. When vaporized, the FOTS molecule (B) reacts with siloxane surface of the fumed silica surface of the previously coated samples. Samples are suspended in the jar by steel mesh platforms for maximum exposure to the FOTS vapor.....	28
Figure 2.3: Fluorescence microscopy images of BSA coated nonwovens (A) show at low magnification uniformity of unfolded protein adsorption on fiber surfaces. Individual fibers are shown at high magnification (B) under visible spectrum illumination, and (C) dense coating of individual fibers with protein is demonstrated through excitation of fluorescent dye under TRITC filter.....	32
Figure 2.4: Water contact angle of the polymer thin film is monitored throughout the coating process. Contact angles are highly repeatable and representative of the bulk material properties, indicating good uniformity of the coating. Of note are the moderately hydrophobic neat PP surface, hydrophilic silica surface and superhydrophobic FOTS-modified silica of the final product.....	34
Figure 2.5: SEM images of complete sequentially deposited coatings generating dense fumed silica surface decoration on flat silica surface, at low (A) and high (B) magnification. The same coatings, on nonwoven polypropylene meltblown fabrics, result in highly conformal and dense silica decoration, imaged here at low (C) and high magnification (D). .....	36
Figure 2.6: Changes in atomic composition of nonwoven coating after each sequentially deposited coating step as measured by XPS. ....	38

Figure 2.7: Contact angle linearized as  $1-\cos(\theta)$  for a range of test fluids and mixtures. Contact angles shown were measured on: control substrates (neat PP, black); flat, coated thin-film substrates (red); and coated nonwoven mats (blue). Below surface tension values of 30 mN/m apparent contact angles on nonwoven substrates were unmeasurable due to droplet wicking.....41

Figure 2.8: Schematics of test substrates with contact angle of mineral oil on neat PP thin film substrates (left), FOTS modified coating of PP thin film substrates (center) and FOTS modified coating of nonwoven PP substrates (right). .....44

Figure 2.9: Isolated characteristic peaks for elements of interest from XPS survey scans of sequentially coated PP nonwovens. In each sub-plot the XPS signal for each peak is shown with multiple curves. Color of the curves indicates the surface layer of the coating: neat polypropylene with no coating (black), soy coated polypropylene (red), polyDADMAC surface over preceding layers (blue), fumed silica over preceding layers (magenta), and FOTS modified complete coating (green). .....50

Figure 3.1: Characterization of the influence of processing parameters on resulting nonwoven web formation by median fiber diameter analysis. Median fiber diameter of samples was shown to be independent of additive concentration (B) in the range tested, and to be moderately impacted by air pressure (A) and polymer throughput (D), and unaffected by DCD (C), as expected. ....62

Figure 3.2: Additive containing samples were characterized by XPS to demonstrate, (a) the initial (red) and fully migrated or equilibrated (black) additive distribution states at a range of bulk loading concentrations and (b) migration behavior in fibers containing 1.2% (black), 1.6% (red) or 2.0% (blue) additive over the first 72 hrs post-manufacturing. ....65

Figure 3.3: Apparent contact angle of isopropanol/water mixtures were measured as a function of surface fluorine content of nonwoven webs. Data was drawn from samples of varying bulk additive concentrations (as indicated by symbol shape according to the inset legends), and each were allowed to migrate to generate a range of samples with increasing F/C ratios. Both pure water (blue) and 25% isopropanol solution (green) droplets were supported by the web without wicking at all F/C ratios, while 50% (red) and pure (black) isopropanol droplets wick through nonwovens with insufficient surface concentration of fluorine.as indicated by dashed lines...67

Figure 3.4: Cross-sectional view of migrated, low DCD, Reicofil nonwovens with 4 wt% additive (F/C ratio  $\approx 0.56$ ) by ToF-SIMS. (A) Total ToF-SIMS signal across all ions, (B) Concentration of characteristic epoxy matrix ion, (C) Concentration of fluorine (characteristic additive ion), (D)

Overlay of characteristic epoxy and additive scans ( $F^-$  in green,  $C_3NO^-$  in yellow), (E) and (F) composition line scans of fibers (as indicated in D),  $F^-$  (red) and  $C_3NO^-$  (blue). The concentration of fluorine at the fiber surface observed here as an outline or halo structure is a clear indication of significant migration of the surface. Also demonstrated here is the formation of a depletion zone with significantly lower fluorine content in the volume of fiber between the core and surface.....70

Figure 3.5: Cross-sectional view of unmigrated, low DCD, Reicofil nonwovens with 4 wt% additive (F/C ratio  $\approx 0.21$ ) by ToF-SIMS. (a) Concentration of fluorine (characteristic additive ion) (b) Overlay of characteristic epoxy and additive scans ( $F^-$  in green,  $C_3NO^-$  in yellow) (c) Concentration of characteristic epoxy matrix ion, (d) and (e) composition line scans of fibers (as indicated in C),  $F^-$  (red) and  $C_3NO^-$  (blue). The concentration of fluorine at the fiber surface is only observed here in the case of very small fibers with short migration distances. ....71

Figure 3.6: Competing influence of migration time and die-to-collector distance on additive surface concentration was measured by XPS. F/C ratio was measured before migration (solid) and after migration (hashed) for samples generated at a DCD of 15 cm (red) and at 40 cm (blue). The effect of DCD prior to migration indicates significant additional mobility during the fiber formation process at larger distances. ....73

Figure 3.7: Fiber size distribution of 500 MFR (black) and 1200 MFR (red) nonwovens at 15 cm (unfilled) and 40 cm (hashed) DCD's and airflow rates of 1100 m<sup>3</sup>/hr and 800 m<sup>3</sup>/hr.....75

Figure 3.8: Initial Surface fluorine content of 1200 MFR polypropylene fiber webs as influenced by air flow rate and DCD. Samples prepared at (A) high (1100 m<sup>3</sup>/hr) air flow rate were found to have larger initial fluorine surface concentrations when compared to samples prepared at (B) low (800 m<sup>3</sup>/hr).....77

Figure 3.9: Comparison of unmigrated surface composition of low (open) and high (closed) MFR samples prepared at 1100 m<sup>3</sup>/hr air flow rate. The impact of DCD was also seen to be influenced by polymer flow rate. While high (40 cm, red) DCD samples exhibited similar F/C ratios independent of polymer flow rate, at low (15 cm, black) DCD higher F/C ratios were observed in the case of high MFR polymer samples.....79

Figure 3.10: Influence of polymer melt flow rate on unmigrated and migrated alcohol repellency scores as determined by the ISO 23232 test method. While 500 MFR polymer samples (red) demonstrated a more significant response to migration at low bulk additive concentrations, 1200 MFR samples achieved superior alcohol repellency without migration at moderate additive concentrations. ....81

Figure 4.1: Reicofil Pilot Scale Nonwoven Manufacturing System. ....89

Figure 4.2: (A) Fiber size distribution of electret filter samples and the effect DCD were characterized by SEM image analysis. Distribution of fibers is represented as a box containing 50% of fibers, whiskers containing 95% of fibers, with the mean (circle) and median (intersecting line). Fibers outside the 95<sup>th</sup> percentile are shown individually (diamonds). (B) The influence of additive concentration on filtration efficiency (red) and pressure drop (blue) was analyzed by fractional filter tester.....94

Figure 4.3: Additive fluorine content present at the surface of electret filter materials as measured by XPS immediately after manufacturing (open) and equilibrated over six months storage (solid). ....96

Figure 4.4: Competing influence of migration state and die-to-collector distance on additive surface concentration. Initial surface fluorine content (solid) is shown to be significantly lower than the fully migrated samples (hashed) for low to moderate bulk additive concentrations. The influence of DCD is shown to be significant in the development of surface fluorine content prior to migration as high, 40 cm DCD samples (blue) exhibit significantly higher F/C ratios than samples prepared at 15 cm DCD (red). At high bulk additive content and high DCD, initial surface concentration of additive is sufficiently high so as to prevent significant improvement through further sample migration. ....98

Figure 4.5: Influence of DCD and bulk additive concentration on initial (red) and equilibrium (blue) alcohol repellency scores as determined by ISO 23232 standard test method. All samples demonstrate significantly improved IPA repellency after additive migration, but samples manufactured at 40 cm DCD exhibit better repellency prior to migration with moderate additive concentrations in the bulk.....100

Figure 4.6: Subset of data from Figure 4.7 showing the impact of discharging of neat PP electret filter media by isopropanol vapor on filtration efficiency performance against 0.3  $\mu\text{m}$  DOP particle test.....102

Figure 4.7: Comparison of discharging performance of unmigrated (circles) and migrated (triangles) filter materials. Filtration performance against a 0.3  $\mu\text{m}$  particle was evaluated before corona charging (“uncharged”, black), after corona charging (“charged”, red) and after IPA vapor discharging of charged samples (“discharged”, green). At or above 1.2% bulk additive concentration, migration does not play a significant role in charge protection due to the diminishing returns of additional additive content at already high F/C ratios. At 0.6% bulk additive concentration there is a drastic response in charge protection performance due to additive migration, nearly doubling the effective filtration efficiency. ....103

Figure 4.8: Charge protection in electret filter media as influenced by additive content and migration.....	105
Figure 4.9: Charge retention of electret filter media as characterized by fractional filtration testing with 0.3 $\mu\text{m}$ DOP particles. The importance of additive migration is highlighted by the difference between % charge retention values of unmigrated (red) and migrated (blue) samples at extremely low additive loadings.....	107
Figure A.1.1: Thermal Gravimetric Analysis of neat 500 MFR PP and additive containing nonwovens. ....	118
Figure A.2.1: Differential Scanning Calorimetry of neat 500 MFR PP and additive containing nonwovens. ....	119
Figure A.2.2: Differential Scanning Calorimetry of neat 1200 MFR PP and additive containing nonwovens. ....	120
Figure B.1.1: Fourier Transform Infrared Spectroscopy absorption spectra of neat 500 MFR PP and additive containing nonwovens from 700 $\text{cm}^{-1}$ to 3500 $\text{cm}^{-1}$ . ....	121
Figure B.1.2: Fourier Transform Infrared Spectroscopy absorption spectra of neat 500 MFR PP and additive containing nonwovens focused upon the fingerprint region from 1000 $\text{cm}^{-1}$ to 1800 $\text{cm}^{-1}$ .....	122

## CHAPTER 1. INTRODUCTION

### *1.1 Motivation and Goals*

The modification of chemistry at polymer interfaces for a wide range of applications has been an important area of research for many years. The chemistries and methods used vary significantly depending upon the materials and desired resultant functionality of the surface. The literature has established a multitude of approaches for interfacial property manipulation with the goal of improved properties such as increased durability,<sup>1-4</sup> flame-retardancy,<sup>5-7</sup> conductivity,<sup>8-10</sup> and surface energy control,<sup>11-13</sup> among others. This dissertation details research into two primary methods for the creation of low surface energy polymer substrates; the development of a novel sequentially deposited surface coating with facile CVD functionalization approach, and the investigation of surface active fluorochemical melt additives.

The overarching goal of this research effort has been to design nonwoven materials with oil and alcohol repellent surfaces for electret air filtration applications. These devices, which utilize electrostatic attraction to increase capture efficiency, suffer severe and rapid charge loss when exposed to low surface tension fluids.<sup>14,15</sup> While there is some debate as to the mechanism by which charge loss takes place, it is clear that minimizing contact area between the probing liquid and the charged surface is key to the prevention of charge loss.<sup>16,17</sup> Therefore, decreasing the surface energy of the nonwoven and as a result increasing repellency towards these fluids was tested as a potential method for protecting charge and preventing the associated decrease in filtration efficiency.

## *1.2 Background*

In this section, a brief overview of relevant background information from the literature is provided on a number of topics critical to the research performed in this dissertation. Through this discussion of the prior art, specific goals will be highlighted as necessary contributions to the field which will be addressed through the work presented in the following chapters. These studies are all at various stages of the publication process and as such are presented here as independent, stand-alone works; however, through the context of this dissertation, the separate chapters will work in concert to address the research challenges highlighted in the following sections.

### *1.2.1 Nonwovens Manufacturing*

Nonwovens are a class of textile materials which are composed of fibers which are laid down randomly and bonded to one another in one of several ways. These fibers can be synthetic, natural, or a mixture of the two, and can be engineered in a plethora of ways yielding highly variable textile properties depending upon the materials and manufacturing methods used. Among the most commonly used methods for the manufacturing of nonwoven materials are processes that can be divided broadly into three main web forming methods: air-laid methods, wet-laid methods, and polymer-laid methods.

The first two of these require the use of staple fibers: namely natural fibers such as cotton, wool, or rayon; or synthetic fibers such as polypropylene, polyester, or nylon. These fibers are made prior to nonwoven manufacturing and are assembled into a mat or web. In the case of air-laid materials this can be done through the use of various carding processes where large clumps of staple fibers are first separated into individual fibers and then laid down in a

relatively unidirectional manner by a series of drums with fine toothed comb-like structures on their face. Alternatively, air-laid materials can be made through the use of aerodynamic methods where staple fibers are separated by carding, before lofting the individual fibers in an air-stream where they are captured by a condenser screen in a highly random orientation. Both the largely ordered structures formed by carding, and the random structures of aerodynamic air-laid fiber mats are then often layered by cross-lapping and bonded by processes such as needle-punching, calendaring or chemical bonding to improve the strength of the material and further engineer key properties for the intended application.<sup>18</sup>

Polymer-laid methods differ substantially from air and wet-laid methods, in that they effectively combine the fiber formation process and the fiber laydown process into a single step. In some cases, particularly meltblowing, fiber bonding also naturally occurs during the nonwoven production process. Due to the economy of performing so many manufacturing functions in a single process, and the relatively low cost of synthetic polymer materials, polymer-laid nonwovens are extremely cheap to produce. As a result, materials produced by these methods have found widespread use in applications requiring extreme cost-efficiency such as wipes, diapers, medical garments, and other disposables.<sup>19</sup> Another benefit of these processes is the highly tunable nature of the resulting textiles. As all of the major processes affecting the structure of the resultant nonwoven are occurring within the same process, it is possible to engineer key properties for the intended application, while maintaining low costs. Such highly engineered, low cost technical textiles make ideal products in many industries including insulating materials, hygienic products, protective apparel, and most commonly, filtration.<sup>20</sup> Of the polymer-laid methods, melt-blown nonwovens are the most commonly used

for filtration applications, and therefore were the materials used for the research in this dissertation.<sup>21</sup>

Meltblowing is a polymer-laid manufacturing process, unique for its fiber attenuation method. In the meltblowing process, polymer melt is extruded at high pressure through a die containing a large number of orifices and then propelled toward a collecting belt by a high velocity hot air stream, as shown in Figure 1.1. This process attenuates the fibers while still molten, significantly decreasing fiber diameter and bonding them through random contacts between molten fibers. This results in relatively strong fiber webs composed of fibers primarily between 1 and 10  $\mu\text{m}$ , and allows for tailored control many of the properties of the web.<sup>22</sup> Control over both machine and operational parameters allow for the manipulation of web properties including basis weight, loft, pore size, fiber diameter, and more.<sup>19,20</sup>

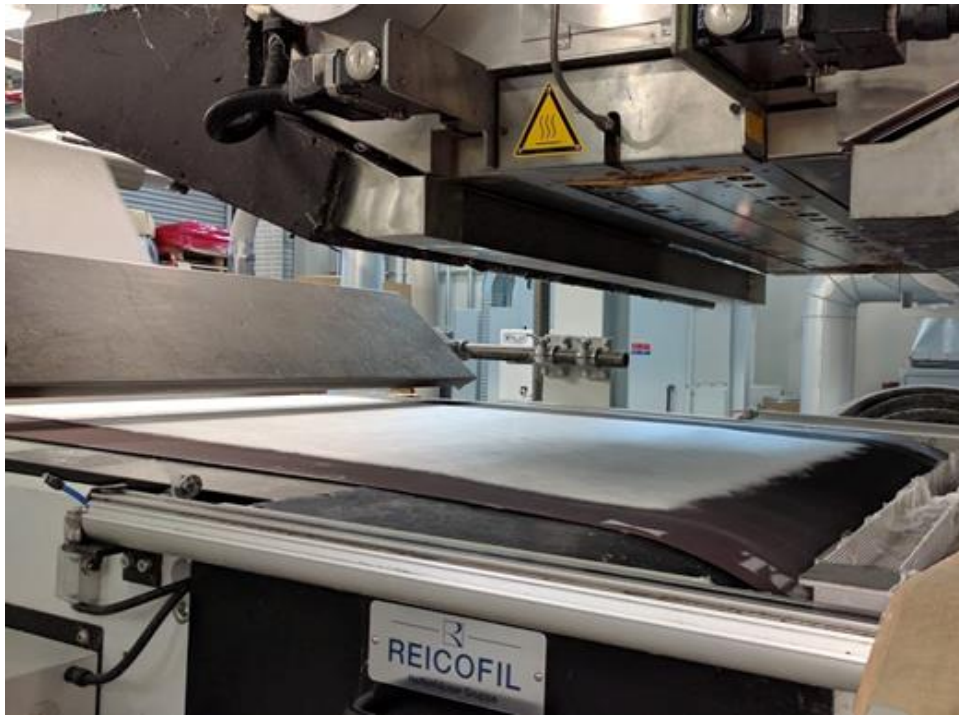


Figure 1.1: Reicofil pilot scale meltblown nonwoven manufacturing line at The Nonwovens Institute.

### 1.2.2 *Air Filtration*

A large and quickly growing market for nonwoven materials, and meltblown materials specifically, is filtration.<sup>23,24</sup> Many of the key benefits on nonwoven materials, such as controlled pore size, high surface area, and low cost, make them ideal for use in filtration applications where highly engineered materials are required while maintaining low costs such that disposability is feasible. As a result, the filtration sector of the nonwovens market has seen significant growth in recent years, and is expected to approach \$5 billion worldwide by 2019.<sup>25</sup>

This growth has been fueled by an emerging industries seeking to address emergent problems in a modern world; burgeoning development in fields such as water purification and air quality management are strong examples of this response. Driving growth in the industry is the need for extremely high efficiency air filters in applications such as home and industrial heating, ventilation and air conditioning (HVAC), cabin air filters, personal respirators, and clean room environment particulate control.<sup>26,27</sup> While generally a high efficiency air filter is capable of capturing particles at its specified efficiency, a greater constraint on long term performance of the filter is pressure drop. Initial pressure drop across the filter is largely a function of filter web solidity and thickness, however as the filter is subjected to particle loading, pressure drop increases as a result.<sup>28</sup> This imposes increased workload on air handling equipment as particle loading increases over the course of the life of the filter. In an effort to improve energy efficiency and mitigate effects of particle loading on filter life, a number of approaches have been developed including the use of electrostatics to maximize particle capture at lower pressure drop levels.

### 1.2.3 *Electrets*

Electret air filters are most commonly polymer-laid nonwoven filters made from a dielectric polymer such as polypropylene, polyethylene or polybutylene terephthalate. These materials are capable of being imbued with a quasi-permanent electrostatic charge, which allows for the capture of particles by electrostatic interaction. This charge can be induced in several different ways, including triboelectric charging, hydrocharging, and corona charging, among others.<sup>29,30</sup> Triboelectric charging is the well characterized effect of two dissimilar materials becoming charged through coming into contact with one another.<sup>31</sup> This allows for the passive generation of charge in textile applications where the textile is composed of multiple materials, typically in the form of a web composed of heterogeneous fibers with significantly different triboelectric properties.<sup>32</sup> Hydrocharging requires the nonwoven web be subjected to high pressure water jets, which induce a charge upon the fibers due to a similar phenomenon as tribocharging.<sup>33</sup>

Corona charging is a distinct method in which a dielectric material is charged through the use of an electrode which is energized with a high voltage power source. This electrode generates a strong electric field, ionizing molecules in the air, and then driving them toward the material to be charged. These ions become embedded in the insulating polymer and remain charged through the life of the filter. This concentration of embedded charges generate a permanent electric field, allowing for capture of particles by electrostatics and in general allowing for similar or improved capture efficiencies, as shown in Figure 1.2, at lower pressure drop values.<sup>34,35</sup>

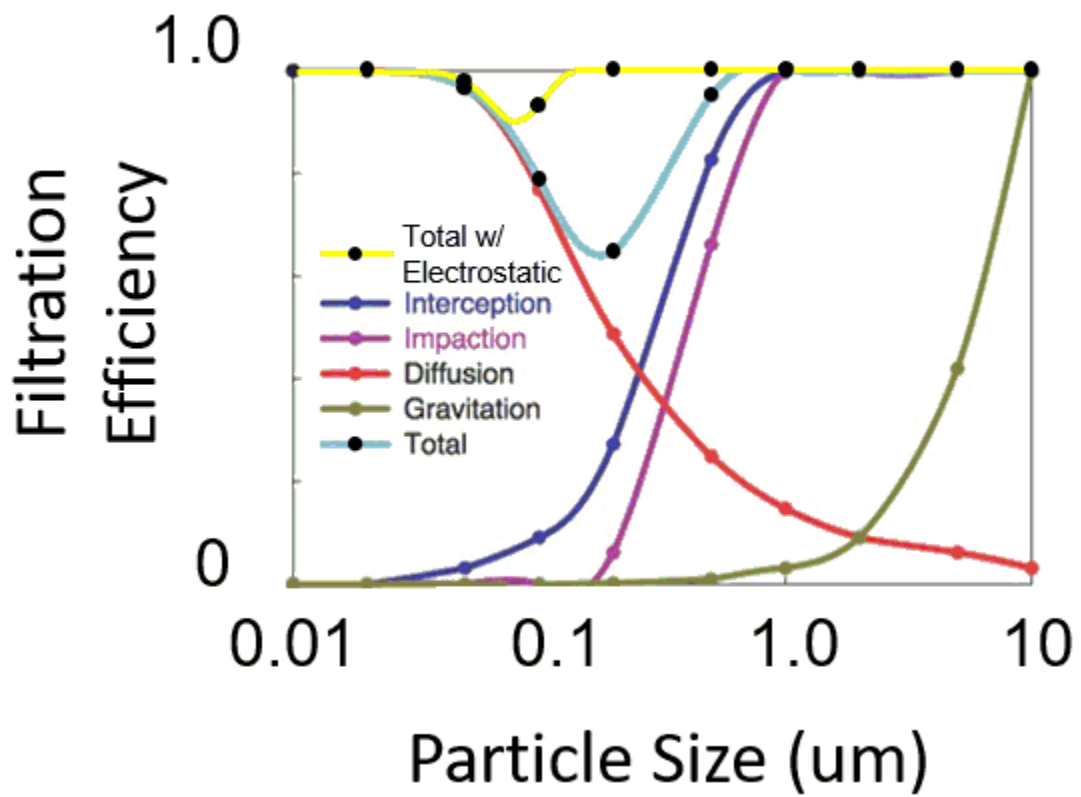


Figure 1.2: Contributions of filtration mechanisms to overall filtration efficiency.

In recent years, a significant portion of the literature surrounding electret filter materials has focused on the use of various additives for the purposes of increased chargeability or charge stability.<sup>36</sup> The focus of these efforts has been to show that changing the polymer morphology through the use of nucleating agents<sup>37,38</sup>, antioxidants,<sup>39,40</sup> or other means of crystallinity control<sup>41-43</sup> can have a significant impact on electret performance. Unfortunately, a significantly neglected aspect of these investigations and other investigations is the protection of the charge after it has been acquired.

#### *1.2.4 Charge Protection*

While the embedded charges utilized for increased capture efficiency in electrets are stable over very long time periods, they are unfortunately not immune to the effects of various external effects. One of the most prevalent mechanisms by which charge can be lost is through exposure of the charged media to oil and alcohol mists. This issue is commonly encountered in real world applications, including automotive cabin air filters, engine air intake filters, clean room and hospital HVAC systems, and other industrial applications.<sup>44,45</sup> As shown in Figure 1.3, the effect of these fluids on filtration performance can be extremely rapid and catastrophic, even at low concentrations.

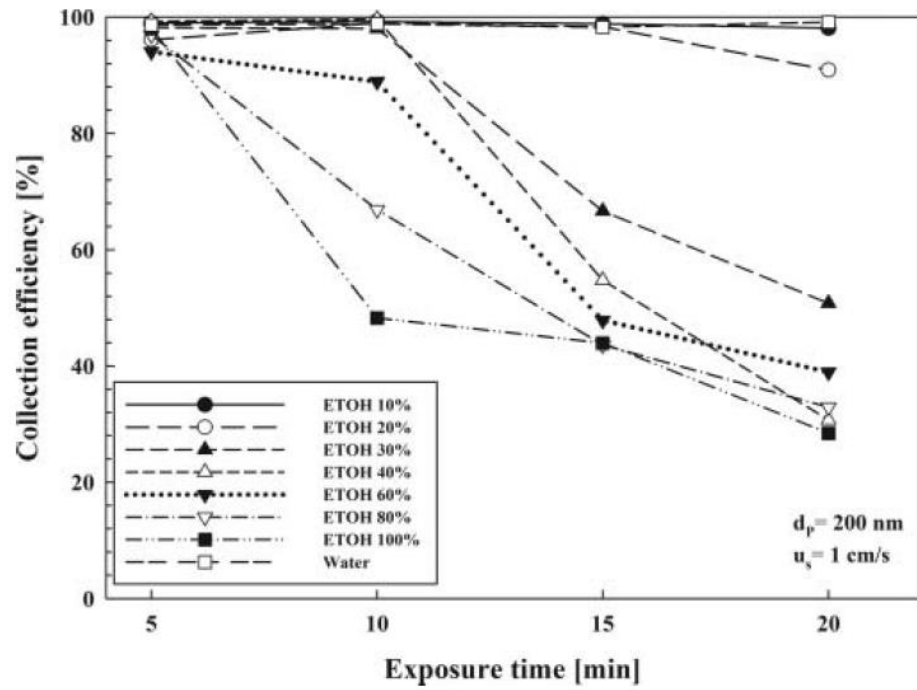


Figure 1.3: Effect of ethanol exposure on particle collection efficiency in electret filter materials (Choi et al, 2015).

While the mechanism by which oil and alcohol exposure is thought to cause discharging is a matter of some debate, there are three primary mechanisms which are thought to contribute to discharging in general. The first is recombination of charges with oppositely charged captured particles. The second is the capture of conducting species which screen the environment from the embedded charges. The final proposed mechanism is that the captured aerosol in some way alters the morphology of the fiber, allowing charges to move and recombine or otherwise inhibit the polymers capacity for holding charge.<sup>46</sup> While clearly the second mechanism is the most likely to play a role during the adsorption of oil or alcohol on the surface, the role of the first mechanism is unclear, though the third is unlikely in the case of an inert polymer such as polypropylene which was used in this study.

#### *1.2.5 Repellency*

The control of fluid surface wetting is a well characterized field of research with significant impact on many industries spanning from prevention of marine biofouling to anti-icing coatings for aircraft and everything in between. It has been understood since the seminal works of Cassie and Baxter that the two most critical design criteria for controlling wetting behavior are the chemistry of the surface, that is, the surface energy of the compounds which occupy the interface between the substrate and the fluid, and the roughness of that interface.<sup>47-49</sup> Roughness plays a key role, particularly in the design of systems for extreme repellency applications such as superhydrophobicity, as surface energy constraints are limited to relatively moderate levels of repellency.<sup>50,51</sup> The most drastic change in wetting behavior is often observed due to the inclusion of hierarchical, or multi-scale, roughness.<sup>52-55</sup> These structures enable the formation of a porous interface where the substrate and liquid are separated by air

pockets, effectively decreasing the surface energy of the interface to levels far below those possible for a homogeneous material.

These considerations are key to the effort to generate nonwoven substrates capable of repelling the most challenging of fluids, oils and alcohols. In this dissertation, two methods for the control of nonwoven surface energy were pursued: surface modification through the use of physisorbed coatings; and bulk, surface-active polymer melt additives.

### *1.2.6 Surface Modification of Polymers by Sequential Deposition*

Surface coatings for polymeric materials can be developed through a large number of different methods, however the modification of certain, highly inert polymers can prove to be difficult, and have had to be circumvented in the past.<sup>56,57</sup> Due to the unavailability of reactive sites in the backbone of saturated polymers like polypropylene, it is necessary to use highly energetic methods, or harsh chemical treatments, to generate sites for covalent attachment of coatings.<sup>58,59</sup> While these methods can be effective, such treatments, by definition, are detrimental to the integrity of the polymer structure and, as a result, can negatively impact bulk polymer properties in the final product.<sup>60</sup>

Alternatively, in recent years methods which utilize non-covalent bonding mechanisms such as ionic or van der Waals interactions have been presented in the literature.<sup>61,62</sup> The use of non-specific binding interactions as a means of coating inert polymer substrates has become more prevalent and there are several examples in the literature of the use of denatured proteins as an activation layer for further modification on substrates of various compositions and geometries.<sup>63-65</sup> These methods can be effective at generating durable and functional coatings on a wide range of substrates which would be difficult to modify by covalent modification

methods, but come with a separate set of challenges; namely, the less specific interactions of these methods frequently generate coatings with poor conformality and density of decoration.<sup>66-68</sup>

### *1.2.7 Surface Active Bulk Polymer Melt Additives*

The use of polymer melt additives to impart specific properties in the resulting material is a common practice in the polymer processing industries.<sup>69-71</sup> The effect of included additives vary greatly depending upon the intended application, and even within the field of nonwovens, additives can be used to address issues such as: lubricants for the reduction of melt viscosity, dyes for pigmentation, anti-oxidants or peroxides to limit degradation and flame retardant compounds.<sup>20</sup> Some additive molecules are designed such that they migrate to the surface of the material and form a region of higher concentration at or near the interface.<sup>72-76</sup> These types of additives are termed “blooming agents” and are particularly effective for applications which are relegated strictly to the fiber surface, such as control of wetting behavior. The blooming of surface active molecules to the surface causes an increased concentration of the desired compound localized at the interface, thus providing increased efficacy while decreasing the required bulk additive concentration.

While such phenomena are relatively well understood in the literature, the quantitative tracking of repellency performance with migration behavior, particularly with respect to challenging fluids such as oils and alcohols, is not as well characterized.<sup>71,77</sup> In the case of discharging due to oil aerosol contact, it has been demonstrated that repellency of these fluids has some beneficial effect, but this has not been thoroughly demonstrated for alcohols.<sup>78,79</sup>

### *1.3 Organization of Dissertation*

The structure for this dissertation will be the presentation of three studies detailing different phases of the above described effort. The first and second chapters describe the fundamental efforts to develop coated and additive containing fibers, respectively, and quantitatively evaluate repellency performance and impact on the nonwoven manufacturing process and resultant surface properties. The third chapter discusses the filter charging and discharging processes and establishes relationships between surface chemistry and charge protection as demonstrated by filtration performance tests.

#### 1.4 Works Cited

1. Jing, J. *et al.* Layer by layer deposition of polyethylenimine and bio-based polyphosphate on ammonium polyphosphate: A novel hybrid for simultaneously improving the flame retardancy and toughness of polylactic acid. *Polym. (United Kingdom)* **108**, 361–371 (2017).
2. Sellinger, A. *et al.* Continuous self-assembly of organic-inorganic nanocomposite coatings that mimic nacre. *Nature* **394**, 256–260 (1998).
3. Suriano, R., Ciapponi, R., Griffini, G., Levi, M. & Turri, S. Fluorinated zirconia-based sol-gel hybrid coatings on polycarbonate with high durability and improved scratch resistance. *Surf. Coatings Technol.* **311**, 80–89 (2017).
4. Riau, A. K. *et al.* Functionalization of the Polymeric Surface with Bioceramic Nanoparticles via a Novel, Nonthermal Dip Coating Method. *ACS Appl. Mater. Interfaces* **8**, 35565–35577 (2016).
5. Lv, P., Wang, Z., Hu, K. & Fan, W. Flammability and thermal degradation of flame retarded polypropylene composites containing melamine phosphate and pentaerythritol derivatives. *Polym. Degrad. Stab.* **90**, 523–534 (2005).
6. Du, M., Guo, B. & Jia, D. Thermal stability and flame retardant effects of halloysite nanotubes on poly(propylene). *Eur. Polym. J.* **42**, 1362–1369 (2006).
7. Li, B. & Xu, M. Effect of a novel charring-foaming agent on flame retardancy and thermal degradation of intumescent flame retardant polypropylene. *Polym. Degrad. Stab.* **91**, 1380–1386 (2006).
8. Prolongo, S. G., Printz, A. D., Rolston, N., Watson, B. L. & Dauskardt, R. H. Poly(triarylamine) composites with carbon nanomaterials for highly transparent and conductive coatings. *Thin Solid Films* **646**, 61–66 (2018).
9. Leterrier, Y. *et al.* Mechanical integrity of transparent conductive oxide films for flexible polymer-based displays. *Thin Solid Films* **460**, 156–166 (2004).
10. Lee, J. Y., Bashur, C. A., Goldstein, A. S. & Schmidt, C. E. Polypyrrole-coated electrospun PLGA nanofibers for neural tissue applications. *Biomaterials* **30**, 4325–4335 (2009).
11. Hardman, S. J. *et al.* Electrospinning Superhydrophobic Fibers Using Surface Segregating End-Functionalized Polymer Additives. 6461–6470 (2011).
12. Genzer, J. Creating Long-Lived Superhydrophobic Polymer Surfaces Through Mechanically Assembled Monolayers. *Science (80-. )*. **290**, 2130–2133 (2000).
13. Spataru, C. I., Purcar, V., Ghiurea, M., Somoghi, R. & Donescu, D. Superhydrophobic surfaces obtained from bilayer hybrids and silica nanoparticles. **15**, 1438–1444 (2013).
14. Myers, D. L. & Arnold, B. D. Electret Media For HVAC Filtration Applications. *Int. Nonwovens J. Winter*, (2003).
15. Kim, J., Hinestroza, J. P., Jasper, W. & Barker, R. L. Effect of Solvent Exposure on the Filtration Performance of Electrostatically Charged Polypropylene Filter Media. *Text. Res. J.* **79**, 343–350 (2009).
16. Jasper, W. J., Ph, D., Hinestroza, J. & Barker, R. Degradation Processes in Corona-Charged Electret Filter-Media with Exposure to Ethyl Benzene. **2**, 1–6 (2007).
17. Jasper, W. *et al.* Effect of xylene exposure on the performance of electret filter media. *J. Aerosol Sci.* **37**, 903–911 (2006).
18. Jirsak, O. & Wadsworth, L. C. *Nonwoven Textiles*. (Carolina Academic Press, 1999).

19. Zobel, S. & Gries, T. The use of nonwovens as filtration materials. *Appl. Nonwovens Tech. Text.* 160–183 (2010). doi:10.1016/B978-1-84569-437-1.50009-4
20. Dutton, K. Overview and Analysis of the Meltblown Process and Parameters. *J. Text. Appar. Technology Manag.* **6**, (2008).
21. Malkan, S. R. An overview of spunbonding and meltblowing technologies. *TAPPI J.* **78**, 185–190 (1995).
22. Lewandowski, Z., Ziabicki, A. & Jarecki, L. The Nonwovens Formation in the Melt-blown Process. *Fibers Text. East. Eur.* **15**, 77–81 (2007).
23. McIntyre, K. Filtration Market Update. *Nonwovens Ind.* **46**, 38–43 (2015).
24. Analysis, C. P. I. & Version, S. Filtration & Separation Industry CP Industry Analysis – Summary Version. 1–9
25. McIntyre, K. Focus On: Filtration. *Nonwovens Ind.* **45**, 54–60 (2014).
26. McIntyre, K. Filtration Makers Respond to Changing World. *Nonwovens Ind.* **43**, 58–66 (2012).
27. Edelman, L. Air filtration: Air filter media — an industry evolves. *Filtr. Sep.* **45**, 24–26 (2008).
28. Payen, J. *et al.* Influence of fiber diameter, fiber combinations and solid volume fraction on air filtration properties in nonwovens. *Text. Res. J.* **82**, 1948–1959 (2012).
29. Tsai, P. P., Schreuder-Gibson, H. & Gibson, P. Different electrostatic methods for making electret filters. *J. Electrostat.* **54**, 333–341 (2002).
30. Tsai, P. What is an Electret? *American Filtration & Separation Society* (2013).
31. Smith, P., East, G., Brown, R. & Wake, D. Generation of triboelectric charge in textile fibre mixtures, and their use as air filters. *J. Electrostat.* **21**, 81–98 (1988).
32. Horrocks, A. R. & Anand, S. C. *Handbook of technical textiles. Volume 2, Technical Textile Applications.* (Woodhead Publishing, 2016).
33. Angadjivand, S. A., Jones, M. E. & Meyer, D. E. Method Of Charging Electret Filter Media. (1996). doi:Jan, 28, 1997
34. Romay, F. J., Liu, B. Y. H. & Chae, S.-J. Experimental Study of Electrostatic Capture Mechanisms in Commercial Electret Filters. *Aerosol Sci. Technol.* **28**, 224–234 (1998).
35. Tsai, P. P., Qin, G. & Wadsworth, L. C. Theory and techniques of electrostatic charging of melt-blown nonwoven webs. *TAPPI J.* 274–278 (1998).
36. Kilic, A. Improving Electret Filter Efficiency by Modifying Fibrous Webs with Melt Additives. (2012).
37. Behrendt, N. *et al.* Charge storage behavior of isotropic and biaxially-oriented polypropylene films containing alpha and beta nucleating agents. *J. Appl. Polym. Sci.* **99**, 650–658 (2006).
38. Hillenbrand, J., Behrendt, N., Altstadt, V., Schmidt, H. W. & Sessler, G. M. Electret properties of biaxially stretched polypropylene films containing various additives. *J. Phys. D. Appl. Phys.* **39**, 535–540 (2006).
39. Erhard, D. P., Giesa, R., Altstadt, V. & Schmidt, H.-W. Charge Storage Performance of Polyetherimide Ultem 1000 —Influence of Secondary Antioxidants and Purification. *J. Appl. Polym. Sci.* **115**, 1247–1255 (2013).
40. Cartwright, G. A., Davies, A. E., Swingler, S. G. & Vaughan, A. S. Effect of an antioxidant additive on morphology and space-charge characteristics of low-density polyethylene. *Sci. Meas. Technol. IEE Proc.* **143**, 26–34 (1996).
41. Thyssen, A., Almdal, K. & Thomsen, E. V. Electret stability related to the crystallinity

- in polypropylene. *IEEE Trans. Dielectr. Electr. Insul.* **24**, 3038–3046 (2017).
42. Xiao, H., Gui, J., Chen, G. & Xiao, C. Study on correlation of filtration performance and charge behavior and crystalline structure for melt-blown polypropylene electret fabrics. *J. Appl. Polym. Sci.* **132**, 1–6 (2015).
  43. Cheung, Z., Ng, K., Weng, L., Chan, C. & Li, L. Crystallization-driven migration of the low surface energy segment of a copolymer to the bulk. **47**, 3164–3170 (2006).
  44. Heinonen, K. I. M. M. O. Reliability of Electret Filters. **29**, 353–355 (1994).
  45. Choi, H.-J., Park, E.-S., Kim, J.-U., Kim, S. H. & Lee, M.-H. Experimental Study on Charge Decay of Electret Filter Due to Organic Solvent Exposure. *Aerosol Sci. Technol.* **49**, 977–983 (2015).
  46. Brown, R. The behaviour of fibrous filter media in dust respirators. *Ann. Occup. Hyg.* **23**, 367–380 (1980).
  47. Cassie, A. & Baxter, S. Wettability of porous surfaces. *Trans. Faraday Soc.* 546–551 (1944).
  48. Wenzel, R. Resistance of solid surfaces to wetting by water. *Ind. Eng. Chem.* **28**, 988–994 (1936).
  49. Choi, W. *et al.* Fabrics with Tunable Oleophobicity. *Adv. Mater.* **21**, 2190–2195 (2009).
  50. Mammen, L. *et al.* Effect of nanoroughness on highly hydrophobic and superhydrophobic coatings. *Langmuir* **28**, 15005–15014 (2012).
  51. Kulinich, S. A. & Farzaneh, M. On wetting behavior of fluorocarbon coatings with various chemical and roughness characteristics. *Vacuum* **79**, 255–264 (2005).
  52. Taurino, R. *et al.* Facile preparation of superhydrophobic coatings by sol-gel processes. *J. Colloid Interface Sci.* **325**, 149–56 (2008).
  53. Campos, R., Guenther, A. J., Haddad, T. S. & Mabry, J. M. Fluoroalkyl-functionalized silica particles: synthesis, characterization, and wetting characteristics. *Langmuir* **27**, 10206–15 (2011).
  54. Tuteja, A. *et al.* Designing superoleophobic surfaces. *Science* **318**, 1618–22 (2007).
  55. Tuteja, A., Choi, W., Mabry, J. M., McKinley, G. H. & Cohen, R. E. Robust omniphobic surfaces. *Proc. Natl. Acad. Sci. U. S. A.* **105**, 18200–5 (2008).
  56. Arvidson, S. a. *et al.* Modification of Melt-Spun Isotactic Polypropylene and Poly(lactic acid) Bicomponent Filaments with a Premade Block Copolymer. *Macromolecules* **45**, 913–925 (2012).
  57. Özen, I., Rustal, C., Dirnberger, K., Fritz, H. G. & Eisenbach, C. D. Modification of surface properties of polypropylene films by blending with poly(ethylene-b-ethylene oxide) and its application. *Polym. Bull.* **68**, 575–595 (2012).
  58. Szabová, R., Černáková, L., Wolfová, M. & Černák, M. Coating of TiO<sub>2</sub> nanoparticles on the plasma activated polypropylene fibers. *Acta Chim. Slovaca* **2**, 70–76 (2009).
  59. Jois, Y. H. R. & Harrison, J. B. Modification of Polyolefins: An Overview. *J. Macromol. Sci. Part C Polym. Rev.* **36**, 433–455 (1996).
  60. Takke, V., Behary, N., Perwuelz, a. & Campagne, C. Studies on the atmospheric air-plasma treatment of PET (polyethylene terephthalate) woven fabrics: Effect of process parameters and of aging. *J. Appl. Polym. Sci.* **114**, 348–357 (2009).
  61. Pavasupree, S., Dubas, S. T. & Rangkupan, R. Surface modification of polypropylene non-woven fibers with TiO<sub>2</sub> nanoparticles via layer-by-layer self assembly method: Preparation and photocatalytic activity. *J. Environ. Sci. (China)* **37**, 59–66 (2015).
  62. Salas, C., Genzer, J., Lucia, L. a, Hubbe, M. a & Rojas, O. J. Water-wettable

- polypropylene fibers by facile surface treatment based on soy proteins. *ACS Appl. Mater. Interfaces* **5**, 6541–8 (2013).
63. Goli, K. K., Rojas, O. J., Ozçam, a E. & Genzer, J. Generation of functional coatings on hydrophobic surfaces through deposition of denatured proteins followed by grafting from polymerization. *Biomacromolecules* **13**, 1371–82 (2012).
  64. Goli, K. K. *et al.* Generation and properties of antibacterial coatings based on electrostatic attachment of silver nanoparticles to protein-coated polypropylene fibers. *ACS Appl. Mater. Interfaces* **5**, 5298–5306 (2013).
  65. Goli, K. K., Rojas, O. J. & Genzer, J. Formation and antifouling properties of amphiphilic coatings on polypropylene fibers. *Biomacromolecules* **13**, 3769–79 (2012).
  66. Nishizawa, S. & Shiratori, S. Water-based preparation of highly oleophobic thin films through aggregation of nanoparticles using layer-by-layer treatment. *Appl. Surf. Sci.* **263**, 8–13 (2012).
  67. Dubas, S. T., Kumlangdudsana, P. & Potiyaraj, P. Layer-by-layer deposition of antimicrobial silver nanoparticles on textile fibers. *Colloids Surfaces A Physicochem. Eng. Asp.* **289**, 105–109 (2006).
  68. Xu, L., Cai, Z., Shen, Y., Wang, L. & Ding, Y. Facile preparation of superhydrophobic polyester surfaces with fluoropolymer/SiO<sub>2</sub> nanocomposites based on vinyl nanosilica hydrosols. *J. Appl. Polym. Sci.* **131**, (2014).
  69. Allen, M. A. & Crane, P. L. Nonwoven webs manufactured from additive-loaded multicomponent filaments. (2005).
  70. Gardiner, R. A. Durably hydrophilic thermoplastic fiber and fabric made from said fiber. (1994).
  71. Zhang, D., Sun, C. & Xiao, J. Effect of Selected Additives on Surface Energy of Fibers and Meltblown Nonwovens. *Text. Res. J.* **76**, 261–265 (2006).
  72. Nouman, M., Saunier, J., Jubeli, E. & Yagoubi, N. Additive blooming in polymer materials: Consequences in the pharmaceutical and medical field. *Polym. Degrad. Stab.* **143**, 239–252 (2017).
  73. Camós Noguera, A., Olsen, S. M., Hvilsted, S. & Kiil, S. Diffusion of surface-active amphiphiles in silicone-based fouling-release coatings. *Prog. Org. Coatings* **106**, 77–86 (2017).
  74. Dulal, N. *et al.* Slip-additive migration, surface morphology, and performance on injection moulded high-density polyethylene closures. *J. Colloid Interface Sci.* **505**, 537–545 (2017).
  75. Jariwala, C., Klun, T., Dams, R. & Jones, M. Alkylated fluorochemical oligomers and use thereof. *US Patent 6,288,157* (2001).
  76. Quincy III, R. B., Yahiaoui, A. & McManus, J. L. Nonwoven webs having zoned migration of internal additives. (2000).
  77. Wang, Z., Macosko, C. W. & Bates, F. S. Fluorine-Enriched Melt-Blown Fibers from Polymer Blends of Poly(butylene terephthalate) and a Fluorinated Multiblock Copolyester. *ACS Appl. Mater. Interfaces* **8**, 754–761 (2016).
  78. Jones, M., Mei, B. & Rousseau, A. Method of making electret articles and filters with increased oily mist resistance. *US Pat. 6,068,799* (2000).
  79. Jones, M. E. & Rousseau, A. D. Oily mist resistant electret filter media. 1–8 (1995).

**CHAPTER 2. OMNIPHOBIC POLYPROPYLENE NONWOVENS BY SURFACE  
MODIFICATION WITH BIO-HYBRID AND CONFORMABLE COATINGS  
FOLLOWED BY CHEMICAL VAPOR DEPOSITION**

*Joseph H. Lavoie<sup>1</sup>, Eunkyong Shim<sup>2</sup>, Saad Khan<sup>1</sup>, and Orlando J. Rojas<sup>1,3</sup>*

<sup>1</sup>*Department of Chemical Engineering, North Carolina State University, Raleigh NC*

<sup>2</sup>*College of Textiles, North Carolina State University, Raleigh NC*

<sup>3</sup>*Department of Bioproducts and Biosystems, School of Chemical Engineering, Aalto University, Espoo, Finland*

*2.1 Abstract*

A conformal coating system for the preparation of extremely low surface energy nonwoven fibers substrates was developed by using a sequential assembly approach that combined changes in surface roughness and physical deposition of low energy molecules. The coating system exploited hydrophobic interactions between polypropylene (PP) nonwoven substrates and the hydrophobic domains of soy protein isolate molecules, which act as a uniform, conformal foundation for further modification. Poly(diallyldimethylammonium chloride) (polyDADMAC) was bound to the exposed negatively charged residues of soy protein, forming a positively charged polyelectrolyte surface. Following, negatively charged fumed silica nanoparticles formed the outermost layer of the coating, providing nanoscale surface roughness, which was then functionalized by chemical vapor deposition (CVD) with fluorooctyl triethoxysilane (FOTS). The coating process was characterized by spectrometric and microscopy techniques that included X-ray photoelectron spectroscopy (XPS), which confirmed the change in chemical composition of surface-bound compounds after each step of surface modification. Scanning electron microscopy (SEM) confirmed the surface roughness and the quality and conformability of the finished coating structure. Resultant surface

properties of the functionalized coating were quantified by contact-angle goniometry with a wide range of probing liquids. The results indicated successful superhydrophobic and oleophobic behavior, with water contact angles  $> 150^\circ$  and mineral oil contact angles  $> 90^\circ$ . Moderate increases in the contact angle with some alcohols were also observed. Coatings on thin films were used as a reference to elucidate the effect of the substrate geometry on repellency of low surface tension fluids.

## 2.2 *Introduction*

The creation of hydrophobic and oleophobic surfaces is a technical challenge that applies to many different industries, including automotive, consumer electronics, adhesives and many others. Surfaces that are engineered with the goal of attaining oil and water repellency have been possible by a myriad of approaches according to the materials in use and design criteria for the particular field of study. However, repelling ultra low surface energy fluids have not been as widely studied. Due to their extremely low surface tension compared to water and many oils, the creation of a surfaces that induces a significantly increased contact angle with alcohol is extremely challenging. With this in mind, this study sought to utilize many of the principles developed for superhydrophobic and oleophobic surfaces and apply them to the unique challenge of alcohol repellency.

As has been shown in the previous literature, there are two primary considerations for the creation of highly repellent surface properties: combined changes in surface chemistry and roughness.<sup>1-3</sup> The use of textiles as a substrate for repellent surface chemistries is advantageous due to the geometry of the fiber mat, beginning with the seminal works of Cassie and Baxter. In particular, hierarchical and reentrant geometries are key to the creation of surfaces capable

of super-oleophobicity and so-called “omniphobicity.”<sup>4-7</sup> In an effort to combine the natural roughness of textile systems, and to engineer hierarchical roughness into these materials, an organic-inorganic coating method was developed that would bind fumed silica nanoparticles onto the fiber surface. Surface chemistry was then controlled through facile modification of surface groups on the fumed silica particles.

Due to the highly engineered and customizable nature of nonwoven materials, they are utilized in a wide range of technical textile applications. In this case, a meltblown PP nonwoven material was selected as the substrate to be coated. Polypropylene is commonly used in nonwoven applications such as electret air filters, medical and industrial protective apparel, construction materials and home furnishings, among others.<sup>8</sup> It is extremely difficult to perform direct surface functionalization of PP, due to the lack of potential sites for chemical reaction on the polymer backbone. In order combat the inert nature of PP and create a surface conducive to modification, it is necessary to create suitable sites for the grafting of desired chemistries. Most frequently this is done through the creation of hydrophilic groups by oxidation, typically by high energy surface treatments such as plasma, corona, or flame discharge treatments.<sup>9,10</sup> While effective, these treatments can significantly alter fiber morphology and physical properties by polymer degradation. Alternatively, the use of melt additives or bi-component fiber construction have been developed to achieve many of the same goals through the selective incorporation of other polymers into fibers, thereby altering fiber properties. Unfortunately, by moving away from a homopolymer fiber construction, significant changes to the manufacturing process must be made; therefore, the properties of the nonwoven fiber mat may be drastically altered. As an alternative to these methods, a surface modification process was designed that would successfully alter surface properties of the PP nonwoven

material, without interfering with the manufacturing process and avoiding processing steps, which would not be feasible at the rapid, roll-to-roll manufacturing speed necessary for successful nonwovens production.

Soy protein isolate is a widely available material derived from the soybean that is commonly used in the food processing and health foods industries. Due to its established use in other areas and highly renewable nature, it is readily available and inexpensive. This is an important criterion for successful integration into nonwoven product design, which necessitates focus upon rapid, cheap manufacturing processes. Key to the utilization of soy protein isolate in this work is the natural biofouling phenomena whereby proteins irreversibly bind to hydrophobic surfaces.<sup>11,12</sup> This phenomena has been observed in many application areas, though it is typically considered an adverse effect, such as the adhesion of biopolymers to biomedical devices in the body or surfaces exposed to marine environments. Previous work has successfully demonstrated the use of soy protein compounds as “activation” layers for further modification by advantageous biofouling coatings, as a means to circumvent the inert nature of some polymer substrates.<sup>13–15</sup>

The activation of the surface by soy protein opens avenues to multiple modification methods. Amino and hydroxyl functionalities present in the protein structure have been used as reactive sites for “grafting-from” polymerization for polymer brush structures with various functionalities.<sup>16</sup> Others have used cellulosic materials as a substrate for layer-by-layer type coating systems,<sup>17</sup> utilizing ionic interactions between oppositely charged molecules to generate self-assembled layers in a sequential fashion. As shown in Figure 2.1, in this work we combine these two concepts, generating a conformal coating of denatured soy protein and modify it through the use of self-assembled adsorbed layers to create a bio-based hybrid

coating with beneficial properties. The creation of organic-inorganic coatings has been shown to be an effective tool for the design of materials and surfaces with unique or improved properties, through control of both topography and functionality.<sup>18</sup> These nanocomposite-type materials and coatings have found applications in a number of growing fields, including medical devices,<sup>19–23</sup> supercapacitors,<sup>24,25</sup> protective coatings,<sup>26–28</sup> and others. In particular, there is great interest in the use of bio-based materials in order to avoid synthetic polymers derived from petroleum sources. In addition, improved environmental impacts can be gained due to biodegradability, resulting in bio-based hybrid materials where the organic component of the material is a biopolymer such as those derived from soy, chitosan, or lignin.<sup>29–31</sup>

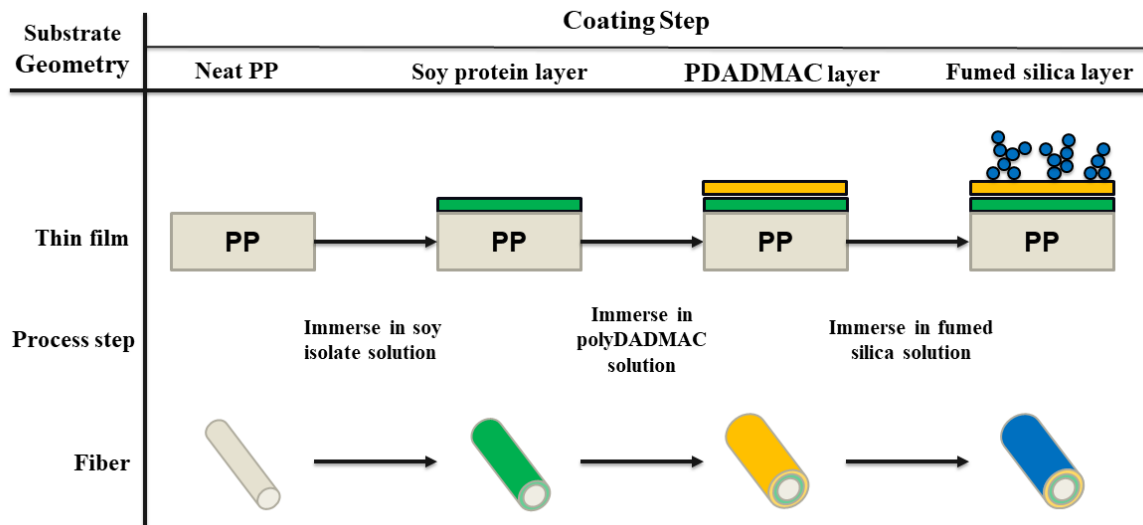


Figure 2.1: Coating schematic for both flat and fiber substrate geometries, showing the development of self-assembled layers on polypropylene. Sequential adsorption of unfolded soy protein isolate (green), polyDADMAC (yellow) and fumed silica (blue) from solutions, results in a dense coating of fumed silica for further functionalization by CVD approaches.

Perhaps the most beneficial property of the resulting coated surface is the presence of silane groups for chemical modification. While many methods for the grafting of chemical moieties require numerous steps, hazardous solvents or damaging sample preparation methods, CVD of organosilane groups is a facile process that is safe for many substrates. For the purposes of this study, fluorooctyl triethoxysilane (FOTS) was selected as a organosilane compound with a sufficiently large perfluorinated chain to ensure extremely high contact angles with many liquids, which has been demonstrated to effectively graft through the CVD process.<sup>32</sup>

## 2.3 *Experimental*

### 2.3.1 *Materials & Methods.*

Water soluble soy protein isolate (Clarisoy 150, Soy Protein Isolate) was obtained from Archer Daniels Midland (ADM, Decatur, IL). Nonwoven polypropylene (PP) substrates and metallocene homopolymer PP resin (Metocene MF650X, LyondellBasell, Houston, TX, USA) for spin coated thin-films were provided by The Nonwovens Institute at North Carolina State University (Raleigh, NC, USA). Poly(diallyldimethyl ammonium chloride), fumed silica, fluorooctyl triethoxysilane (FOTS), bovine serum albumin, and isopropyl alcohol (IPA) were obtained from Sigma Aldrich (St. Louis, MO). Alexa Fluor 555 labeled bovine serum albumin (BSA) was obtained from Invitrogen (Thermo Fisher Scientific, Waltham, MA).

### 2.3.2 *Preparation of Polypropylene Thin Films*

Thin films of PP on silica substrates were prepared by a spin coating method reported previously.<sup>33</sup> In this method, polypropylene was dissolved in 140 °C xylene at a concentration of 2 mg/mL under constant stirring. The solution was boiled for 2 hours under a reflux

condenser, utilizing cold tap water as the cooling medium, to prevent the loss of solvent to atmosphere. While this was being done, silicon substrates were cleaned by submersion in a 30% hydrogen peroxide, 70% sulfuric acid “piranha” etch acid bath for 20 minutes. After removal from the acid bath, samples were triple rinsed to ensure complete removal of the acid solution. Just prior to spin coating, the silicon wafers were placed in an oxygen plasma chamber for 20 minutes to ensure the surface was clean, and to promote adhesion between the PP and silicon.

The wafer to be coated was then placed on the spin coating rotor, and heated under an infrared lamp (250W) for several minutes. At this time the reflux condenser was removed from the polypropylene-xylene solution, and the temperature was dropped to just below the boiling point to allow for effective pipetting. An infrared thermometer gun was used to assess the temperature of the surface, and when the temperature had reached approximately 85 °C, about 100 µL of the solution was pipetted onto the center of the silicon surface using disposable glass pipettes. Immediately after pipetting the spin coater was activated, spinning the substrate at 3000 rpm for 20 seconds, removing any excess solution. After coating, samples were removed and immediately transferred to an oven, preheated to 80 °C, to remove any excess xylene overnight.

### *2.3.3 Preparation of Coating layers*

Dispersions were first prepared for each layer of the coating system. The soy protein isolate dispersion was prepared from a 1.0 mg/ml solution of Clarisoy in Milli-Q water. In order to enhance adhesion of the soy protein onto the substrate, it was thermally unfolded at 95 °C for 2 hours, under constant stirring by magnetic stir bar. A 0.2 wt% solution of pDADMAC in

water was prepared, and stirred continuously to ensure a well-mixed, homogeneous solution. The fumed silica dispersion was prepared at a 1 wt% concentration in isopropanol, and stirred continuously.

PP nonwoven and thin films were first treated with IPA to facilitate wetting in subsequent steps involving treatments from aqueous dispersions. Small, roughly 1 inch square samples of nonwoven PP were cut and placed into a beaker of IPA and stirred by magnetic stir bar for 20 minutes to allow wetting in subsequent aqueous solutions. In the case of thin film samples, PP coated wafers were soaked in IPA, but not stirred. The samples were then rinsed by sequential submersion in two baths of purified water, taking care to drain as much liquid from the samples as possible before moving to the next bath. After the second rinse step, the samples were transferred directly to the previously described Clarisoy solution. Adsorption of denatured soy onto the PP substrates occurred under constant stirring by magnetic stir bar. After 30 minutes of adsorption, the samples were removed from the solution, rinsed thoroughly by immersion in a beaker of water with mild agitation, and transferred to the pDADMAC solution. Adsorption of the pDADMAC was carried out under constant agitation as well, for a duration of 20 minutes, before rinsing as in the previous step. Lastly, the samples were submerged in the fumed silica solution and stirred for 1 hour to encourage uniform and complete coating coverage. Samples were then rinsed and placed on a Teflon sheet to dry overnight.

After the samples dried completely, they were placed into a simple glass reactor for the chemical vapor deposition of the FOTS molecule. The glass reactor, shown in Figure 2.2, included a vial loaded with a small quantity of FOTS (50 – 100  $\mu$ L, depending upon the number of samples) which was placed at the bottom of the reactor. A metal mesh was compressed into

the reactor to form suspended sample holders in the head space of the reactor chamber, and samples were arranged on the mesh such that they did not overlap. Multiple layers of mesh were used to increase sample loadings for some experiments, as depicted in the schematic. The reactor was sealed and then placed in an oven at 125 °C for 2 hours. At this time the reactor was then removed from the oven and opened in a fume hood to vent the remaining FOTS vapor. After the vapors clear (about 30 seconds), the vial of FOTS was removed, the reactor resealed, and placed back in the oven for an additional hour in order to re-vaporize any unbound FOTS from the reactor assembly and samples. The reactor was then vented in the fume hood again, and the samples removed.

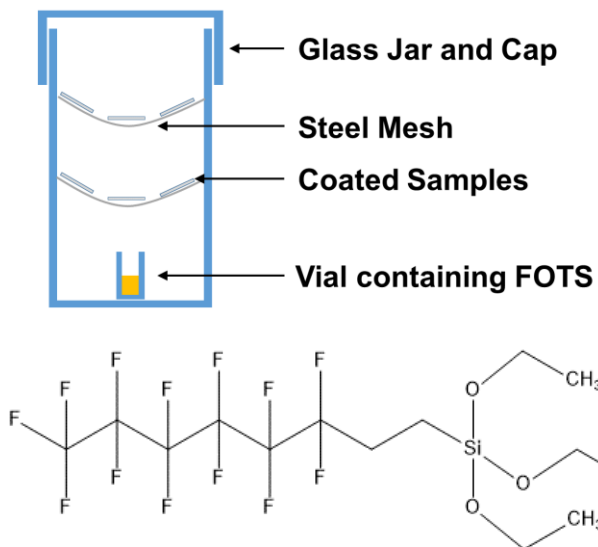


Figure 2.2: The reactor chamber used for the CVD functionalization process (A) was composed of a sealed glass jar with a small volume of FOTS contained in a vial. When vaporized, the FOTS molecule (B) reacts with siloxane surface of the fumed silica surface of the previously coated samples. Samples are suspended in the jar by steel mesh platforms for maximum exposure to the FOTS vapor.

#### 2.3.4 *Scanning Electron Microscopy*

Coating uniformity was evaluated visually through the use of scanning electron microscopy. Images were captured on the Verios High Resolution SEM at the AIF. Various beam conditions were used to capture images of the different samples generated as a part of this effort. Thin film coatings were imaged at a voltage of 2 kV and 13 pA at a working distance of 4 mm. In order to avoid charging of nonwoven samples during imaging, low current of 3.1 pA was used at a voltage of 3 kV, and the higher working distance of 6 mm. All images were captured using the Through Lens Detector.

#### 2.3.5 *Fluorescence Microscopy*

Adsorption of proteins onto PP nonwovens was qualitatively evaluated using fluorescence microscopy. Bovine serum albumin (MW 67 000 Da, isoelectric point (pI) 4.7) labelled with Alexa Fluor 555 fluorescent dye was purchased from Invitrogen.<sup>34</sup> The fluorescent BSA molecule was considered to be a suitable analog for soy protein, insofar as surface adsorption through physical interactions of hydrophobic residues after denaturation should be consistent between the two molecules. Nonwoven PP samples were treated with IPA to promote wetting, placed into a dilute solution of Alexa Fluor 555 tagged BSA (approximately 10 µg/mL).<sup>34</sup> The solution was then stirred for 30 minutes, before rinsing and drying overnight. Samples were imaged using an excitation wavelength of 555 nm and images were captured on a fluorescence microscope using the standard TRITC filter set.

#### 2.3.6 *X-Ray Photoelectron Spectroscopy*

Coated nonwoven substrates were characterized by XPS. Analysis was performed on a SPECS system with PHOIBOS 150 Analyzer at the Analytical Instrumentation Facility (AIF) at NC

State University (Raleigh, NC). The analysis was done using a Mg K $\alpha$  x-ray source operated at 300 W (10 kV and 30 mA) and at room temperature and pressures in the 10<sup>-8</sup> Torr range or lower. Survey scans were collected from 0 to 1100 eV and atomic compositions were derived from peak areas with Shirley backgrounds using CasaXPS processing software version 2.3.16.

### 2.3.7 *Contact Angle Goniometry*

To evaluate repellency of both flat and nonwoven substrates, initial sessile drop contact angles of water and other solvents were measured using an SEO Phoenix 300 Goniometer (Surface Electro Optics, Suwon City, South Korea). Measurements were performed at room temperature. Images were captured by the manufacturer provided frame grabbing software “Image XP”, and contact angle analysis was performed using “ImageJ” image processing software with the “DropSnake” analysis plugin. Solvents with varying surface tensions used for quantifying repellency towards oils and alcohols included IPA, dodecane, ethylene glycol, octane, hexadecane, hexane, and mineral oil. Due to the porous nature of nonwoven materials, reported contact angles for these materials are apparent contact angles and cannot be directly related to the surface energy of the coating.

## 2.4 *Results and Discussion*

### 2.4.1 *Surface Morphology of Coating Layers*

Alexa Fluor 555 tagged BSA proteins were unfolded and adsorbed onto PP nonwovens according to the same procedure used for unlabeled soy protein. The images in Figure 2.3 illustrate the coating of nonwoven fibers with denatured proteins. Figure 2.3C, at 40X magnification, shows the conformal nature of the coating, as the light emitted by the fluorescent dye clearly outlines each individual fiber, matching the visible spectrum image

shown in Figure 2.3B. Fibers which are too deep into the fiber mat, or that rise above the surface of the mat, become out of focus and the diffuse light is not as easily detectable at this high magnification, however Figure 2.3A shows the same sample at lower magnification (10X). While individual fibers are not visible, it is clear that the proteins are uniformly distributed throughout the nonwoven, as there are no significant, visible irregularities in brightness of the fluorescent image.

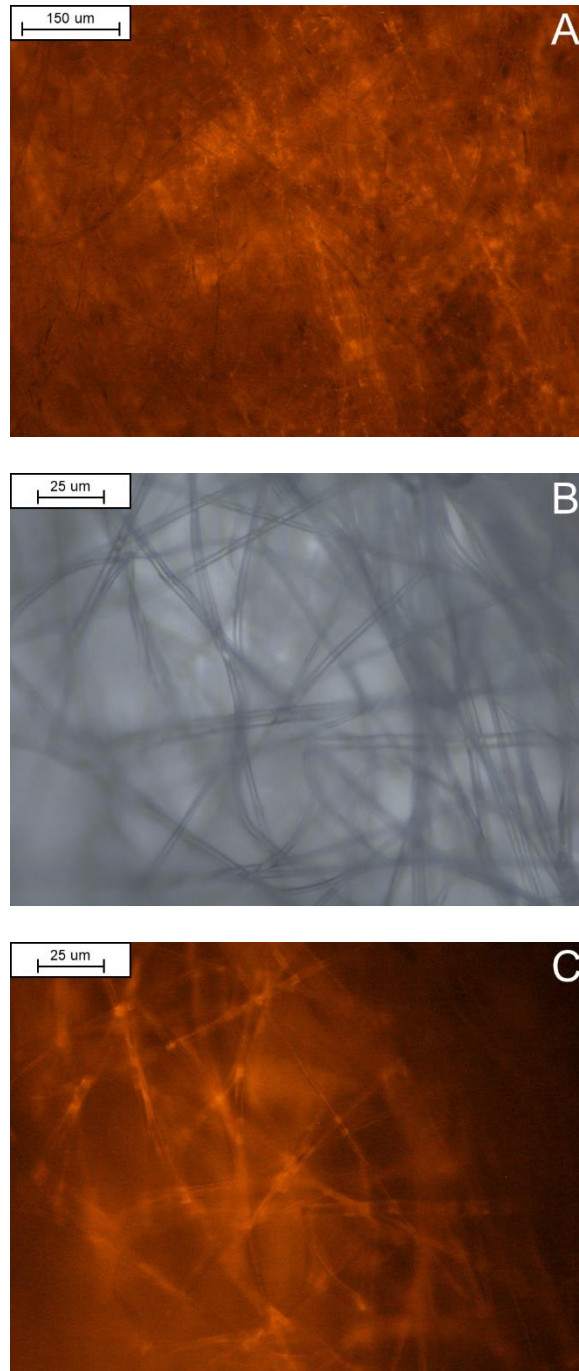


Figure 2.3: Fluorescence microscopy images of BSA coated nonwovens (A) show at low magnification uniformity of unfolded protein adsorption on fiber surfaces. Individual fibers are shown at high magnification (B) under visible spectrum illumination, and (C) dense coating of individual fibers with protein is demonstrated through excitation of fluorescent dye under TRITC filter.

Throughout the coating process, reference thin film samples on spun-coated silica substrates were used to monitor the evolution of each coating layer. In Figure 2.4 we see the water contact angle of the coating after each phase of deposition. The adsorption of soy protein isolate causes an immediate reduction in contact angle to approximately 45°. This agrees with the proposed hydrophobic interaction binding mechanism, which would result in hydrophilic moieties of the substrate bound protein species being left exposed at the interface. After the subsequent adsorption of polyDADMAC, the surface remains moderately hydrophilic as expected.<sup>35,36</sup> The silica surface is extremely hydrophilic, and therefore exhibits the lowest contact angle of all the coating layers, prior to functionalization with the FOTS molecule, which produces a superhydrophobic surface. These values align with expectations from the literature for a cohesive layer of the appropriate materials, verifying the integrity of the coating process throughout.<sup>16,37,38</sup>

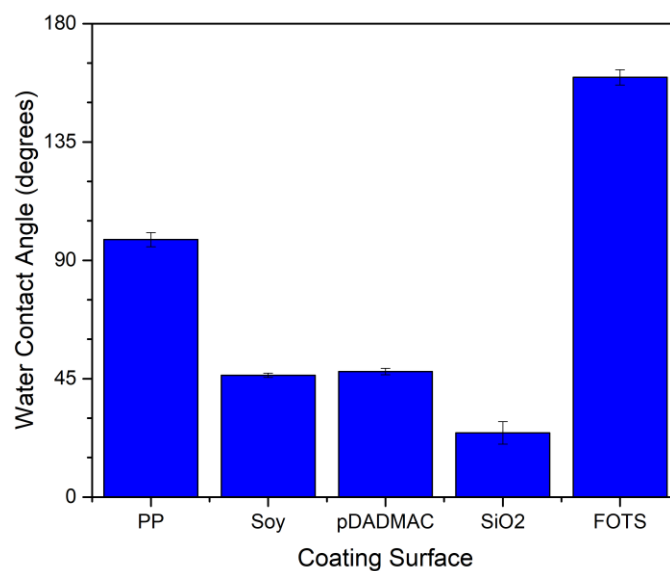


Figure 2.4: Water contact angle of the polymer thin film is monitored throughout the coating process. Contact angles are highly repeatable and representative of the bulk material properties, indicating good uniformity of the coating. Of note are the moderately hydrophobic neat PP surface, hydrophilic silica surface and superhydrophobic FOTS-modified silica of the final product.

Confirmation of the resultant nanoparticle coatings was obtained via SEM. Figure 2.5 shows the completed coating on thin film samples and nonwoven PP substrates. On the flat substrate (top) we see that the coating of nanoparticles on the surface is dense; however, it is also shown at higher magnifications (top-right) that the coating formed on the flat substrate is subject to aggregation of the particles into nanoscale clusters. This creates a heterogeneous, non-uniform surface that may have nontrivial impact on coating properties. Coatings on nonwoven substrates were also investigated in this manner. The low magnification images (bottom-left) illustrate the highly conformal nature of the coatings on fibers. Each fiber is shown to be uniformly coated, with minimal webbing between fibers. The high magnification image (25000X, bottom-right) shows the extremely dense coverage of nanoparticles on the fiber surface. The aggregation of particles which was shown on flat substrates does not present itself on the surface of the fibers. Most significantly, it is clear from these images that the generation of an extremely rough, nanoscale coating, with the potential for reentrant curvature has been generated.

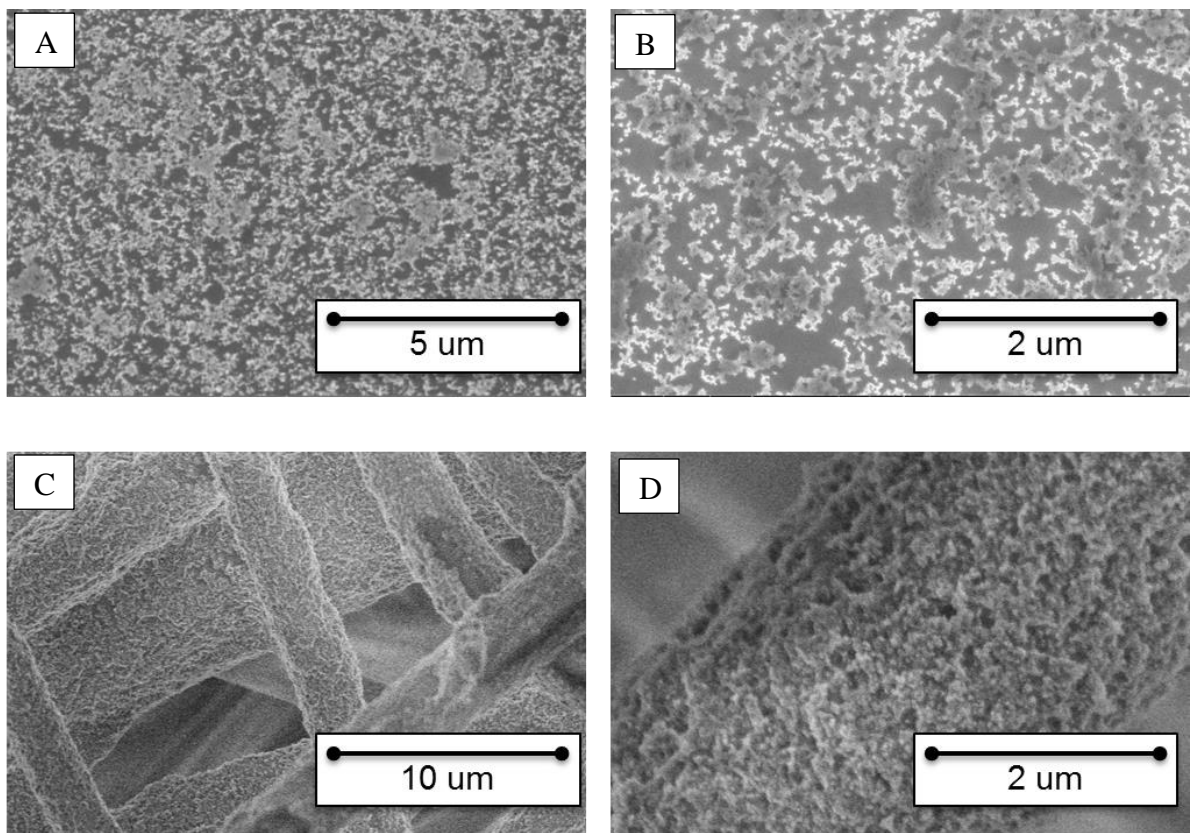


Figure 2.5: SEM images of complete sequentially deposited coatings generating dense fumed silica surface decoration on flat silica surface, at low (A) and high (B) magnification. The same coatings, on nonwoven polypropylene meltblown fabrics, result in highly conformal and dense silica decoration, imaged here at low (C) and high magnification (D).

#### 2.4.2 *Surface chemical composition*

The chart in Figure 2.6, and numerical data in Table 2.1, show the change in surface chemical composition through XPS. Over the course of the formation of the complete coating, each layer of the coating was characterized on the nonwoven substrates. The initial scan (A), shows the composition of the neat PP nonwoven substrate, with a single carbon 1s peak at 285 eV. After the adsorption of soy protein isolate (B), XPS reveals the added presence of oxygen and nitrogen containing molecules at the interface by peaks at 400 eV (N 1s) and 532 (O 1s), characteristic of naturally occurring protein compounds. With the addition of bound pDADMAC onto the soy-coated fibers (C), a small peak at 197 eV (Cl 2p) indicates the added presence of chlorine atoms. The addition of fumed silica nanoparticles generates silicon peaks at 104 eV (Si 2p) and 155 eV (Si 2s), as well as significantly increased intensity of the oxygen peak at 532 eV (O 1s) and 26 eV (O 2s). Lastly, the modification of the silica nanoparticles by the FOTS CVD process introduces significant peaks at 690 eV (F 1s) and 36 eV (F 2s) resulting in a final compositional analysis of approximately 40% C, 15% O, 9% Si, 2% N, and 34% F. This final composition, due to its deviation from the structure of the pure FOTS molecule, illustrates the heterogeneity of the coating within the penetration depth of XPS. As each layer is composed of various geometries and thicknesses, at each stage of this XPS analysis it was clear that scans were sensitive to the presence of prior layers and the compositions calculated represent this sensitivity.

Table 2.1: Atomic composition values of coating after each processing step as measured by XPS.

	<b>C</b>	<b>O</b>	<b>N</b>	<b>Cl</b>	<b>Si</b>	<b>F</b>
<b>Neat PP</b>	99	1	0	0	0	0
<b>Soy Isolate</b>	78	15	7	0	0	0
<b>pDADMAC</b>	77	13	9	2	0	0
<b>Fumed Silica</b>	53	31	2	4	11	0
<b>FOTS</b>	43	16	3	0	6	32

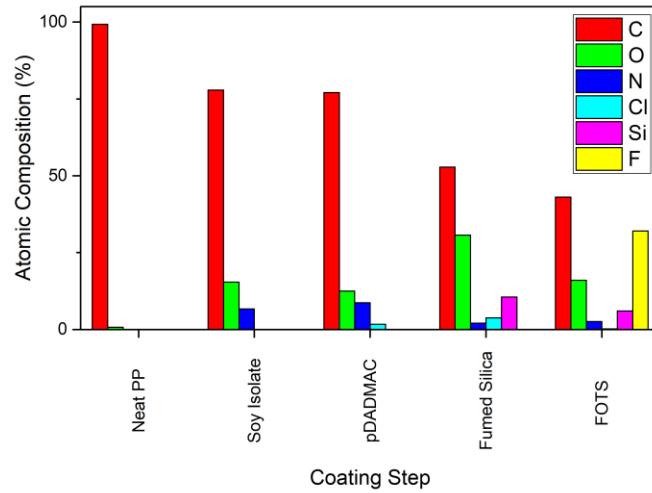


Figure 2.6: Changes in atomic composition of nonwoven coating after each sequentially deposited coating step as measured by XPS.

### 2.4.3 *Wetting with fluids of different surface tensions*

Contact angles of a range of fluids on both flat and nonwoven substrates were tested. In order to best illustrate the impact of both the nonwoven geometry and the FOTS coating on the apparent contact angle of the solvents, three substrates were evaluated. Neat PP thin films were prepared on silicon wafers to establish a baseline contact angle for the solvent. Coated thin films resulting in a FOTS modified 2D surface demonstrate the impact of the change in surface energy alone on the resultant contact angle of the solvent. Coated nonwovens illustrate the impact of hierarchical roughness by comparing the solvent apparent contact angle and the true contact angle on the flat substrate with the same chemistry.

The resulting data from these tests, shown in Figure 2.7, shows that there is a significant improvement to the repellency behavior of the substrate due to changes in both surface energy and morphology as a result of the coating system. Surface chemistry of course plays a critical role; in several cases solvents which completely wetted a neat PP surface had contact angles of  $45^\circ$  or more after coating. Roughness, as expected, plays a critical role in determining repellency. In the case of water, which PP readily repels prior to coating (contact angle of  $\sim 140^\circ$  on nonwoven substrate), the FOTS chemistry provided additional benefits as far as repellency, increasing apparent contact angles up to  $150^\circ$ . Low challenge solvents such as ethylene glycol (47.7 mN/m) and ethylene glycol-water mixtures (between 50 and 65 mN/m) showed significant gains in repellency due to the introduction of both hierarchical roughness and changing surface chemistry. The introduction of the FOTS chemistry was similarly significant to the repellency of more challenging solvents, though efficacy of the treatment varied more greatly from liquid to liquid. Oleophobicity toward mineral oil (30 mN/m) was

drastic, resulting in overall increase of contact angle from  $13^\circ$  (for flat PP substrate) to  $117^\circ$  (for FOTS coated nonwoven substrate).

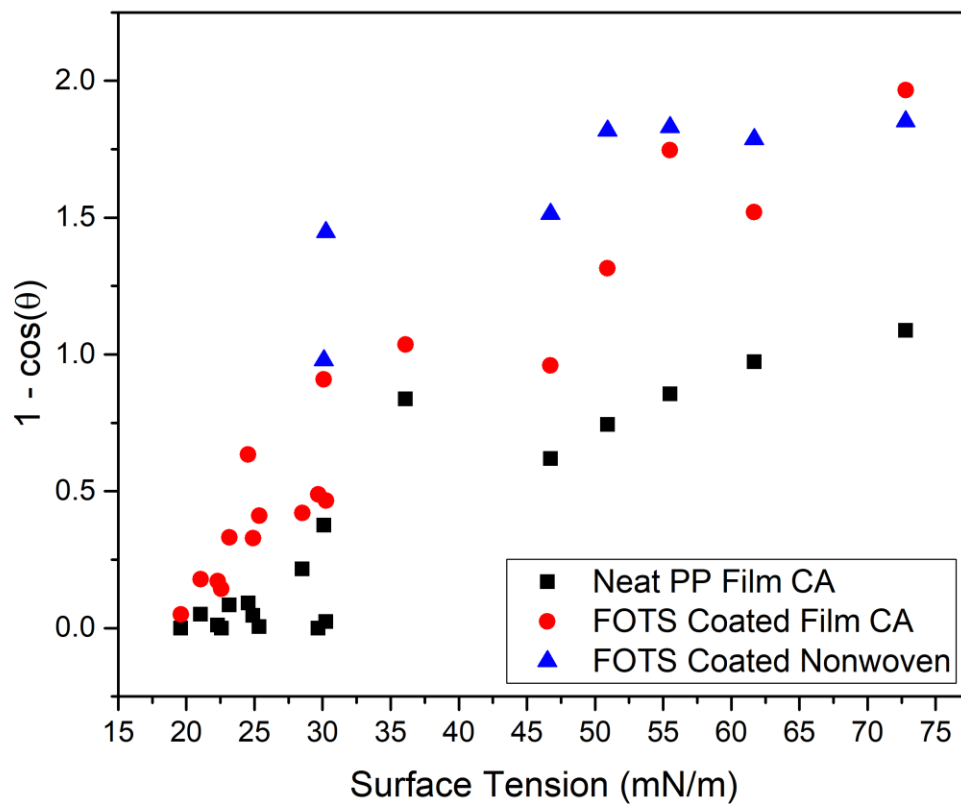


Figure 2.7: Contact angle linearized as  $1 - \cos(\theta)$  for a range of test fluids and mixtures. Contact angles shown were measured on: control substrates (neat PP, black); flat, coated thin-film substrates (red); and coated nonwoven mats (blue). Below surface tension values of 30 mN/m apparent contact angles on nonwoven substrates were unmeasurable due to droplet wicking.

Alcohol repellency proved to be significantly more challenging. IPA repellency of neat PP was minimal, having an average contact angle of  $18^\circ$ , comparable to the contact angle of mineral oil. However, upon coating the FOTS surface only yielded a 2x increase in contact angle to  $35^\circ$ . As a result, the additional repellency afforded by hierarchical roughness due to the nonwoven substrate was not sufficient to significantly increase contact angle. As shown in Figure 2.7, for IPA and other low surface tension fluids, when the apparent contact angle approaches  $90^\circ$  or less, droplets wick through the substrate and apparent contact angle becomes unmeasurable.

While the requirements for achieving true omniphobicity (contact angle of  $>90^\circ$  with all fluids) are not met by these results, many advantages of this method are worth noting. The large majority of omniphobic surfaces reported in the literature require either the use of labor intensive microfabrication methods for the creation of reentrant nanostructures<sup>39,40</sup> or to synthesize molecules unavailable for industrial use.<sup>41,42</sup> With this method, we achieve significant increases in contact angle against a wide range of fluids while utilizing facile coating methods and commercially available components. This is illustrated effectively in Figure 2.8. Here, three surface preparations are represented in schematic form, and paired with their respective contact angles for a sessile droplet of mineral oil. Mineral oil is an example of a challenging fluid to repel, due to its low surface tension of 31 mN/m. As such, the static contact angle of mineral oil on a neat PP thin film substrate was shown to be very small, approximately  $10^\circ$ . However, after the application of the proposed, sequentially deposited surface coating, the static contact angle of mineral oil on the flat substrate increased to  $60^\circ$ . Further improvement still was shown for nonwoven web substrates, where the porous web structure and low surface energy of the FOTS modified surface together yield a chemically

heterogeneous interface. The result is a highly repellent nonwoven substrate, exhibiting an apparent contact angle with mineral oil of  $120^\circ$ .

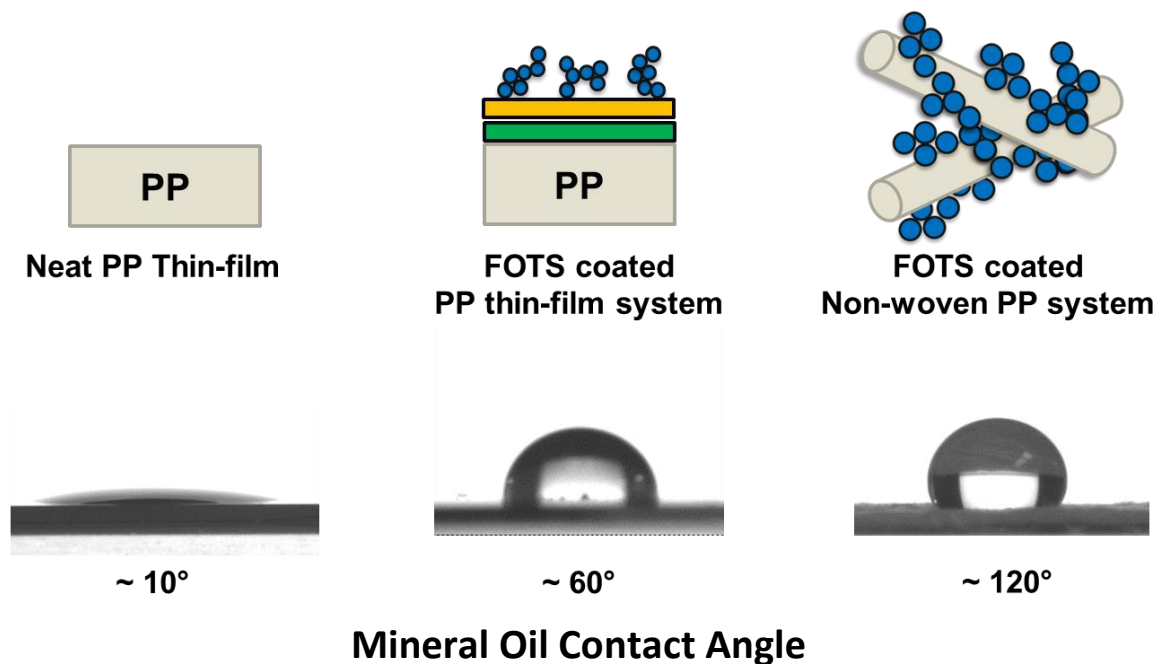


Figure 2.8: Schematics of test substrates with contact angle of mineral oil on neat PP thin film substrates (left), FOTS modified coating of PP thin film substrates (center) and FOTS modified coating of nonwoven PP substrates (right).

While wicking of extremely challenging fluids such as isopropanol (21.1 mN/m), octane (22.6 mN/m) and hexadecane (29.7 mN/m) prevents the demonstration of similar improvements to apparent contact angles on nonwoven substrates, significantly improved repellency was observed on flat substrates nonetheless. When comparing results between flat, neat PP substrates and those which have been prepared with the FOTS coating, it was found that the isopropanol contact angle improved from 18.2° to 34.8°, a 91% improvement. More significant is the result observed for octane and hexadecane, which both wet neat PP completely (~0° contact angle), but exhibit contact angles of 31.1° and 59.2° respectively on the treated surface. This is a promising result which indicates that many extremely challenging fluids could be repelled by similar compositions with only minor optimizations. Rougher surfaces, generated through the use of larger fumed silica particles, mixtures of large and small particles, or through a multilayered sequential deposition could have beneficial effects on observed contact angles for all fluids. Additional optimizations to the nonwoven fabric such as fiber size, fiber shape, or web solidity would likely have further beneficial effects as well and could be a worthwhile are for further research.

## 2.5 *Conclusions*

In this work, we have demonstrated the use of self-assembly techniques to modify highly inert polyolefinic substrates. The extremely low surface energy molecule, FOTS, was successfully grafted onto the completed coating, yielding nonwoven substrates which exhibit highly repellent surface behavior. It has been shown that these coatings increase the contact angle of a wide range of solvents due to the combination of highly fluorinated surface chemistry and multi-scale “hierarchical” roughness, when used to coat nonwoven substrates. Though extremely low surface tension fluids do not show a measurable apparent contact angle on the

nonwoven surfaces tested, it is clear that by further optimizing the chemistry and scale of the geometries involved that improvements may be made toward the achievement of truly superoleophobic surfaces and increased alcohol repellency.

## 2.6 Works Cited

- 1 Baxter, S.; Cassie, a. B. D. The Water Repellency of Fabrics and a New Water Repellency Test. *J. Text. Inst. Trans.* **1945**, *36* (4), T67–T90.
- 2 Cassie, A.; Baxter, S. Wettability of Porous Surfaces. *Trans. Faraday Soc.* **1944**, No. 5, 546–551.
- 3 Choi, W.; Tuteja, A.; Chhatre, S.; Mabry, J. M.; Cohen, R. E.; McKinley, G. H. Fabrics with Tunable Oleophobicity. *Adv. Mater.* **2009**, *21* (21), 2190–2195.
- 4 Gao, L.; McCarthy, T. J. The “Lotus Effect” Explained: Two Reasons Why Two Length Scales of Topography Are Important. *Langmuir* **2006**, *22* (7), 2966–2967.
- 5 Gao, L.; McCarthy, T. J. “Artificial Lotus Leaf” prepared Using a 1945 Patent and a Commercial Textile. *Langmuir* **2006**, *22* (14), 5998–6000.
- 6 Feng, L.; Li, S.; Li, Y.; Li, H.; Zhang, L.; Zhai, J.; Song, Y.; Liu, B.; Jiang, L.; Zhu, D. Super-Hydrophobic Surfaces: From Natural to Artificial. *Adv. Mater.* **2002**, *14* (24), 1857–1860.
- 7 Tuteja, A.; Choi, W.; Mckinley, G. H.; Cohen, R. E.; Rubner, M. F. Design Parameters for Superhydrophobicity and Superoleophobicity. *MRS Bull.* **2008**, *33* (August), 752–758.
- 8 Price, D. (Price H. C. Spunmelt Polypropylene - The Leading Global Technology for Nonwoven Supply and Demand. *Nonwovens Industry.* 2016, pp 1–2.
- 9 Garbassi, F.; Morra, M.; Occhiello, E. *Polymer Surfaces: From Physics to Technology*; West Sussex, England, 1998.
- 10 Jois, Y. H. R.; Harrison, J. B. Modification of Polyolefins: An Overview. *J. Macromol. Sci. Part C Polym. Rev.* **1996**, *36* (3), 433–455.
- 11 Wei, Q.; Becherer, T.; Angioletti-Uberti, S.; Dzubiella, J.; Wischke, C.; Neffe, A. T.; Lendlein, A.; Ballauff, M.; Haag, R. Protein Interactions with Polymer Coatings and Biomaterials. *Angew. Chemie Int. Ed.* **2014**, n/a-n/a.
- 12 Salas, C.; Rojas, O. J.; Lucia, L. a; Hubbe, M. a; Genzer, J. Adsorption of Glycinin and  $\beta$ -Conglycinin on Silica and Cellulose: Surface Interactions as a Function of Denaturation, pH, and Electrolytes. *Biomacromolecules* **2012**, *13* (2), 387–396.
- 13 Salas, C.; Genzer, J.; Lucia, L. a; Hubbe, M. a; Rojas, O. J. Water-Wettable Polypropylene Fibers by Facile Surface Treatment Based on Soy Proteins. *ACS Appl. Mater. Interfaces* **2013**, *5* (14), 6541–6548.
- 14 Liu, X.; Goli, K. K.; Genzer, J.; Rojas, O. J. Multilayers of Weak Polyelectrolytes of Low and High Molecular Mass Assembled on Polypropylene and Self-Assembled Hydrophobic Surfaces. *Langmuir* **2011**, *27* (8), 4541–4550.
- 15 Goli, K. K.; Rojas, O. J.; Genzer, J. Formation and Antifouling Properties of Amphiphilic Coatings on Polypropylene Fibers. *Biomacromolecules* **2012**, *13* (11), 3769–3779.
- 16 Goli, K. K.; Rojas, O. J.; Ozçam, a E.; Genzer, J. Generation of Functional Coatings on Hydrophobic Surfaces through Deposition of Denatured Proteins Followed by Grafting from Polymerization. *Biomacromolecules* **2012**, *13* (5), 1371–1382.
- 17 Castro, C.; Zuluaga, R.; Putaux, J.-P.; Osorio, M.; Caro, G.; Rojas, O.; Gañán, P. In Situ Self-Assembly and Hydrophobization of Gluconacetobacter Bacterial Cellulose. In *2013 Tappi International Conference on Nanotechnology for Renewable Materials*; 2013.

- 18 Silva, S. S.; Oliveira, J. M.; Benesch, J.; Caridade, S. G.; Mano, J. F.; Reis, R. R. Hybrid Biodegradable Membranes of Silane-Treated Chitosan/soy Protein for Biomedical Applications. *J. Bioact. Compat. Polym.* **2013**, *28* (4), 385–397.
- 19 Vallet-Regí, M.; Colilla, M.; González, B. Medical Applications of Organic–inorganic Hybrid Materials within the Field of Silica-Based Bioceramics. *Chem. Soc. Rev.* **2011**, *40* (2), 596–607.
- 20 Yoneda, M.; Terai, H.; Imai, Y.; Okada, T.; Nozaki, K.; Inoue, H.; Miyamoto, S.; Takaoka, K. Accelerated Repair of a Bone Defect with a Synthetic Biodegradable Bone-Inducing Implant. *J. Orthop. Sci.* **2006**, *11* (5), 505–511.
- 21 Simchi, A.; Tamjid, E.; Pishbin, F.; Boccaccini, A. R. Recent Progress in Inorganic and Composite Coatings with Bactericidal Capability for Orthopaedic Applications. *Nanomedicine Nanotechnology, Biol. Med.* **2011**, *7* (1), 22–39.
- 22 Messori, M.; Toselli, M.; Pilati, F.; Fabbri, E.; Fabbri, P.; Pasquali, L.; Nannarone, S. Prevention of Plasticizer Leaching from PVC Medical Devices by Using Organic-Inorganic Hybrid Coatings. *Polymer (Guildf)*. **2004**, *45* (3), 805–813.
- 23 Doraiswamy, A.; Jin, C.; Narayan, R. J.; Mageswaran, P.; Mente, P.; Modi, R.; Auyeung, R.; Chrisey, D. B.; Ovsianikov, A.; Chichkov, B. Two Photon Induced Polymerization of Organic-Inorganic Hybrid Biomaterials for Microstructured Medical Devices. *Acta Biomater.* **2006**, *2* (3), 267–275.
- 24 Kim, S. Y.; Kim, B. H. Silica Decorated on Porous Activated Carbon Nanofiber Composites for High-Performance Supercapacitors. *J. Power Sources* **2016**, *328*, 219–227.
- 25 Gómez-Romero, P.; Chojak, M.; Cuentas-Gallegos, K.; Asensio, J. A.; Kulesza, P. J.; Casañ-Pastor, N.; Lira-Cantú, M. Hybrid Organic-Inorganic Nanocomposite Materials for Application in Solid State Electrochemical Supercapacitors. *Electrochem. commun.* **2003**, *5* (2), 149–153.
- 26 Ren, Y.; Zhang, Y.; Zhao, J.; Wang, X.; Zeng, Q.; Gu, Y. Phosphorus-Doped Organic–inorganic Hybrid Silicon Coating for Improving Fire Retardancy of Polyacrylonitrile Fabric. *J. Sol-Gel Sci. Technol.* **2017**, *82* (1), 280–288.
- 27 Jing, J.; Zhang, Y.; Tang, X.; Zhou, Y.; Li, X.; Kandola, B. K.; Fang, Z. Layer by Layer Deposition of Polyethylenimine and Bio-Based Polyphosphate on Ammonium Polyphosphate: A Novel Hybrid for Simultaneously Improving the Flame Retardancy and Toughness of Polylactic Acid. *Polym. (United Kingdom)* **2017**, *108*, 361–371.
- 28 Christopher, G.; Kulandainathan, M. A.; Harichandran, G. Biopolymers Nanocomposite for Material Protection: Enhancement of Corrosion Protection Using Waterborne Polyurethane Nanocomposite Coatings. *Prog. Org. Coatings* **2016**, *99*, 91–102.
- 29 Fabra, M. J.; López-Rubio, A.; Lagaron, J. M. Use of the Electrohydrodynamic Process to Develop Active/bioactive Bilayer Films for Food Packaging Applications. *Food Hydrocoll.* **2016**, *55*, 11–18.
- 30 Bari, S. S.; Chatterjee, A.; Mishra, S. Biodegradable Polymer Nanocomposites: An Overview. *Polym. Rev.* **2016**, *56* (2), 287–328.
- 31 Fernández-Solis, C.; Erbe, A. Waterborne Chitosan–Epoxy-silane Hybrid Pretreatments for Corrosion Protection of Zinc. *Biointerphases* **2016**, *11* (2), 21001.
- 32 Yang, H.; Deng, Y. Preparation and Physical Properties of Superhydrophobic Papers. *J. Colloid Interface Sci.* **2008**, *325* (2), 588–593.

- 33 Song, J.; Liang, J.; Liu, X.; Krause, W. E.; Hinestroza, J. P.; Rojas, O. J. Development and Characterization of Thin Polymer Films Relevant to Fiber Processing. *Thin Solid Films* **2009**, *517* (15), 4348–4354.
- 34 Langdon, B. B.; Mirhossaini, R. B.; Mabry, J. N.; Sriram, I.; Lajmi, A.; Zhang, Y.; Rojas, O. J.; Schwartz, D. K. Single-Molecule Resolution of Protein Dynamics on Polymeric Membrane Surfaces: The Roles of Spatial and Population Heterogeneity. **2015**.
- 35 Deng, Y. L.; Abazeri, M. Contact Angle Measurement of Wood Fibers in Surfactant and Polymer Solutions. *Wood Fiber Sci.* **1998**, *30* (2), 155–164.
- 36 Yu, L.; Yuan, W.; Liu, X.; Xu, X.; Ruan, S. Asymmetry of the Free-Standing Polyelectrolyte Multilayers. *Appl. Surf. Sci.* **2017**, *422*, 46–55.
- 37 Williams, R.; Goodman, A. M. Wetting of Thin Layers of SiO<sub>2</sub> by Water. *Appl. Phys. Lett.* **1974**, *25* (10), 531–532.
- 38 Wang, B.; Feng, J.; Gao, C. Surface Wettability of Compressed Polyelectrolyte Multilayers. *Colloids Surfaces A Physicochem. Eng. Asp.* **2005**, *259* (1–3), 1–5.
- 39 Tuteja, A.; Choi, W.; Mabry, J. M.; McKinley, G. H.; Cohen, R. E. Robust Omniphobic Surfaces. *Proc. Natl. Acad. Sci. U. S. A.* **2008**, *105* (47), 18200–18205.
- 40 Domingues, E.; Arunachalam, S.; Mishra, H. Doubly Reentrant Cavities Prevent Catastrophic Wetting Transitions on Intrinsically Wetting Surfaces. *ACS Appl. Mater. Interfaces* **2017**, acsami.7b03526.
- 41 Meuler, A. J.; Chhatre, S. S.; Nieves, A. R.; Mabry, J. M.; Cohen, R. E.; McKinley, G. H. Examination of Wettability and Surface Energy in Fluorodecyl POSS/polymer Blends. *Soft Matter* **2011**, *7* (21), 10122.
- 42 Srinivasan, S.; Chhatre, S. S.; Mabry, J. M.; Cohen, R. E.; McKinley, G. H. Solution Spraying of Poly(methyl Methacrylate) Blends to Fabricate Microtextured, Superoleophobic Surfaces. *Polymer (Guildf)*. **2011**, *52* (14), 3209–3218.

2.7 Appendix – Supplementary Material

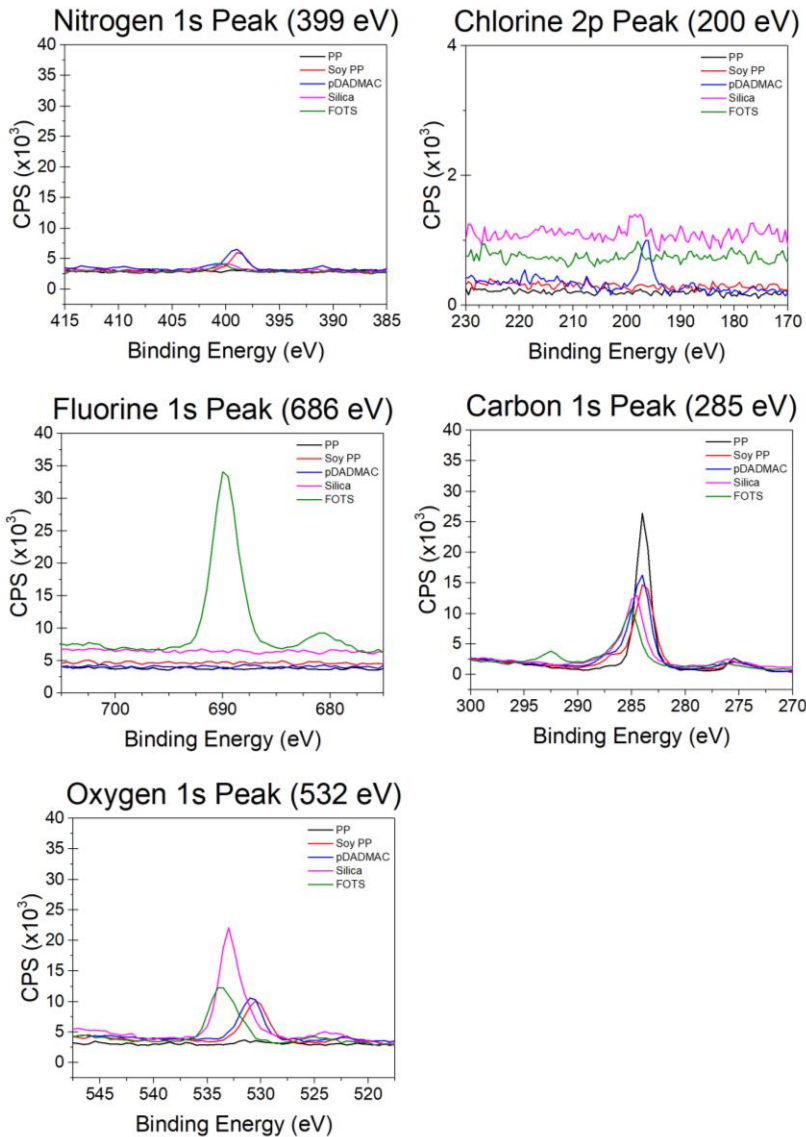


Figure 2.9: Isolated characteristic peaks for elements of interest from XPS survey scans of sequentially coated PP nonwovens. In each sub-plot the XPS signal for each peak is shown with multiple curves. Color of the curves indicates the surface layer of the coating: neat polypropylene with no coating (black), soy coated polypropylene (red), polyDADMAC surface over preceding layers (blue), fumed silica over preceding layers (magenta), and FOTS modified complete coating (green).

**CHAPTER 3. CHARACTERIZATION OF FLUOROCHEMICAL MELT ADDITIVE  
MIGRATION FOR ALCOHOL REPELLENCY IN ELECTRET FILTER  
MATERIALS**

*Joseph H. Lavoie<sup>1</sup>, Orlando Rojas<sup>1,3</sup>, Saad Khan<sup>1</sup>, and Eunkyong Shim<sup>2</sup>*

*<sup>1</sup>Department of Chemical Engineering, North Carolina State University, Raleigh, NC*

*<sup>2</sup>College of Textiles, North Carolina State University, Raleigh, NC*

*<sup>3</sup>Department of Forest Biomaterials, Aalto University, Espoo, Finland*

*3.1 Abstract*

When customizing the properties of polymer surfaces, the use of bulk polymer melt additives is a facile, industrially relevant method for many different applications. These melt additives, when blended with polymers prior to melt spinning, migrate to the fiber surface and influence surface energy and therefore repellency behavior. While the use of bulk polymer melt additives to impart hydrophilicity or oleophobicity is well studied, the impact of the fiber formation process on additive migration and resultant repellency of nonwoven media products is not fully characterized. In this work we have produced meltblown nonwovens containing fluorochemical melt additive, and established methods for their characterization. Fiber formation was monitored through the use of Scanning Electron Microscopy (SEM) by characterizing changes in median fiber size due to changing processing parameters and additive content. The additive migration process was quantitatively evaluated by X-ray Photoelectron Spectroscopy (XPS) and time-of-flight secondary ion mass spectroscopy (ToF-SIMS). Contact angle goniometry was used to evaluate apparent contact angles of isopropyl alcohol solutions on nonwoven fiber mats. Migration of additives was monitored over several

months, allowing for the evaluation of compositional changes over multiple timescales. This changing composition was then related to repellency of alcohol solutions via contact angle data. By collecting composition and contact angle data in tandem, it was found that for the samples tested a fluorine to carbon ratio of 0.35 was sufficient to prevent wicking of isopropanol droplets. In other tests it was demonstrated that migration of additives is key to performance of samples with low additive loadings, and that these phenomena are heavily influenced by many nonwoven manufacturing parameters including fiber size, die-to-collector distance, and polymer resin melt flow rates.

### *3.2 Introduction*

Modification of polymer interfaces for surface energy control is a critical challenge for many industries where liquid compatibility or repellency is required. Many different approaches have been established in the literature for various applications, whether they require hydrophilicity/phobicity, oleophilicity/phobicity, or more specific targeted wetting behavior. Such approaches include surface coatings,<sup>1-4</sup> direct chemical modification, and the inclusion of bulk additives.<sup>5</sup> Depending upon the specific chemistry of the application, each approach has significant advantages and disadvantages which might influence the design process. The use of surface coatings or chemical modification after manufacturing of the nonwoven media have been demonstrated to varying levels of effectiveness; however, these methods require additional processing steps during the manufacturing process, and depending upon the chemistry used can pose additional concerns such as requiring the use of harsh chemicals, limited durability of coatings, and others.

In the case of nonwoven polymer textiles, the considerations of processing speed, cost effectiveness, and uniformity place tight constraints on the surface functionalization process. Because of this, the use of bulk polymer melt additives have been established as a facile, industrially relevant method for surface energy control in extruded fibers.<sup>6-8</sup> Melt additives, which are blended with the base polymer during the compounding and extrusion process, are immiscible in the polymer bulk to some degree and therefore segregate to the surface, influencing interfacial properties.<sup>9,10</sup> The process of surface segregation of partially immiscible polymer mixtures is well understood in the literature, whether considering the formation of phase separated block copolymer mixtures<sup>11-13</sup> or surface active small molecule or nanoparticle additives<sup>14-16</sup>, though the large majority of these studies were performed on films. Of those studies performed on fibers, very few are conducted on meltblown nonwoven systems, as research is most frequently conducted on small scale fiber production systems, such as electrospun fiber mats.<sup>17-19</sup> While the research on electrospun fibers is of great value, the difference between fibers formed through solvent casting and melt-spinning processes is not insignificant; and as will be shown in the results from this effort, fiber size has significant impact on the migration process.

Due to the low concentrations of additive used in these applications, surface concentrations of the additive can be significantly elevated compared to the bulk, thereby achieving the desired functionality without significantly changing the bulk polymer properties. This phenomenon allows for the creation of fiber surfaces with controlled wettability useful in many industries, including protective medical garments, consumer textile garments, oil spill cleanup materials, self-cleaning materials, and filters.<sup>20,21</sup>

There are commercially available bulk polymer additives, including those for increased repellency toward various liquids.<sup>22-25</sup> While these products have demonstrated effectiveness, questions remain surrounding the observed migration phenomenon of surface active small molecules in polymer matrices. Though the process of migration of low surface energy additive species is well known, the impact of additive migration and correlation of nonwoven meltblown processing parameters on resultant product design has not been fully characterized in the literature.<sup>26,27</sup> In this work we seek to explore the interconnected considerations of additive loading and migration effects with traditional nonwoven manufacturing parameters and their impacts upon repellency of nonwoven products.

### 3.3 *Experimental*

#### 3.3.1 *Materials & Methods.*

Nonwoven substrates were prepared from metallocene homopolymer PP of two different melt flow rates (MFR) (MF650W, 500 MFR and MF650X, 1200 MFR, LyondellBasell, Houston, TX) and a small molecule, fluorochemical melt additive “HydRepel A-204M” (Goulston Technologies Inc., Monroe, NC) at 20% concentration in 1200 MFR polypropylene masterbatch. Both were provided by The Nonwovens Institute at North Carolina State University. Research grade, 99.9% pure isopropyl alcohol (IPA) was obtained from Sigma Aldrich (St. Louis, MO) for alcohol repellency testing.

#### 3.3.2 *Meltblown Nonwoven Manufacturing*

Samples for experimentation were manufactured on both a small scale research line and a pilot scale manufacturing line. The first set of samples were prepared using the Biax Meltblown Research Line with a 38 cm width Biax die with a total of 368 holes. The die temperature was

held at 220 °C, and high pressure air for fiber attenuation at the die was heated to 180 °C. LyondellBasell MF650W, 500 MFR polypropylene was mixed with additive containing masterbatch pellets, then loaded into the hopper of the Biax system at designated concentrations. As shown in Table 3.1, processing parameters including air pressure, polymer throughput, and die-to-collector distance were varied to assess their impact upon additive performance and migration. The second set of samples were prepared using the Reicofil Meltblown Pilot Line with a 1.3 meter, 35 hole per inch (HPI) Exxon die and polypropylene polymer resins of two melt flow rates.

Of the samples prepared using the Reicofil system, the first study, shown in Table 3.2, was conducted with varying die-to-collector distance and additive concentrations, in order to more thoroughly understand the influence of these parameters on repellency performance of nonwoven samples in an industrially relevant manufacturing process.

The second study, detailed in Table 3.3, utilized a 1200 MFR polypropylene resin, compared to the 500 MFR polymer used in the previous study. The change in flow rate of these resins is largely attributed to changing molecular weight of the polymer; this allows for the characterization of molecular weight effects on the migration and repellency behavior of the resulting nonwoven webs. Run parameters were constrained to match the previous, 500 MFR manufacturing run wherever possible in order to enable comparison between the two materials, however necessary adjustments to die and air temperature were made to ensure that high quality and representative samples were produced. Air flow rate was also varied between the 1100 m<sup>3</sup>/h set point used in the first study and a lower 800 m<sup>3</sup>/h value to establish a wider range of fiber diameters among the samples generated. In order to limit the size of the design of experiment for the high MFR samples, additive concentration was limited to 1.6% or lower,

as this was the region that had shown the most significant response to variable processing conditions in the previous study.

Table 3.1: Biax Research Line Conditions

Biax Meltblown Research Line Run Conditions			
Die Temperature	220 °C		
Die Air Temperature	180 °C		
Die Air Pressure	55.2 kPa (8 PSI)	75.8 kPa (11 PSI)	
Throughput	2.4 kg/h	4.5 kg/h	
Die-to-Collector Distance	30 cm	40 cm	
Die	38 cm, 368 holes		
Die Capillary Diameter	508 μm		
Additive Concentration	0.0%	1.2%	1.6%   2.0%

Table 3.2: Reicofil Pilot Line 500 MFR Run Conditions

Reicofil Meltblown Pilot Line Run Conditions						
Polymer	LyondellBasell MF650W (500 MFR)					
Die Temperature	240 °C					
Die Air Temperature	255 °C					
Die Air Flow Rate	1100 m <sup>3</sup> /h					
Throughput	53 kg/h					
Die-to-Collector Distance	15 cm	40 cm				
Die	Exxon (35 HPI)					
Die Capillary Diameter	400 μm					
Additive Concentration	0.0%	0.6%	1.2%	1.6%	2.0%	4.0%

Table 3.3: Reicofil Pilot Line 1200 MFR Run Conditions

Reicofil Meltblown Pilot Line Run Conditions				
Polymer	LyondellBasell MF650X (1200 MFR)			
Die Temperature	220 °C			
Die Air Temperature	235 °C			
Die Air Flow Rate	800 m <sup>3</sup> /h	1100 m <sup>3</sup> /h		
Throughput	53 kg/h			
Die-to-Collector Distance	15 cm	40 cm		
Die	Exxon (35 HPI)			
Capillary Diameter	400 μm			
Additive Concentration	0.0%	0.6%	1.2%	1.6%

### 3.3.3 *X-Ray Photoelectron Spectroscopy*

Surface composition of nonwoven substrates with fluorochemical melt additive were characterized by XPS. A portion of nonwoven web from each experiment were stored in the freezer at -20 °C immediately after manufacturing, effectively stopping additive migration. For samples analyzed with respect to migration time, the reported time is measured as time since removed from the freezer. Migration was allowed to occur on the laboratory benchtop, where conditions were typically 20 °C and 30% relative humidity with moderate variability. Compositional analysis was performed on a SPECS XPS system with PHOIBOS 150 Analyzer at the Analytical Instrumentation Facility (AIF) at NC State University (Raleigh, NC). The analysis was done using a Mg K $\alpha$  x-ray source operated at 300 W (10 kV and 30 mA) with vacuum chamber at room temperature and pressures in the 10<sup>-8</sup> torr range or lower. Survey scans were collected from 0 to 1100 eV and atomic compositions were derived from peak areas using CasaXPS processing software version 2.3.16.

### 3.3.4 *Contact Angle Goniometry*

To evaluate repellency of nonwoven substrates, sessile drop contact angles of water, IPA, and water/isopropanol mixtures were measured using an SEO Phoenix 300 Goniometer (Surface Electro Optics, Suwon City, South Korea). Images were captured by the manufacturer provided frame grabbing software “Image XP”, and contact angle analysis was performed using “ImageJ” image processing software with the “DropSnake” analysis plugin. Due to the porous nature of nonwoven materials, reported contact angles for these materials are apparent contact angles and cannot be directly related to the surface energy of the fiber.

### 3.3.5 *ToF-SIMS*

Cross-sectional images of fiber composition were obtained through the use of the ION-TOF ToF-SIMS instrument at the Analytical Instrumentation Facility (AIF) at NC State University. Bundles of nonwoven fibers and individual fiber samples were encased in an epoxy matrix. The epoxy blocks containing fiber mats were then cut perpendicular to the fiber direction using a microtome to create cross-sections that could be analyzed. Samples composed of nonwoven fiber bundles generated more feature rich images, but in some cases wetting of the bundle interior by the epoxy proved to be infeasible, and for those samples individual fibers were removed from the bundle and encased separately.

### 3.3.6 *Scanning Electron Microscopy*

Fiber diameter was evaluated through the use of scanning electron microscopy. Images were captured on the Verios High Resolution SEM at the AIF. In order to avoid charging of nonwoven samples during imaging, samples were sputter coated with 50 nm of gold using the Hummer II sputter coater at the AIF. Images were captured at 13 nA and 2 kV using the Everhart-Thornley Detector in secondary electron mode, at a working distance of approximately 8 mm to maximize depth of field.

## 3.4 *Results and Discussion*

### 3.4.1 *Fiber Size Analysis*

The first consideration to properly understand the influence of additive content on the fiber formation process was to evaluate the effect of meltblowing processing parameters on fiber diameter. Figure 3.1 compares the effect of process parameters which were controlled during

nonwoven manufacturing on fiber diameters of meltblown samples produced with Biax lab line. Die-to-collector distance is shown to have no impact on the median fiber diameter, as expected. Increased air pressure is shown to decrease fiber diameter due to greater fiber attenuation, and increased polymer throughput yields substantially increased fiber sizes. Most interesting is the top-right chart in Figure 3.1, where the influence of additive concentration on fiber diameter is shown to be negligible. For this reason it is reasonable to assume that small amounts of additive loading would not significantly alter relevant polymer melt properties such as viscosity or crystallization temperature.

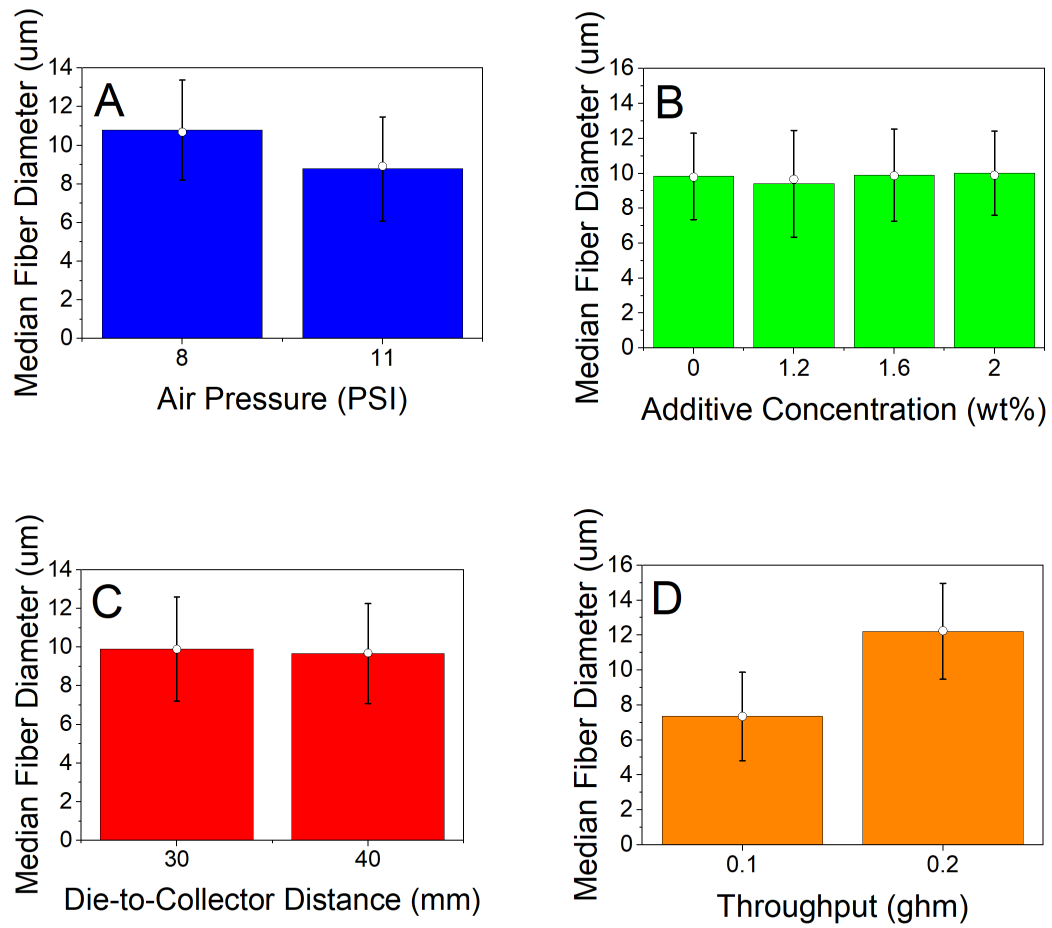


Figure 3.1: Characterization of the influence of processing parameters on resulting nonwoven web formation by median fiber diameter analysis. Median fiber diameter of samples was shown to be independent of additive concentration (B) in the range tested, and to be moderately impacted by air pressure (A) and polymer throughput (D), and unaffected by DCD (C), as expected.

### 3.4.2 Additive surface migration characterization

In an effort to quantitatively track the surface concentration of fluorochemical melt additive in the sample, we utilized XPS and carefully controlled the migration state of the samples being measured. Figure 3.2A demonstrates the quantification of additive migration by XPS through the comparison of two sets of samples: samples which have not experienced any appreciable additive migration post manufacturing (pre-migration, in red), and samples which have been stored at room temperature for six months and can be considered fully migrated (equilibrated, in black). A few principles are clearly illustrated by this analysis. First and foremost, control samples containing only polypropylene and no additive are free from contamination and reliably contain no fluorine down to the detection limit of XPS ( $<0.1$  at%). Second, migration is shown to play a significant role in determining surface fluorine concentration, independent of initial bulk additive content. In each case, the equilibrated samples have demonstrably larger F/C ratio values than the pre-migration samples; however, the magnitude of the increase in fluorine content due to migration is significantly greater when initial bulk additive content is lower. Third, the diminishing effects of additional additive content beyond moderate loadings are observed both before and after migration. This is confirmed in Figure 3.2B, which shows the kinetics of the process over the first 72 hours of migration after manufacturing. Here, once again it is clear that samples containing either 1.6% additive or 2.0% additive exhibit significantly higher surface concentration of additive, but the difference between the two is negligible. While there is some noise in the data (representative error bars are shown on only two points for clarity) it is clear that the sample with the lowest initial additive loading (1.2%) shows relatively rapid increase in surface fluorine content when compared to the higher initial additive loadings which show limited migration on the short time-scales investigated here. This

is most likely due to additive saturation of the interface. As the mechanism for migration is most likely random movement of small molecules within the non-crystalline domains of the PP fiber, increased loading at the interface would significantly inhibit the movement of additional additive molecules to the surface.

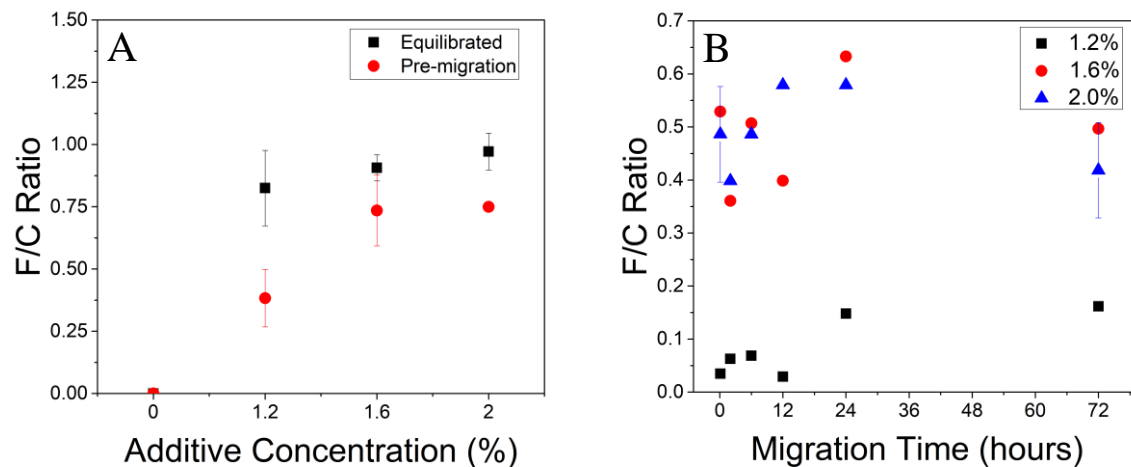


Figure 3.2: Additive containing samples were characterized by XPS to demonstrate, (a) the initial (red) and fully migrated or equilibrated (black) additive distribution states at a range of bulk loading concentrations and (b) migration behavior in fibers containing 1.2% (black), 1.6% (red) or 2.0% (blue) additive over the first 72 hrs post-manufacturing.

### 3.4.3 *Dependence of Repellency Performance on Surface Composition*

The result of increased fluorine content at the surface is invariably increased repellency towards water and alcohol containing solutions. In an effort to elucidate the direct correlation between increased surface content of fluorine containing moieties, contact angle data was collected via sessile drop contact angle goniometry. For this study, we conducted XPS tests where multiple samples from the Biax small scale meltblown line had been permitted to migrate, yielding increased F/C ratio measurements over time. Samples were then tested to determine water and alcohol contact angle values over the same intervals. In this manner, it was possible to determine thresholds for repellency as values in F/C ratio data where droplet wicking ceased and a stable “apparent” contact angle was observed for the substrate. As shown in Figure 3.3, the threshold for repellency is directly correlated with the decrease in surface tension associated with increasing alcohol content of the probing solution. While both pure water and 25 vol% IPA in water solution do not wick through the nonwoven substrate when the surface is effectively pure polypropylene (F/C ratio approaches zero), an associated reduction in the contact angle of the droplet is shown for the lower surface tension, 25% isopropanol solution. Further reduction of the surface tension of the solution through increased isopropanol content causes wicking to occur at low fluorine surface concentrations. A 50% isopropanol solution requires at least 0.16 fluorine atoms per carbon at the interface before wicking is prevented and an apparent contact angle is observed; while a 100% IPA test requires an F/C ratio approaching 0.2 or more before wicking is prevented.

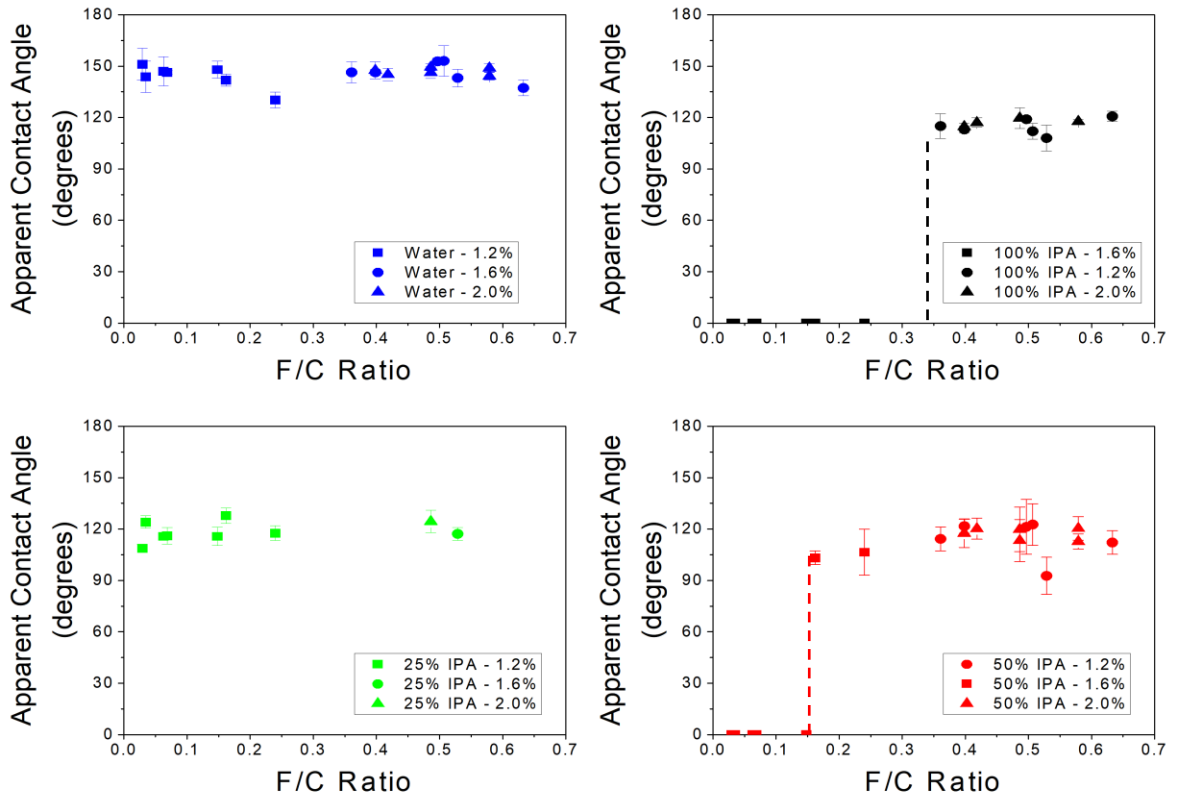


Figure 3.3: Apparent contact angle of isopropanol/water mixtures were measured as a function of surface fluorine content of nonwoven webs. Data was drawn from samples of varying bulk additive concentrations (as indicated by symbol shape according to the inset legends), and each were allowed to migrate to generate a range of samples with increasing F/C ratios. Both pure water (blue) and 25% isopropanol solution (green) droplets were supported by the web without wicking at all F/C ratios, while 50% (red) and pure (black) isopropanol droplets wick through nonwovens with insufficient surface concentration of fluorine, as indicated by dashed lines.

#### 3.4.4 *High-resolution investigation of cross-sectional composition by ToF-SIMS*

We have also developed, for the purpose of characterizing additive distribution, the use of ToF-SIMS on cross-sectional samples of fibers in an epoxy matrix. In these experiments we visualize the concentration of additive within the fiber, and by creating overlays with scans of ions characteristic of the epoxy matrix, understand the impact of migration on composition at the interface. In Figure 3.4, an example of this analysis is shown for Reicofil meltblown samples that have been allowed to fully migrate. The total signal across all analyzed fragments, as well as the individual scans for the characteristic ions for both the fluorocarbon melt additive and epoxy are shown in Figure 3.4A-C. The overlay of the  $F^-$  (green) and  $C_3NO^-$  (yellow) in Figure 3.4D clearly illustrates the migration phenomenon. Here we see significantly increased concentrations of fluorine at the fiber-epoxy interface, and the generation of a depletion zone between the core of the fiber and the surface. This is represented in another way in Figure 3.4E-F where line scans of the characteristic ions have been drawn across fiber cross-sections. In these examples, we again see the sharp contrast between the pure epoxy surrounding the polypropylene fiber, and the fluorine containing, additive-rich surface of the fiber. The sharp decrease in detected counts of  $C_3NO^-$  ions occurs in conjunction with local maxima in detected counts of  $F^-$  ions. Fluorine ion counts decrease for 3-5  $\mu m$  before increasing again through the core of the fiber. The size of the fiber “core,” where additive content as measured by fluorine ion counts remains at levels comparable to that detected at the interface, seems to depend mainly upon the fiber diameter. The depletion zone, formed by the movement of additive molecules to the surface without equivalent replacement by migration from the bulk, appears to remain constant, independent of fiber diameter.

In contrast, when migration is not allowed to occur, the segregation of additive to the surface is only observed in the smallest fibers, as shown Figure 3.5. These pre-migration samples, prepared through the encapsulation of individual fibers as opposed to the bundled fibers shown in Figure 3.4, do not exhibit the formation of a depletion zone after surface segregation of additive in moderately sized fibers more than a few  $\mu\text{m}$  in diameter. Instead, we observe the same core additive containing bulk polymer, without the interfacial fluorine content shown in the previous example.

The difference between the pre-migration and fully migrated samples illustrated in Figure 3.4 and Figure 3.5 corroborates the surface changes observed through XPS, and yields additional insight into the changing internal composition of the fiber.

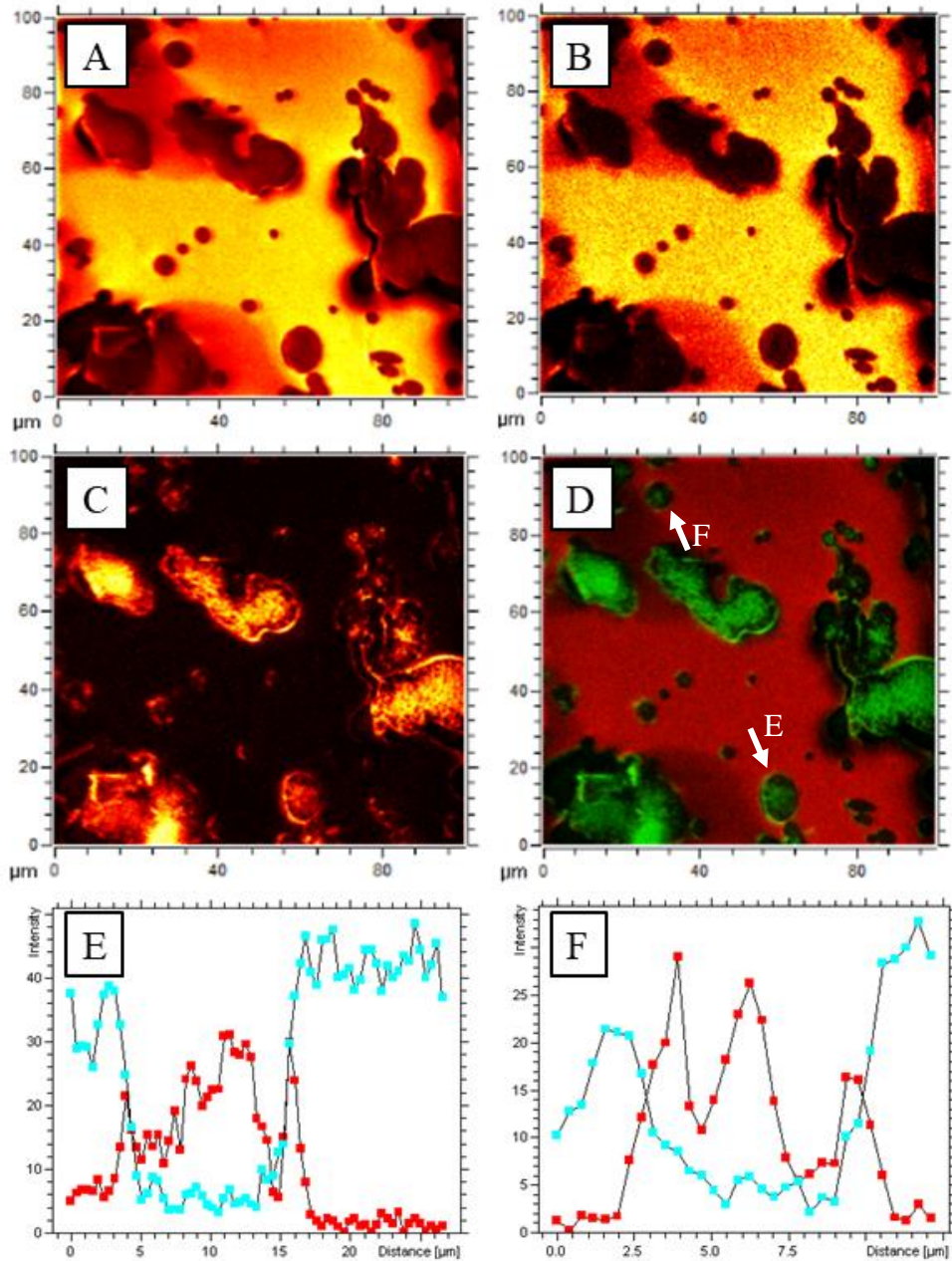


Figure 3.4: Cross-sectional view of migrated, low DCD, Reicofil nonwovens with 4 wt% additive (F/C ratio  $\approx$  0.56) by ToF-SIMS. (A) Total ToF-SIMS signal across all ions, (B) Concentration of characteristic epoxy matrix ion, (C) Concentration of fluorine (characteristic additive ion), (D) Overlay of characteristic epoxy and additive scans (F<sup>-</sup> in green, C<sub>3</sub>NO<sup>-</sup> in yellow), (E) and (F) composition line scans of fibers (as indicated in D), F<sup>-</sup> (red) and C<sub>3</sub>NO<sup>-</sup> (blue). The concentration of fluorine at the fiber surface observed here as an outline or halo structure is a clear indication of significant migration of the surface. Also demonstrated here is the formation of a depletion zone with significantly lower fluorine content in the volume of fiber between the core and surface.

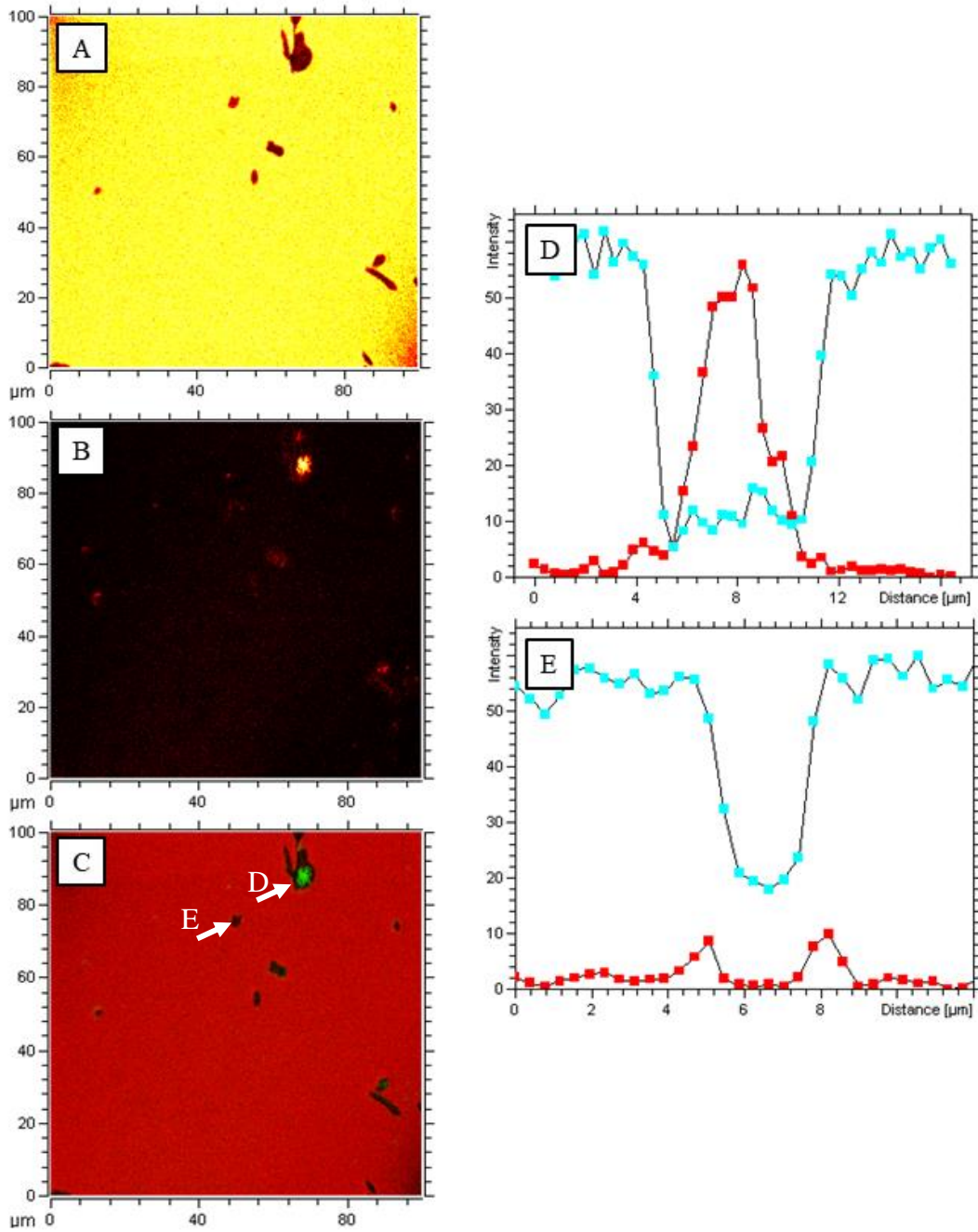


Figure 3.5: Cross-sectional view of un migrated, low DCD, Reicofil nonwovens with 4 wt% additive (F/C ratio  $\approx 0.21$ ) by ToF-SIMS. (a) Concentration of fluorine (characteristic additive ion) (b) Overlay of characteristic epoxy and additive scans ( $\text{F}^-$  in green,  $\text{C}_3\text{NO}^-$  in yellow) (c) Concentration of characteristic epoxy matrix ion, (d) and (e) composition line scans of fibers (as indicated in C),  $\text{F}^-$  (red) and  $\text{C}_3\text{NO}^-$  (blue). The concentration of fluorine at the fiber surface is only observed here in the case of very small fibers with short migration distances.

### 3.4.5 *Effects of processing parameters on migration*

#### 3.4.5.1 *Die-to-collector distance*

While migration time is a significant driving force for the changing composition of the surface, it is clear that other factors also play a role, including fiber size and certain manufacturing parameters. Among the parameters tested, the most significant impact on migration state was found to be the die-to-collector distance used during the manufacturing process. This is shown in Figure 3.6 where unmigrated samples manufactured at 40 cm DCD exhibited as much as a three-fold increase in initial surface concentration compared to samples prepared at lower DCD's. This is likely due to significant changes in the thermal environment for fiber formation under different DCD conditions. When the DCD is large, the duration of the fiber formation process is extended, and fibers remain in the melt phase longer.<sup>28</sup> This allows for more aggressive migration in these samples, as migration is significantly inhibited in the solid, crystalline state after web formation. The resulting final surface concentration of additive after migration remains largely independent of DCD, indicating that the effect being observed does not significantly impact the equilibrium state, but rather the kinetics of the equilibration process. It is also worth noting that while this effect is significant at large additive loadings, it is of limited impact at low additive loadings. While the mechanism behind this limitation is not clear, it is likely simply attributed to the extremely low concentration of additive in the system.

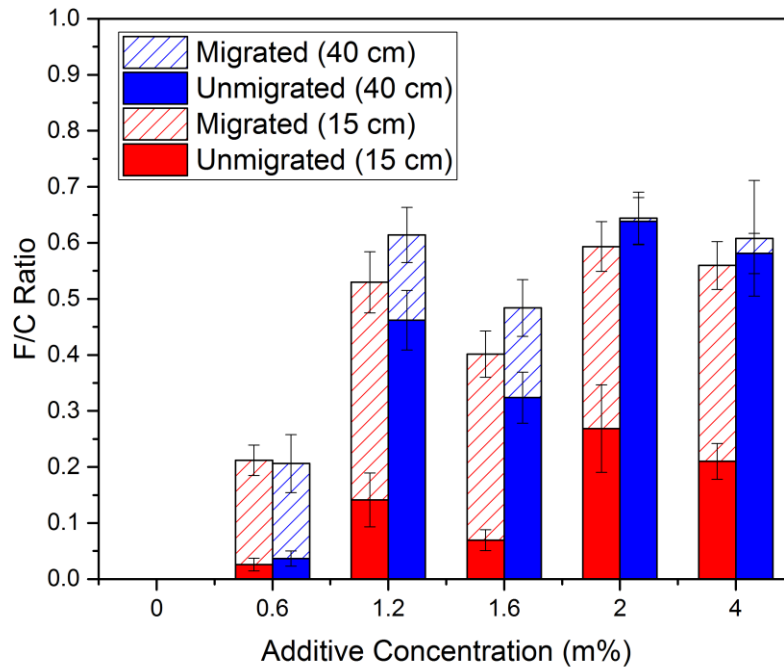


Figure 3.6: Competing influence of migration time and die-to-collector distance on additive surface concentration was measured by XPS. F/C ratio was measured before migration (solid) and after migration (hashed) for samples generated at a DCD of 15 cm (red) and at 40 cm (blue). The effect of DCD prior to migration indicates significant additional mobility during the fiber formation process at larger distances.

#### 3.4.5.2 *Molecular weight*

In an effort to characterize the role of molecular weight on the migration process, a new set of samples were prepared on the Reicofil manufacturing line. These samples were formed from polypropylene having a melt flow rate of 1200 g/10 min (1200 MFR), compared to the previous samples of 500 g/10 min (500 MFR) polypropylene. The manufacturing process was also controlled to generate samples with high and low air flow rates as well as high and low die-to-collector distances. As shown below in Figure 3.7, when compared to the previous trial of 500 MFR fibers, most conditions did not show significant changes in fiber size distribution; the only exception being the samples prepared at 800 m<sup>3</sup>/hr air flow rate and 40 cm die-to-collector distance. These samples exhibited a slightly larger median fiber diameter, approximately 7 μm, while all other conditions yielded a median fiber diameter of 5 μm or less. The large number of fibers which were found to be between 10 and 20 μm, and as high as 26 μm, likely played a large role in this shift in the overall distribution of fiber sizes in these samples.

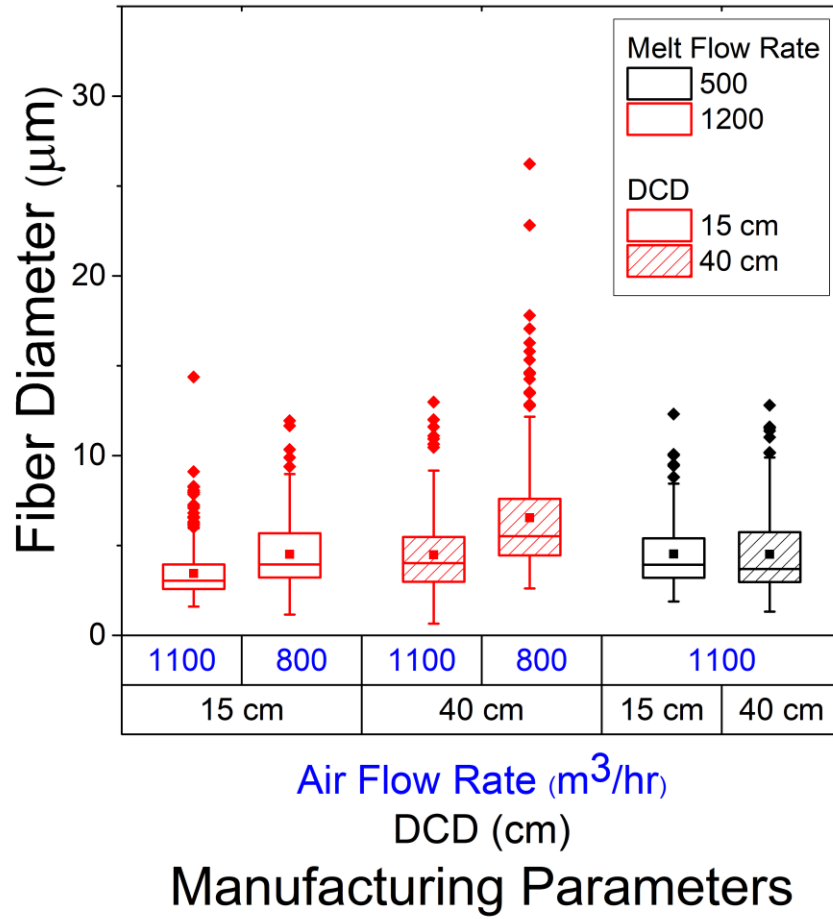


Figure 3.7: Fiber size distribution of 500 MFR (black) and 1200 MFR (red) nonwovens at 15 cm (unfilled) and 40 cm (hashed) DCD's and airflow rates of 1100  $\text{m}^3/\text{hr}$  and 800  $\text{m}^3/\text{hr}$ .

### 3.4.5.3 *Air flow rate*

Having determined through the analysis of Figure 3.6 that all samples with sufficiently high bulk additive loading exhibit an equivalent saturation concentration of fluorine after significant migration, in these high MFR samples we sought to characterize changes to the initial additive distribution, as measured in unmigrated samples. By comparing the effect of changing air flow rate, as shown in Figure 3.8, we see that samples prepared at higher air flow rates exhibit higher initial surface additive concentrations. This is most likely attributable to decreased fiber diameter. As was shown in Figure 3.5d, smaller fibers exhibit more complete migration during the fiber formation process. We do notice a significant decrease in the influence of this effect at lower additive concentration, and similarly note that the effect of DCD on the initial surface additive concentration is mitigated under these conditions as well. This is clearly demonstrated in the case of Figure 3.6 where the high and low DCD samples are shown to have statistically insignificant differences in initial surface additive concentration at low bulk additive concentrations and is likely a result of the overall lower potential surface concentration of these samples.

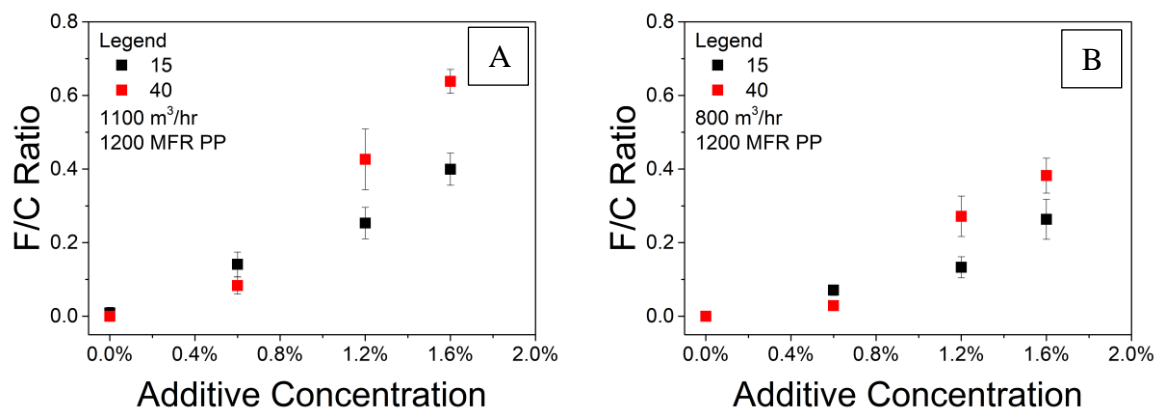


Figure 3.8: Initial Surface fluorine content of 1200 MFR polypropylene fiber webs as influenced by air flow rate and DCD. Samples prepared at (A) high (1100 m<sup>3</sup>/hr) air flow rate were found to have larger initial fluorine surface concentrations when compared to samples prepared at (B) low (800 m<sup>3</sup>/hr).

Further comparing these results to those obtained in the previous, low MFR polymer studies, the competing influence of MFR and DCD are observed in Figure 3.9. In both cases, low or high MFR, it was observed that high DCD yields a larger initial surface concentration of the fluorochemical melt additive. However, it was found that this effect is much more drastic in the case of the low MFR polymer fibers, while the high MFR samples showed higher F/C ratios at equivalent conditions. This is likely an effect of the increased mobility of the surfactant-like fluorochemical melt additive molecule in the lower molecular weight polymer matrix. In this environment, diffusion of the additive is likely to be more rapid, and potential migration distances are likely to be longer, resulting in higher concentrations at the surface after the rapid manufacturing process.

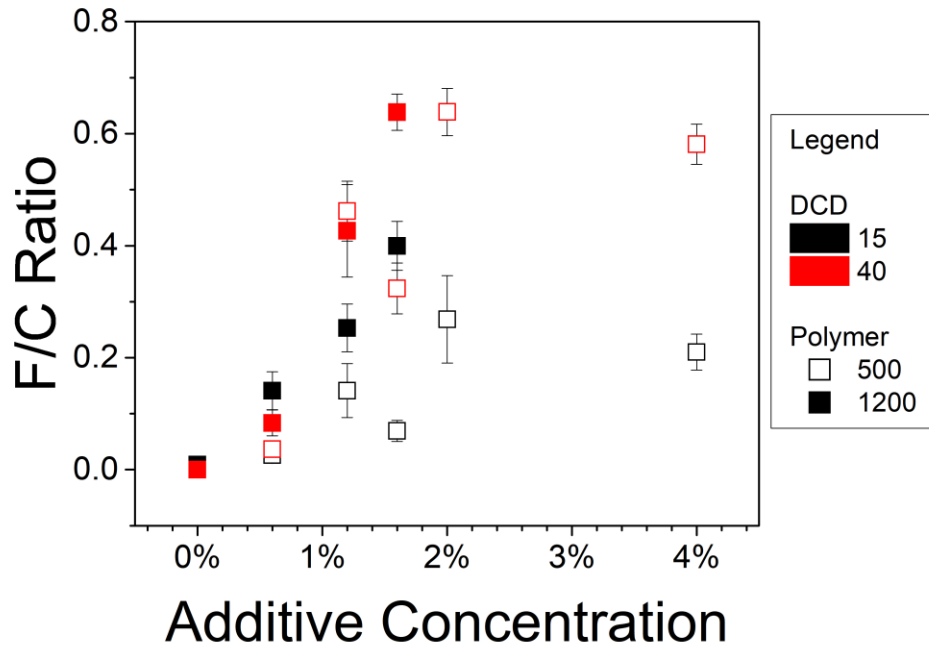


Figure 3.9: Comparison of unmigrated surface composition of low (open) and high (closed) MFR samples prepared at 1100 m<sup>3</sup>/hr air flow rate. The impact of DCD was also seen to be influenced by polymer flow rate. While high (40 cm, red) DCD samples exhibited similar F/C ratios independent of polymer flow rate, at low (15 cm, black) DCD higher F/C ratios were observed in the case of high MFR polymer samples.

### 3.4.6 *Repellency of resulting fiber mats*

These results ultimately are corroborated by alcohol repellency tests. As shown in Figure 3.10, alcohol repellency scores of tested samples are poor when the nonwoven contains no fluorochemical melt additive but are drastically improved through even small concentrations of additive in the bulk. With the understanding of fluorochemical melt additive migration generated in the previous sections it is possible to control various processing conditions and material considerations in order to generate highly repellent nonwoven mats. For example, when 0.6% loading of additive is used repellency values are highly variable, and consistent alcohol repellency results are only obtained after migration of 1.6% additive samples. However, by allowing migration in the lower concentration samples, and utilizing the 500 MFR polymer, comparable performance is achieved to that of significantly higher additive content samples.

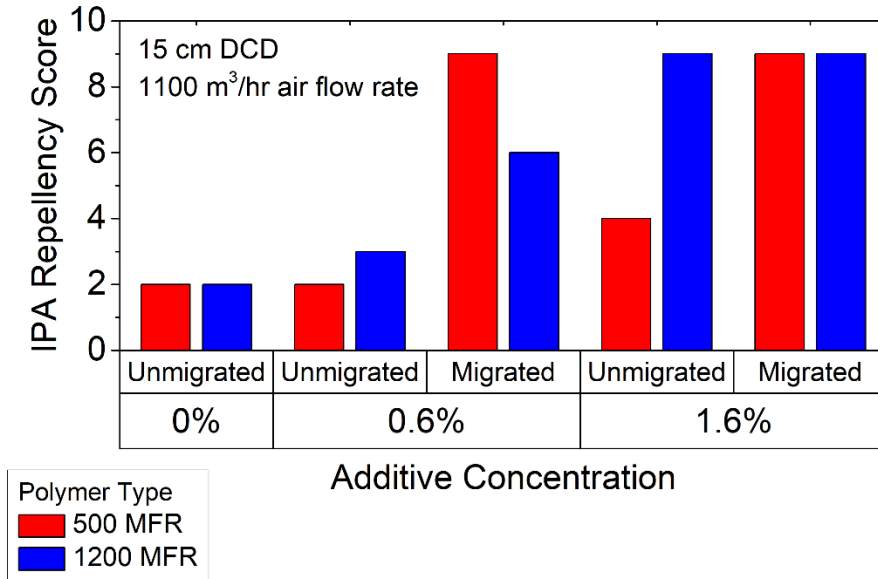


Figure 3.10: Influence of polymer melt flow rate on unmigrated and migrated alcohol repellency scores as determined by the ISO 23232 test method. While 500 MFR polymer samples (red) demonstrated a more significant response to migration at low bulk additive concentrations, 1200 MFR samples achieved superior alcohol repellency without migration at moderate additive concentrations.

### 3.5 *Conclusions*

Our study shows that migration plays a significant role in the determination of the final properties of surface active additive containing nonwoven materials. While moderate concentrations of additive yield sufficient surface concentrations of fluorine compounds to prevent discharging, lower additive concentrations are unable to achieve this goal prior to migration. These effects are demonstrated through the use of contact angle measurement of nonwoven materials, where thresholds for the prevention of droplet wicking are observed. Increasing the F/C ratio of the substrate, either through increased loading of additive or through migration of additive, prevents wicking of droplets for even the lowest surface tension fluids. The die-to-collector distance used during manufacturing is shown to have a significant impact upon initial additive distribution. Samples prepared at higher die-to-collector distances show significantly higher initial concentrations of additive at the surface. Samples prepared using lower molecular weight polypropylene exhibited higher additive concentrations overall, and showed less susceptibility to the influence of DCD. Overall, this work demonstrates the effect of many interdependent manufacturing parameters and highlights key considerations for the successful design of nonwoven materials containing surface active melt additives.

### 3.6 Works Cited

1. Sarmadi, A. M., Kwon, Y. A. & Young, R. A. Wettability of Nonwoven Fabrics . 1 . Effect of Fluorochemical Finishes on Water Repellency COS e. 279–287 (1993).
2. Otozawa, N., Sugiyama, K., Shimada, M. & Oomori, Y. Water/Oil Repellent Composition, Method for its Production and Method for Treating Article. **1**, (2012).
3. Goli, K. K., Rojas, O. J. & Genzer, J. Formation and antifouling properties of amphiphilic coatings on polypropylene fibers. *Biomacromolecules* **13**, 3769–79 (2012).
4. Salas, C., Genzer, J., Lucia, L. a, Hubbe, M. a & Rojas, O. J. Water-wettable polypropylene fibers by facile surface treatment based on soy proteins. *ACS Appl. Mater. Interfaces* **5**, 6541–8 (2013).
5. Fitting, S. W. (2) Patent Application Publication (10) Pub. No.: US 2002/0142691A1. **1**, (2002).
6. Jones, M., Mei, B. & Rousseau, A. Method of making electret articles and filters with increased oily mist resistance. *US Pat.* 6,068,799 (2000).
7. Jones, M. E. & Rousseau, A. D. Oily mist resistant electret filter media. 1–8 (1995).
8. Zhang, D., Sun, C. & Xiao, J. Effect of Selected Additives on Surface Energy of Fibers and Meltblown Nonwovens. *Text. Res. J.* **76**, 261–265 (2006).
9. Quincy III, R. B., Yahiaoui, A. & McManus, J. L. Nonwoven webs having zoned migration of internal additives. (2000).
10. Du, K., Yang, G., Yuan, Z., Xu, W. & Liang, X. Migration of additives toward the surface during aging of epoxy coating by infrared spectroscopy. *J. Appl. Polym. Sci.* **131**, 1–8 (2014).
11. Wang, N., Wang, T. & Hu, Y. Tailoring Membrane Surface Properties and Ultrafiltration Performances via the Self-Assembly of Polyethylene Glycol-block-Polysulfone-block-Polyethylene Glycol Block Copolymer upon Thermal and Solvent Annealing. *ACS Appl. Mater. Interfaces* **9**, 31018–31030 (2017).
12. Yang, B. *et al.* PVDF blended PVDF-g-PMAA pH-responsive membrane: Effect of additives and solvents on membrane properties and performance. *J. Memb. Sci.* **541**, 558–566 (2017).
13. Özen, I., Rustal, C., Dirnberger, K., Fritz, H. G. & Eisenbach, C. D. Modification of surface properties of polypropylene films by blending with poly(ethylene-b-ethylene oxide) and its application. *Polym. Bull.* **68**, 575–595 (2012).
14. Camós Noguera, A., Olsen, S. M., Hvilsted, S. & Kiil, S. Diffusion of surface-active amphiphiles in silicone-based fouling-release coatings. *Prog. Org. Coatings* **106**, 77–86 (2017).
15. Pesek, S. L. *et al.* Synthesis of bottlebrush copolymers based on poly(dimethylsiloxane) for surface active additives. *Polym. (United Kingdom)* **98**, 495–504 (2015).
16. Datla, V., Shim, E. & Pourdeyhimi, B. Surface Modifications of Polypropylene With Nonylphenol Ethoxylates Melt Additives. 1–8 (2012). doi:10.1002/pen
17. Hardman, S. J. *et al.* Electrospinning Superhydrophobic Fibers Using Surface Segregating End-Functionalized Polymer Additives. 6461–6470 (2011).
18. Tuteja, A. *et al.* Designing superoleophobic surfaces. *Science* **318**, 1618–22 (2007).
19. Saquing, C. D., Manasco, J. L. & Khan, S. A. Electrospun nanoparticle-nanofiber composites via a one-step synthesis. *Small* **5**, 944–51 (2009).
20. Kutsenko, M. & Fox, S. Polymer Additive for Providing an Alcohol Repellency for

- Polypropylene Nonwoven Medical Barrier Fabrics. (2009).
21. Oxenrider, B. & Woolf, C. Synthetic fibers having improved soil and stain repellency. *US Patent 3,899,563* (1975).
  22. Jariwala, C., Klun, T., Dams, R. & Jones, M. Alkylated fluorochemical oligomers and use thereof. *US Patent 6,288,157* (2001).
  23. Gardiner, R. A. Durably hydrophilic thermoplastic fiber and fabric made from said fiber. (1994).
  24. Crater, D., Howells, R., Stern, R. & Temperante, J. Fluorochemical oxazolidinones. *US Patent ...* (1991).
  25. Buckanin, R. S. Fluorochemical aminoalcohols. (1995).
  26. Wang, Z., Macosko, C. W. & Bates, F. S. Fluorine-Enriched Melt-Blown Fibers from Polymer Blends of Poly(butylene terephthalate) and a Fluorinated Multiblock Copolyester. *ACS Appl. Mater. Interfaces* **8**, 754–761 (2016).
  27. Arvidson, S. a. *et al.* Modification of Melt-Spun Isotactic Polypropylene and Poly(lactic acid) Bicomponent Filaments with a Premade Block Copolymer. *Macromolecules* **45**, 913–925 (2012).
  28. Bresee, R. R. & Ko, W. Fiber Formation During Melt Blowing. *Inj* 21–28 (2003).

## CHAPTER 4. CHARGE PROTECTION AND ADDITIVE MIGRATION IN ELECTRET AIR FILTRATION MATERIALS

*Joe Lavoie<sup>1</sup>, Orlando Rojas<sup>1,3</sup>, Saad Khan<sup>1</sup>, and Eunkyong Shim<sup>2</sup>*

*<sup>1</sup>Department of Chemical Engineering, North Carolina State University, Raleigh, NC*

*<sup>2</sup>College of Textiles, North Carolina State University, Raleigh, NC*

*<sup>3</sup>Department of Bioproducts and Biosystems, Aalto University, Espoo, Finland*

### *4.1 Abstract*

In the field of electret air filter materials, nonwoven media are embedded with charges in order to improve capture efficiency. Unfortunately, these charged filters are susceptible to charge loss when exposed to oils and alcohols. In this work, we endow charge protection through increased repellency toward these fluids through the use of surface active melt additives. Nonwovens containing fluorochemical melt additives were produced, and methods were established for their characterization. This included quantitative investigation of the additive migration process through the use of X-ray Photoelectron Spectroscopy (XPS). Samples were monitored over the days and weeks post-manufacturing and the surface chemistry was evaluated with respect to repellency and associated charge protection. Repellency was quantified through contact angle goniometry of isopropyl alcohol, a standard discharging liquid, and fractional filter testing was used to measure discharge protection. It was found that the associated increase in filtration efficiency due to electret charging can be protected through the use of alcohol repellent surfaces, and this was directly related to fluorine content in the nonwoven media.

## 4.2 Introduction

When customizing the properties of polymer fibers, the use of bulk melt additives is a facile, industrially relevant method for many different applications.<sup>1-3</sup> One field in which the use of polymer melt additives has been shown to be effective is surface energy control of nonwoven fibers.<sup>4,5</sup> These melt additives, when blended with polymers prior to melt spinning, migrate to the fiber surface and influence surface functionality without significantly changing the bulk polymer properties.<sup>6,7</sup> This phenomenon allows for the creation of fiber surfaces with controlled wettability useful in many industries, including protective medical and consumer textile garments, oil spill cleanup materials, self-cleaning materials, and filters. One application of particular importance, is in the field of electret air filter materials, where embedded charges provide improved filtration efficiency, but are susceptible to losses when exposed to oils and alcohols.

Electret air filters are used in a diverse range of environments where high particle capture efficiency with minimal pressure drop across the filter media are required; however, in many of these environments exposure of the electret filter media to oil and alcohol aerosols or mists is not uncommon.<sup>8-11</sup> These low surface tension fluids easily wet even highly hydrophobic polymer fibers such as polypropylene (PP).<sup>12,13</sup> The wetting of charged fibers has been shown to have a rapid and permanent discharging effect via electric shielding by conductive sheath coatings.<sup>14-16</sup> As these products are designed around the utilization of the electrostatic capture mechanism, the loss of charge has drastic negative effects on filter performance and lifetime.<sup>17,18</sup>

Other methods for the prevention of discharging due to oil and alcohol aerosol exposure include the use of pre-filters to remove aerosolized liquid particles from the feed stream prior to high efficiency particulate filtration.<sup>19,20</sup> This is effective, but introduces additional complexity to the system in the form of multiple filtration steps or complex filter media. The use of surface coatings or chemical modification after manufacturing of the nonwoven media has also been demonstrated to varying levels of effectiveness.<sup>21,22</sup> These methods require additional processing steps during the manufacturing process, and depending upon the chemistry used can pose additional concerns such as requiring the use of harsh chemicals, limited durability of coatings, and others. Alternatively, the use of bulk polymer additives is a facile and industrially proven process for modification of many polymer properties.<sup>23</sup> There are some commercially available products in this area, including those for increased repellency toward various liquids.<sup>24-26</sup> While these products have demonstrated effectiveness, questions remain surrounding the observed migration phenomenon of surface active small molecules in polymer matrices. Though the process of additive migration is well known, the impact of additive migration and correlation of nonwoven meltblown processing parameters on resultant product design has not been fully characterized in the literature. In this work we seek to explore additive loading and migration effects with traditional nonwoven manufacturing parameters and their impacts upon repellency of nonwoven products.

### 4.3 *Experimental*

#### 4.3.1 *Materials & Methods.*

Nonwoven substrates were prepared from metallocene homopolymer PP (MF650W, 500 MFR, LyondellBasell, Houston, TX) and the small molecule fluorochemical melt additive HydRepel A-204M (Goulston Technologies Inc., Monroe, NC) in polypropylene masterbatch. Both were provided by The Nonwovens Institute at North Carolina State University. Research grade, 99.9% pure isopropyl alcohol (IPA) was obtained from Sigma Aldrich (St. Louis, MO) for discharge testing.

#### 4.3.2 *Meltblown Nonwoven Manufacturing*

Samples were manufactured using the Reicofil Meltblown Pilot Line (see Figure 4.1) with a 1.3 meter, 35 hole per inch (HPI) Exxon die. The extrusion die was held at 240 °C, while the air curtain was heated to 255 °C and a volumetric flowrate of 1100 m<sup>3</sup>/h. Polypropylene was mixed with additive containing masterbatch composed of 20 wt% additive in 1200 MFR (melt flow rate) PP resin, by the automated feed system, then fed to the extruder at designated concentrations. Additive concentration was controlled to six levels, in order to more thoroughly understand the influence of additive concentration on repellency properties of the resulting nonwoven samples. Samples were also prepared under two die-to-collector distances (DCD) conditions. Values were selected such that both samples representative of typical air filter materials (high DCD) and samples designed for liquid barrier testing (low DCD) were prepared.

Table 4.1: Reicofil Pilot Line DoE and Run Conditions

Reicofil Meltblown Pilot Line Run Conditions						
Die Temperature	240 °C					
Die Air Temperature	255 °C					
Die Air Pressure	144.8 kPa (21 PSI)					
Throughput	53 kg/h					
Die-to-Collector Distance	15 cm	40 cm				
Die	Exxon (35 HPI)					
Capillary Diameter	400 μm					
Additive Concentration	0.0%	0.6%	1.2%	1.6%	2.0%	4.0%

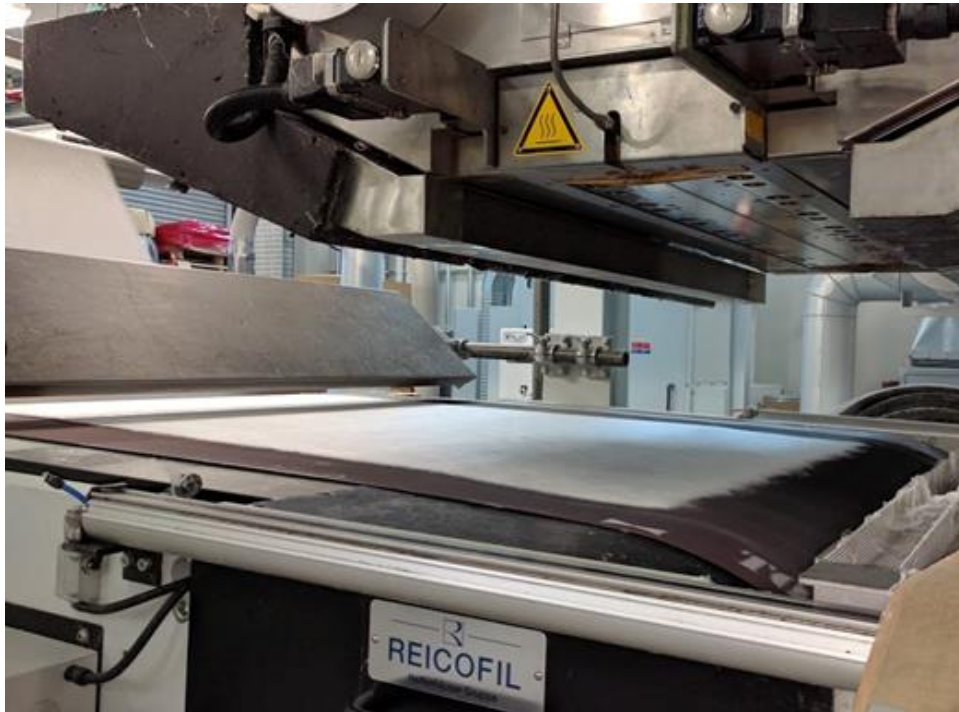


Figure 4.1: Reicofil Pilot Scale Nonwoven Manufacturing System.

#### 4.3.3 *X-Ray Photoelectron Spectroscopy*

Surface composition of nonwoven substrates with fluorochemical melt additive were characterized by XPS. Samples were stored in the freezer at -20 °C after manufacturing, effectively stopping additive migration. For samples analyzed with respect to migration time, the reported time is measured as time since removed from the freezer. Migration was allowed to occur on the laboratory benchtop at room conditions, typically 20 °C and 30% relative humidity. Compositional analysis was performed on a SPECS XPS system with PHOIBOS 150 Analyzer at the Analytical Instrumentation Facility (AIF) at NC State University (Raleigh, NC). The analysis was done using a Mg K $\alpha$  x-ray source operated at 300 W (10 kV and 30 mA) with vacuum chamber at room temperature and pressures in the 10<sup>-8</sup> torr range or lower. Survey scans were collected from 0 to 1100 eV and atomic compositions were derived from peak areas using CasaXPS processing software version 2.3.16.

#### 4.3.4 *Contact Angle Goniometry*

Wicking and repellency of nonwoven substrates were evaluated using sessile drop goniometry of isopropanol. Samples were measured under standard laboratory conditions, around 20 °C and approximately 30% humidity, using an SEO Phoenix 300 Goniometer (Surface Electro Optics, Suwon City, South Korea). Images were captured by frame grabbing software “Image XP”, and contact angle analysis was performed using “ImageJ” image processing software with the “DropSnake” analysis plugin. Due to the porous nature of nonwoven materials, reported contact angles for these materials are apparent contact angles and cannot be directly related to the surface energy of the fiber.

#### 4.3.5 *Scanning Electron Microscopy*

Fiber diameter was evaluated through the use of scanning electron microscopy. Images were captured on the Verios High Resolution SEM at the AIF. In order to avoid charging of nonwoven samples during imaging, samples were sputter coated with 50 nm of gold using the Hummer II sputter coater at the AIF. Images were captured at 13 nA and 2 kV using the Everhart-Thornley Detector in secondary electron mode, at a working distance of approximately 8 mm to maximize depth of field.

#### 4.3.6 *Charge State Preparation*

Charging was performed using a benchtop corona charging system. Samples were placed upon a grounded metal plate, centered under the bar electrode, and adjusted to a distance of 3 cm. Samples were charged on both sides using a negative bias at 11 kV for 10 seconds per side. After charging, samples which did not require discharging were immediately placed into the fractional filter tester to be evaluated. Samples to be discharged were immediately placed into a large polyethylene container and suspended individually above an isopropyl alcohol bath. The container was then closed with an air-tight seal and placed into a fume hood for 48 hours. After the discharging process was complete, samples were then removed from the container and immediately evaluated for remaining charge by fractional filtration efficiency testing.

#### 4.3.7 *Fractional Filter Testing*

Fractional filtration testing for the characterization of charged, discharged, and control samples was performed on a TSI 3160 Automated Filter Tester. Tests were performed with a nominal flow rate of 32 liters per minute and face velocity of  $\sim 5.3$  cm/s across  $100$  cm<sup>2</sup>. Particles used were atomized dioctyl phthalate (DOP) with an average diameter of  $0.3$   $\mu$ m. Full fractional

tests, ranging from 0.05  $\mu\text{m}$  to 0.4  $\mu\text{m}$  particle sizes, were performed under many conditions to confirm the use of 0.3  $\mu\text{m}$  as the most penetrating particle size (MPPS). All filtration efficiency tests were performed in triplicate on separate physical samples.

#### *4.4 Results and Discussion*

##### *4.4.1.1 Characterization of Nonwoven Fiber Web Structure*

After sample manufacturing, the first task was to fully characterize the web structure and relative performance of control samples. Previous studies had been conducted on bench scale nonwoven manufacturing equipment with identical chemistry, and these results demonstrated that increasing additive concentration over the range studied had no significant impact on fiber diameter. As shown in Figure 4.2A, samples prepared for this study were found to have median fiber diameters of approximately 3.8  $\mu\text{m}$ , with 95% of fibers falling between 1 and 10  $\mu\text{m}$ . Additive concentration was shown to have moderate impact on nonwoven web structure as characterized by filtration testing shown in Figure 4.2B. Samples were demonstrated to have moderately increased filtration efficiency with increased additive content, likely resulting from changes to web solidity. Increased additive content was found to significantly decrease inter-fiber interactions, preventing bonding during fiber laydown and thereby decreasing solidity. This effect can be easily observed in a qualitative manner through the handling of samples, as the hand feel of the additive containing samples is significantly softer, and more prone to mechanical failure. The reduction in inter-fiber interactions is further verified by the changing pressure drop of the samples as shown in Figure 4.2B. From this chart, we see that increased additive content up to 1.6% in the bulk, causes decreased pressure drop across the filter media, likely due to decreased tortuosity of the pore structure as solidity decreases. Above 1.6%

additional additive content does not yield significant further changes in the observed filtration behavior.

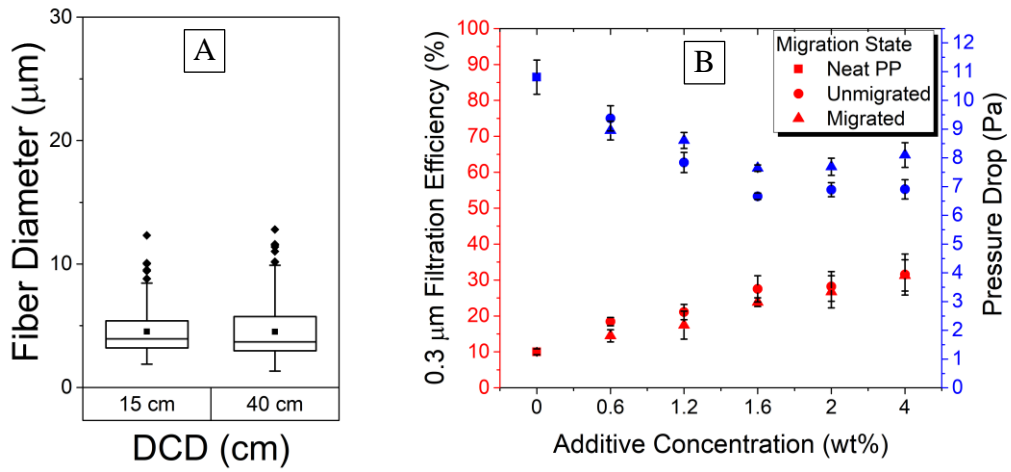


Figure 4.2: (A) Fiber size distribution of electret filter samples and the effect DCD were characterized by SEM image analysis. Distribution of fibers is represented as a box containing 50% of fibers, whiskers containing 95% of fibers, with the mean (circle) and median (intersecting line). Fibers outside the 95<sup>th</sup> percentile are shown individually (diamonds). (B) The influence of additive concentration on filtration efficiency (red) and pressure drop (blue) was analyzed by fractional filter tester.

#### 4.4.2 *Additive surface migration characterization*

In an effort to quantitatively track the surface concentration of fluorochemical melt additive in the sample, we utilized XPS and carefully controlled the migration state of the samples being measured. Due to the extremely surface selective nature of XPS, measurements of the atomic composition of the fibers is relegated to the first 5 to 10 nm at the interface. Through analysis of the signal generated, the atomic composition of this narrow region of the fiber can be quantitatively characterized. For the purposes of this study, the fluorine atoms present in the melt additive compound are the most relevant quantity for characterization, and so we report the atomic ratio of fluorine to carbon atoms (F/C ratio).

Figure 3.2 presents a proof of concept for this kind of analysis. This figure shows a comparison between two sets of samples: samples which have not experienced any appreciable additive migration post manufacturing (unmigrated, in white), and samples which have been stored at room temperature for six months and can be considered fully migrated (migrated, in black). A few principles are clearly illustrated by this analysis. First and foremost, control samples containing only polypropylene and no additive are free from contamination and reliably contain no fluorine down to the detection limit of XPS (<0.1 at%). Second, independent of initial bulk additive content, migration plays a significant role in determining surface fluorine concentration. In each case, the equilibrated samples have demonstrably larger F/C ratio values than the pre-migration samples.

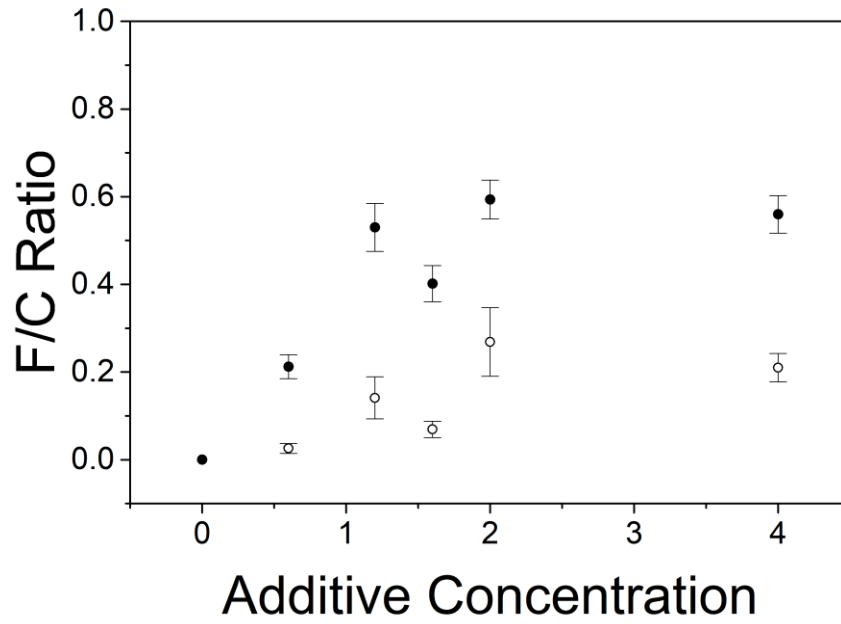


Figure 4.3: Additive fluorine content present at the surface of electret filter materials as measured by XPS immediately after manufacturing (open) and equilibrated over six months storage (solid).

While migration time is a significant driving force for the changing composition of the surface, it is clear that other factors also play a role, including fiber size and certain manufacturing parameters. Among the parameters tested, the most significant impact on migration state was found to be the die-to-collector distance used during the pilot scale manufacturing process. As shown in Figure 3.6, the resulting surface composition of fully migrated fibers is largely independent of other factors at sufficiently high additive concentrations; however, the unmigrated samples exhibit drastic differences in initial additive distribution. While this effect is limited under extremely low additive loading conditions, as much as a three-fold increase in initial surface concentration is observed for even moderate loading conditions when a larger DCD is used during nonwoven manufacturing. This is most likely a result of the increased duration of the fiber formation process when the DCD distance is increased. In many meltblown systems the fibers will not fully solidify until they contact the forming belt and during this time prior to the crystallization of the fiber migration is accelerated.<sup>27</sup>

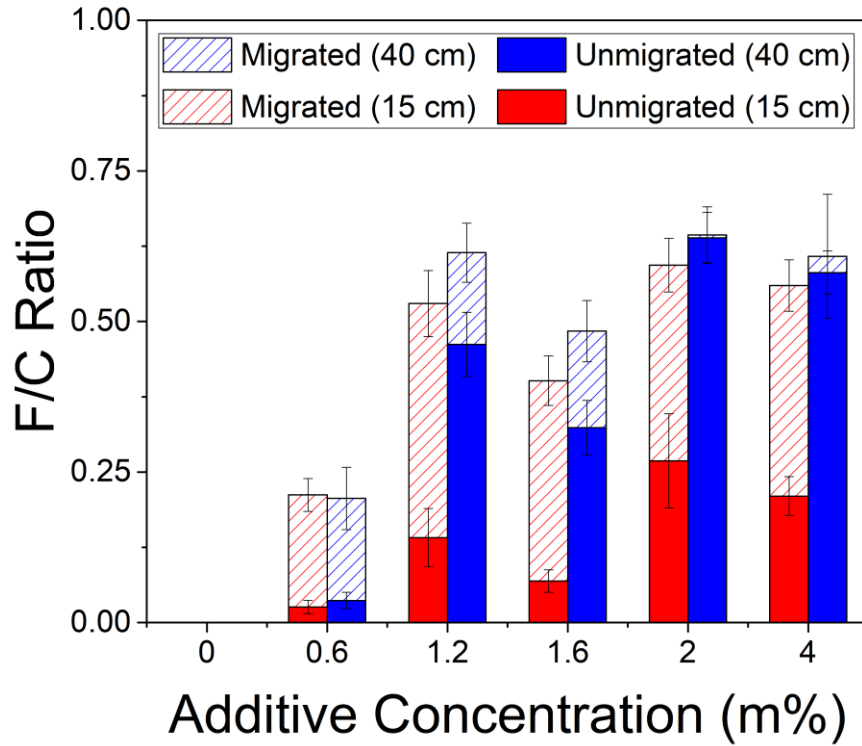


Figure 4.4: Competing influence of migration state and die-to-collector distance on additive surface concentration. Initial surface fluorine content (solid) is shown to be significantly lower than the fully migrated samples (hashed) for low to moderate bulk additive concentrations. The influence of DCD is shown to be significant in the development of surface fluorine content prior to migration as high, 40 cm DCD samples (blue) exhibit significantly higher F/C ratios than samples prepared at 15 cm DCD (red). At high bulk additive content and high DCD, initial surface concentration of additive is sufficiently high so as to prevent significant improvement through further sample migration.

The impact of DCD on the initial surface concentration of additive are corroborated by alcohol repellency tests. For this work, the standard aqueous liquid repellency test for textiles, ISO 23232 was utilized. In this method, aqueous solutions of alcohol are prepared in 10% by volume increments and numbered in ascending fashion, such that test liquid No. 1 is 10% isopropanol, test liquid No. 2 is 20% isopropanol, and so on. Three droplets of test liquid No. 1 are placed on the textile substrate, and if after approximately 10 seconds no penetration or wetting of the fabric is observed, the next test liquid is dispensed onto the substrate. This process is repeated until the sample is determined to have been wetted by test liquid, at which point the samples repellency score is determined to be the number associated with highest alcohol content test liquid which did not wet the substrate.<sup>28</sup> As shown in Figure 4.5, alcohol repellency scores of tested samples are poor when the nonwoven contains no fluorochemical melt additive, and when samples are prepared with 0.6% bulk additive concentration the repellency values are highly dependent upon the migration state of additive to exhibit significant alcohol repellency. However, the initial additive surface concentration does play a significant role in determining the repellency of unmigrated samples as demonstrated by the 1.6% additive sample manufactured at a 15 cm die-to-collector distance. At 40 cm, the pre-migration F/C ratios of these samples is sufficiently high, as shown in Figure 4.4, to significantly increase alcohol repellency.

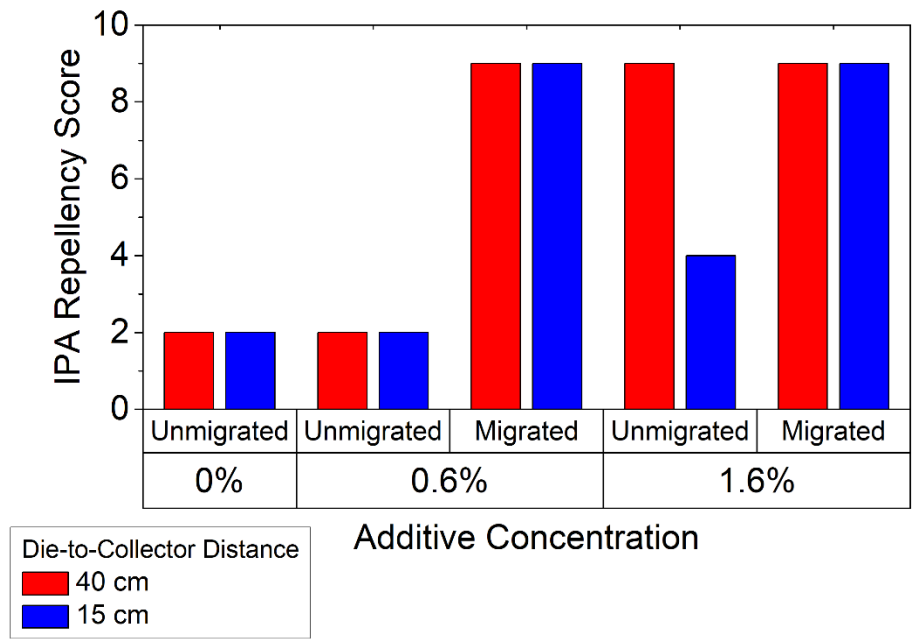


Figure 4.5: Influence of DCD and bulk additive concentration on initial (red) and equilibrium (blue) alcohol repellency scores as determined by ISO 23232 standard test method. All samples demonstrate significantly improved IPA repellency after additive migration, but samples manufactured at 40 cm DCD exhibit better repellency prior to migration with moderate additive concentrations in the bulk.

#### 4.4.3 *Discharging & Filter Performance of Repellent Nonwovens*

As discussed previously, the ultimate goal of this effort is to understand repellency performance as a result of additives and adequate migration in order to generate nonwoven filter materials capable of withstanding isopropanol vapor discharge test methods. For this study we utilized a discharge method designed such that an isopropanol bath was placed in the bottom of a large chamber and filter samples to be discharged were hung from the top of the chamber and exposed to the vapors that developed in the head space. This method was shown to be effective, and demonstrated nearly complete discharging of filter materials as shown in Figure 4.6.

The chart shown in Figure 4.7 illustrates the filtration performance of samples fabricated on the Reicofil pilot scale manufacturing line against 0.3  $\mu\text{m}$  diameter particles, under various charge and migration states. In this study it was noted that samples which had not been exposed to external charging sources exhibited improved filtration efficiency with increased additive content. This is likely a result of passive charging of the filter materials through environmental effects and handling of the materials, in combination with the increased concentration of additive yielding additional charge centers in the polymer matrix.

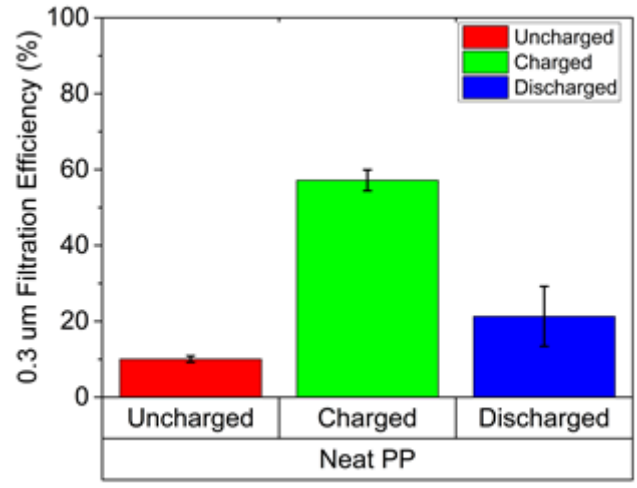


Figure 4.6: Subset of data from Figure 4.7 showing the impact of discharging of neat PP electret filter media by isopropanol vapor on filtration efficiency performance against 0.3 μm DOP particle test.

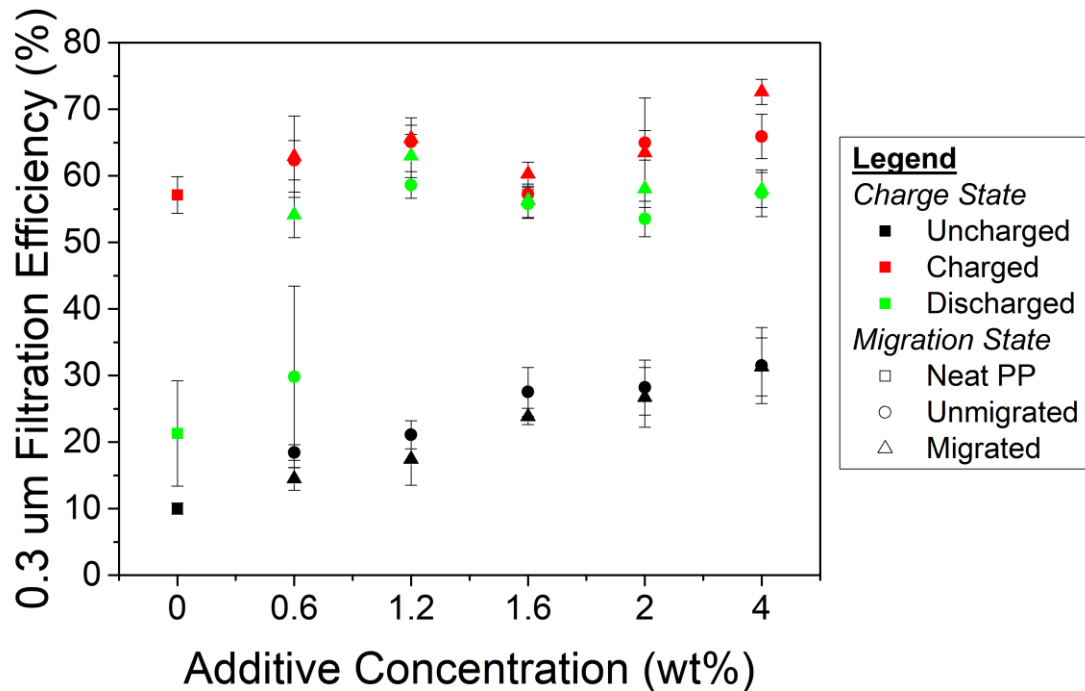


Figure 4.7: Comparison of discharging performance of unmigrated (circles) and migrated (triangles) filter materials. Filtration performance against a 0.3 μm particle was evaluated before corona charging (“uncharged”, black), after corona charging (“charged”, red) and after IPA vapor discharging of charged samples (“discharged”, green). At or above 1.2% bulk additive concentration, migration does not play a significant role in charge protection due to the diminishing returns of additional additive content at already high F/C ratios. At 0.6% bulk additive concentration there is a drastic response in charge protection performance due to additive migration, nearly doubling the effective filtration efficiency.

From these results, it is clear that for meltblown polypropylene nonwoven materials additive loading of 1.2% or higher is sufficient to guarantee adequate surface concentration of fluorine containing additives in order to substantially protect charge. The results shown in Figure 4.7 indicate that at the lowest additive concentration levels tested, charge protection is unreliable and depends greatly on migration state and other potential factors. This is further confirmed by the data shown in Figure 4.8. Here, we see that at additive concentrations of 1.2% and higher, whether samples are migrated or unmigrated, the discharged filtration efficiencies reported are only marginally decreased from the charged filtration values. However, when the bulk additive concentration of the filter media is decreased to 0.6%, we find that the migrated sample are able to protect the samples from discharging, while the unmigrated samples perform comparably to the non-additive containing samples.

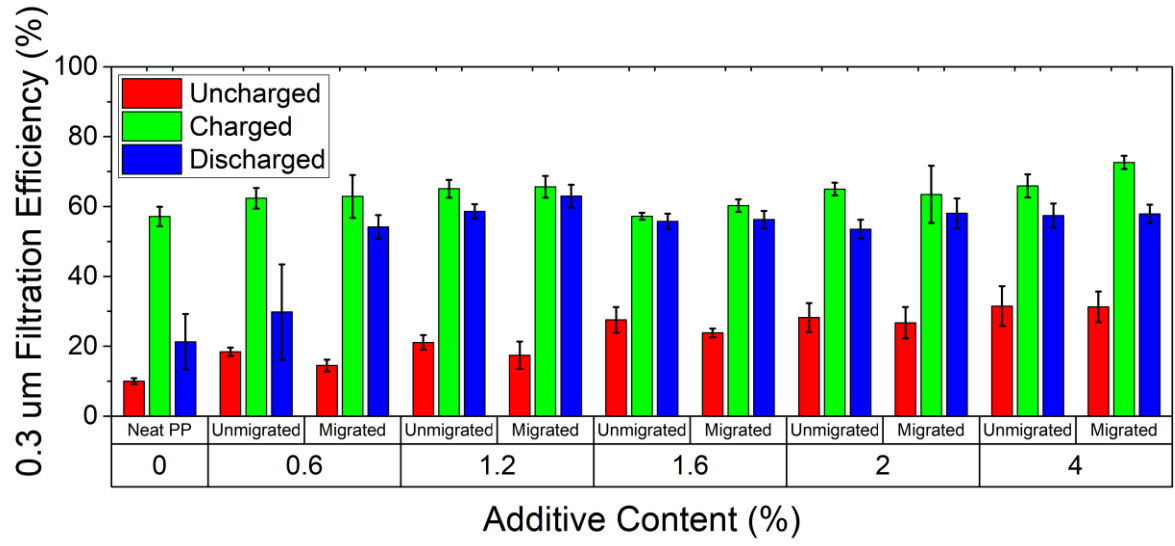


Figure 4.8: Charge protection in electret filter media as influenced by additive content and migration.

Alternatively, this can be seen in Figure 4.9 below, where the filtration efficiency data has been recast from the perspective of performance retained through the discharging process. Here we see that filter media which meet the minimum surface fluorine content required for charge protection (migrated 0.6% additive, and higher loadings), regularly maintain charge retention values of 80% or higher. While individual samples approach 100% protection of charge, performance is largely uncorrelated with additive loading beyond the minimum loading required for charge protection. As such, it appears there are multiple factors involved in the determination of resultant charge protection in electret filter media, and while repellency plays a large role in ensuring effective charge protection, further research is required to identify physical web properties and other parameters necessary to ensure charge protection approaches 100%.

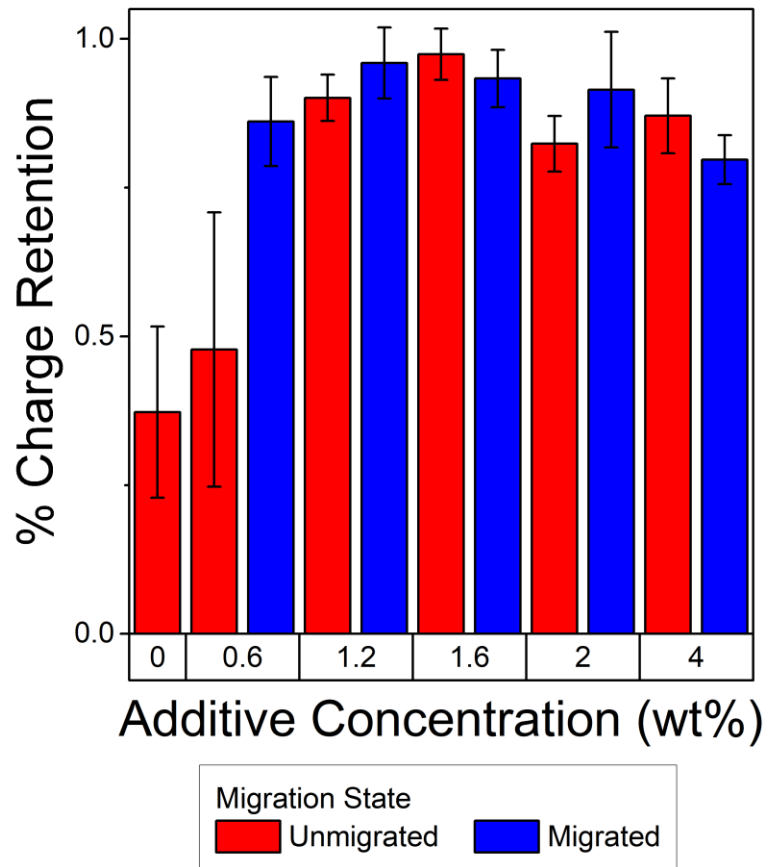


Figure 4.9: Charge retention of electret filter media as characterized by fractional filtration testing with 0.3  $\mu\text{m}$  DOP particles. The importance of additive migration is highlighted by the difference between % charge retention values of unmigrated (red) and migrated (blue) samples at extremely low additive loadings.

Taking into consideration these charge retention values as well as the repellency values shown in Figure 4.5, we find that the critical threshold F/C ratio value for charge protection align with that required for liquid droplet repellency. Cross referencing the demonstrated threshold for repellency of a macroscopic droplet (shown in Figure 4.5) with the samples exhibiting successful charge retention presented in Figure 4.9, we see that in both cases the successful performance of 0.6% additive samples requires migration. As such, it is shown in Figure 4.4 that the F/C ratio required for charge protection in these nonwoven filter media samples lies in the range between 0.02 and 0.2, the change in surface composition observed in 0.6% additive samples due to migration. Overall, the culmination of the presented work in this effort is the successful demonstration of charge protection in electret filter materials with corresponding quantitative evaluation of nonwoven substrate composition. Through the development of this greater understanding of the many correlated and confounding variables in melt additive containing nonwovens, we hope to inform the development of improved technologies and products.

#### 4.5 *Conclusions*

This study shows the successful development of correlations between fluorochemical melt additive surface concentrations and resultant nonwoven filter media and their performance. The impact of DCD and other process parameters which influence fiber surface composition by either encouraging or inhibiting the migration process was demonstrated through characterization of repellency performance through the use of standard methods. The importance of additive migration for achieving elevated surface fluorine content was quantified, and these results were used to assess the changing response of charged electret filter materials to isopropanol vapor exposure. It was found that with elevated surface fluorine

content in the range of  $F/C = 0.2$ , through either increased bulk concentration of additive or through migration, nonwovens could be made to resist wetting by isopropanol vapors and protect charge in electret filter media.

#### 4.6 Works Cited

1. Jones, M., Mei, B. & Rousseau, A. Method of making electret articles and filters with increased oily mist resistance. *US Pat. 6,068,799* (2000).
2. Jones, M. E. & Rousseau, A. D. Oily mist resistant electret filter media. 1–8 (1995).
3. Barrett, L. W. & Rousseau, A. D. Aerosol Loading Performance of Electret Filter Media. *Am. Ind. Hyg. Assoc. J.* **539**, 532–539 (1998).
4. Zhang, D., Sun, C. & Xiao, J. Effect of Selected Additives on Surface Energy of Fibers and Meltblown Nonwovens. *Text. Res. J.* **76**, 261–265 (2006).
5. Wang, Z., Macosko, C. W. & Bates, F. S. Fluorine-Enriched Melt-Blown Fibers from Polymer Blends of Poly(butylene terephthalate) and a Fluorinated Multiblock Copolyester. *ACS Appl. Mater. Interfaces* **8**, 754–761 (2016).
6. Hardman, S. J. *et al.* Electrospinning Superhydrophobic Fibers Using Surface Segregating End-Functionalized Polymer Additives. 6461–6470 (2011).
7. Camós Noguera, A., Olsen, S. M., Hvilsted, S. & Kiil, S. Diffusion of surface-active amphiphiles in silicone-based fouling-release coatings. *Prog. Org. Coatings* **106**, 77–86 (2017).
8. Romay, F. J., Liu, B. Y. H. & Chae, S.-J. Experimental Study of Electrostatic Capture Mechanisms in Commercial Electret Filters. *Aerosol Sci. Technol.* **28**, 224–234 (1998).
9. Taylor, P. *et al.* Aerosol Science and Technology Experimental Study of Electrostatic Capture Mechanisms in Commercial Electret Filters Experimental Study of Electrostatic Capture Mechanisms in Commercial Electret Filters. 37–41
10. Myers, B. D. L. & Arnold, B. D. Electret Media For HVAC Filtration Applications.
11. Kim, J., Hinesroza, J. P., Jasper, W. & Barker, R. L. Effect of Solvent Exposure on the Filtration Performance of Electrostatically Charged Polypropylene Filter Media. *Text. Res. J.* **79**, 343–350 (2009).
12. Price, D. (Price H. C. Spunmelt Polypropylene - The Leading Global Technology for Nonwoven Supply and Demand. *Nonwovens Industry* 1–2 (2016).
13. McIntyre, K. Filtration Market Update. *Nonwovens Ind.* **46**, 38–43 (2015).
14. Mohan, A. Effect Of Organic Solvent Exposure On Electret Filtration. (2005).
15. Choi, H.-J., Park, E.-S., Kim, J.-U., Kim, S. H. & Lee, M.-H. Experimental Study on Charge Decay of Electret Filter Due to Organic Solvent Exposure. *Aerosol Sci. Technol.* **49**, 977–983 (2015).
16. Jasper, W. *et al.* Effect of xylene exposure on the performance of electret filter media. *J. Aerosol Sci.* **37**, 903–911 (2006).
17. Yang, S. *et al.* Aerosol penetration properties of an electret filter with submicron aerosols with various operating factors. *J. Environ. Sci. Health. A. Tox. Hazard. Subst. Environ. Eng.* **42**, 51–7 (2007).
18. Janssen, L. L., Bidwell, J. O., Mullins, H. E. & Nelson, T. J. Efficiency of Degraded Electret Filters : Part I – Laboratory Testing Against NaCl and DOP before and after Exposure to Workplace Aerosols. **20**, (2003).
19. Chang, C., Ji, Z. & Liu, J. The effect of a drainage layer on the saturation of coalescing filters in the filtration process. *Chem. Eng. Sci.* **160**, 354–361 (2017).
20. Letts, G. M., Raynor, P. C. & Schumann, R. L. Selecting fiber materials to improve mist filters. *J. Aerosol Sci.* **34**, 1481–1492 (2003).

21. Wei, X. *et al.* Efficient removal of aerosol oil-mists using superoleophobic filters. *J. Mater. Chem. A* **6**, 871–877 (2018).
22. Agranovski, I. E. & Braddock, R. D. Filtration of liquid aerosols on wettable fibrous filters. *AIChE J.* **44**, 2775–2783 (1998).
23. Dutton, K. Overview and Analysis of the Meltblown Process and Parameters. *J. Text. Appar. Technology Manag.* **6**, (2008).
24. Kutsenko, M. & Fox, S. Polymer Additive for Providing an Alcohol Repellency for Polypropylene Nonwoven Medical Barrier Fabrics. (2009).
25. Crater, D., Howells, R., Stern, R. & Temperante, J. Fluorochemical oxazolidinones. *US Patent ...* (1991).
26. Jariwala, C., Klun, T., Dams, R. & Jones, M. Alkylated fluorochemical oligomers and use thereof. *US Patent 6,288,157* (2001).
27. Bresee, R. R. & Ko, W. Fiber Formation During Melt Blowing. *Inj* 21–28 (2003).
28. ISO. Textiles - Aqueous liquid repellency - Water/alcohol solution resistance test. (2009).

## CHAPTER 5. CONCLUSIONS & FUTURE WORK

Through the course of this dissertation we have worked to design and characterize systems for the creation of highly repellent fiber surfaces. We first developed a conformal and customizable sequential coating method, and characterized its performance against a wide range of low surface tension fluids. We then analyzed the influence of various process parameters on the performance of bulk polymer melt additives due to changes in additive migration. Finally, we quantitatively characterized the impact of alcohol repellency performance on discharge protection in electret air filter materials by measuring particle capture efficiency. A brief summary of the results from these studies is provided below.

### *5.1 CHAPTER 2. Omnipobic Polypropylene Nonwovens By Surface Modification With Bio-Hybrid And Conformable Coatings Followed By Chemical Vapor Deposition*

We have developed a novel, sequentially deposited coating method which exhibits superb coating uniformity, conformity, and roughness on inert polyolefin based nonwoven substrates. The system utilizes hydrophobic interactions between unfolded soy proteins and the hydrophobic polypropylene surface to activate the surface and enable further modification. Subsequent coating layers utilize ionic forces to first bind the cationic polyelectrolyte polyDADMAC to the soy proteins surface, then to decorate the surface with negatively charged fumed silica nanoparticles. This coating was then shown to be easily functionalized through the use of vapor phase silane chemistries. In this case, we utilized a highly fluorinated silane molecule, FOTS, to generate an extremely low surface energy interface. This, in combination with the multi-scale roughness provided by the fumed silica surface and cylindrical geometry of micron scale fibers, generates a highly repellent surface towards a

range of low surface tension fluids. This was exemplified through the response of mineral oil droplets on surfaces treated with this method. Mineral oil droplets on a flat PP film exhibit a static contact angle of  $10^\circ$ , however after preparation of the flat surface with this coating method, mineral oil exhibited a  $60^\circ$  contact angle. As was hypothesized, the combination of this system with the micro-scale roughness of nonwoven webs resulted in a further doubling of the repellency of the surface to a highly repellent contact angle of  $120^\circ$ .

### *5.2 CHAPTER 3. Characterization Of Fluorochemical Melt Additive Migration For Alcohol Repellency In Electret Filter Materials*

In this study, we demonstrated the successful characterization of surface active fluorochemical melt additive migration and the relevant impacts of nonwoven manufacturing parameters on resultant performance. XPS was utilized for its capability to characterize composition in a highly surface selective manner, and with this tool we were able to develop a more complete understanding additive migration kinetics. We demonstrated that the majority of additive migration occurs either during manufacturing, while the fiber is in its molten state, or during the first 72 hours after manufacturing, and characterized the impact of manufacturing parameters such as die-to-collector distance (DCD) and polymer resin melt flow rate (MFR). By monitoring the generated samples over time using both XPS and contact angle goniometry, correlations were developed between the wetting behavior of nonwoven webs and isopropyl alcohol (IPA) solutions. These tests culminate in the identification of threshold atomic composition levels of fluorine at the interface necessary for repellency against IPA. In the case of the samples tested here, it was found that surface fluorine to carbon ratios in excess of  $\sim 0.35$  would result in a surface capable of repelling a macroscopic IPA droplet.

A more comprehensive understanding of additive distribution and migration behavior was developed through the use of Time-of-Flight Surface Ion Mass Spectroscopy (ToF-SIMS) on cross-sectional slices of nonwoven web structures. With these scans, we were able to validate XPS results through the visualization of local maxima in fluorine composition at the fiber surface, but also identified the presence of excess additive in the fiber core, the development of an additive depletion zone, and significant deviations between the compositional profiles of large and small fibers. Finally, standard alcohol repellency test methods were used to demonstrate the impact of additive migration on nonwoven air filter materials. In these tests we found that through the proper selection of processing conditions and additive migration, excellent alcohol repellency can be generated with extremely low additive content samples.

### *5.3 CHAPTER 4. Charge Protection And Additive Migration In Electret Air Filtration Materials*

Fluorochemical melt additive containing meltblown nonwoven webs representative of air filter materials were generated to develop a more complete understanding of the influence of nonwoven manufacturing parameters on resultant charge protection performance. Samples were first characterized by XPS to determine the surface composition of the additive containing fibers, and to monitor the impact of nonwoven manufacturing parameters on resulting product. Standard test methods were used both to monitor the repellency of air filter materials to macroscopic IPA droplets, and to quantify the impact of repellency on the capability for charge retention of electret air filters. These results show that migration plays a key role in the protection of charge, particularly at extremely low additive loadings. Through the comparison of data characterizing the repellency of nonwoven webs towards macroscopic droplets and the charge protection effects in air filter testing, we are able to conclude that the surface

composition for successful alcohol repellency for these samples was indicated by a fluorine to carbon atomic ratio of 0.2 or less.

#### 5.4 *Future Work*

Throughout the planning and execution of these studies, a number of key areas of research were identified as relevant and valuable areas for further investigation. Though these topics were unfortunately outside the scope of the work performed here, we highlight them as recommendations for areas of future study in the field.

In Chapter 2 we discussed the use of sequentially deposited coatings for modification of highly inert polyolefin fibers. In this work we established conformal coatings with extremely dense and rough surface coatings, which when functionalized offer repellency against many challenging, low surface tension fluids. In an effort to improve the repellency of these coated nonwoven materials, future efforts could utilize a multi-layered “layer-by-layer” approach which has been demonstrated previously in the literature. By stacking multiple layers of fumed silica nanoparticles, coating roughness could potentially be increased, resulting in improved repellency performance and likely preventing the wicking of the most challenging fluids through the nonwoven substrate.

Another potential area for future work is in the generalization of these efforts to a wider range of the nonwoven market. Throughout this dissertation we focus largely on the preparation of materials for air filtration applications, and while this is a significant application area for alcohol repellent nonwovens, there are a large number of applications which would benefit from similar treatment to the complex and often confounding effects of nonwoven manufacturing on additive migration. For this reason we would propose that future efforts in

this field seek to generalize the alcohol repellency and charge protection correlations developed here to encompass a range of nonwoven structure properties including fiber size, surface energy, solidity/pore size, to name a few. These are all key parameters that play significant roles in the determination of repellency behavior for nonwoven products, and determining more generally the correlation between the F/C ratio values reported here and repellency for samples varying fiber sizes, for example, would be a logical next step for research in this area.

Similarly, additional understanding of the impact of fluorochemical additive structure on migration behavior, in a general manner, would offer significant value to the nonwovens industry. In this work, we focused on a single, commercially available melt additive. Therefore it would be a valuable addition to the literature for future studies to utilize non-commercial, surfactant-like additives of a known structure, and characterize their migration behavior utilizing the methods described in this dissertation. Due to the shift away from long chain fluorocarbon additives in industrial settings, it is now more critical than ever to understand the practical implications of the differences in migration behavior of C6 fluorocarbons compared to C4, C2, or completely different surface active functional groups in additive structures.

## APPENDICES

## APPENDIX A. THERMAL ANALYSIS

### A.1 Thermal Gravimetric Analysis

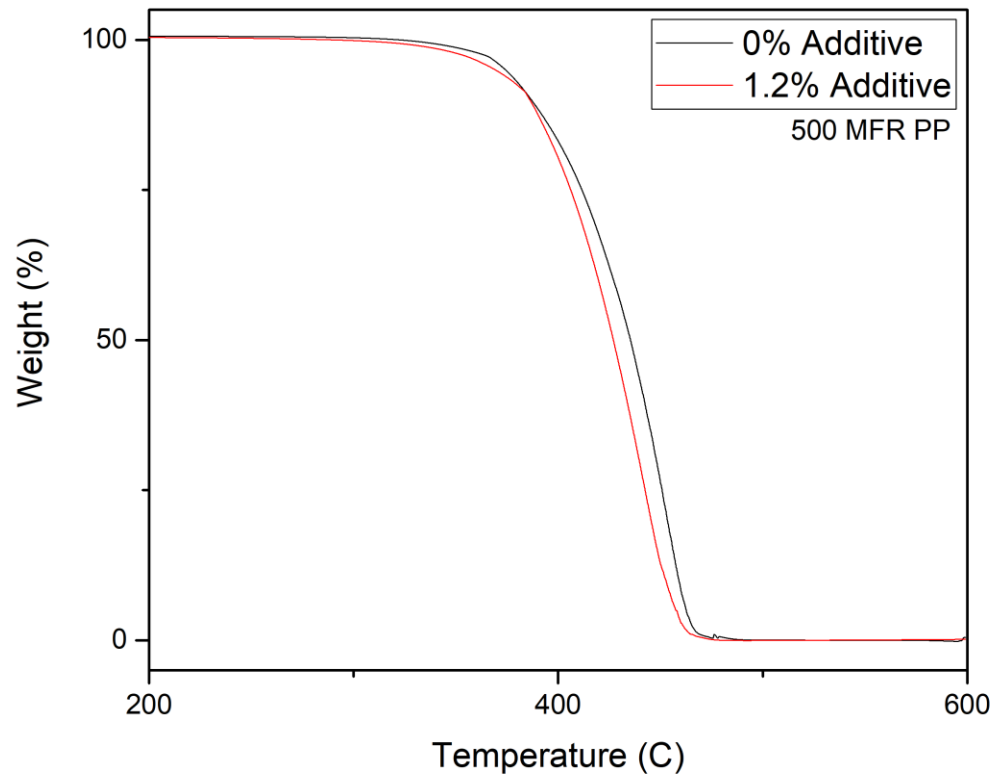


Figure A.1.1: Thermal Gravimetric Analysis of neat 500 MFR PP and additive containing nonwovens.

A.2 *Differential Scanning Calorimetry*

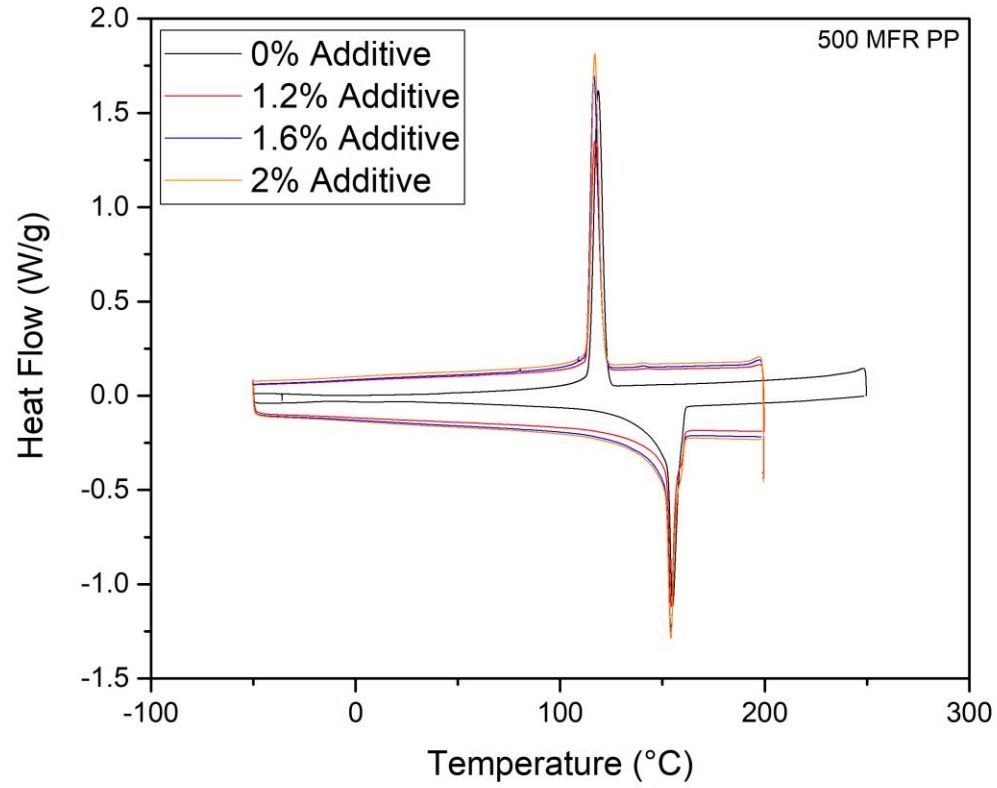


Figure A.2.1: Differential Scanning Calorimetry of neat 500 MFR PP and additive containing nonwovens.

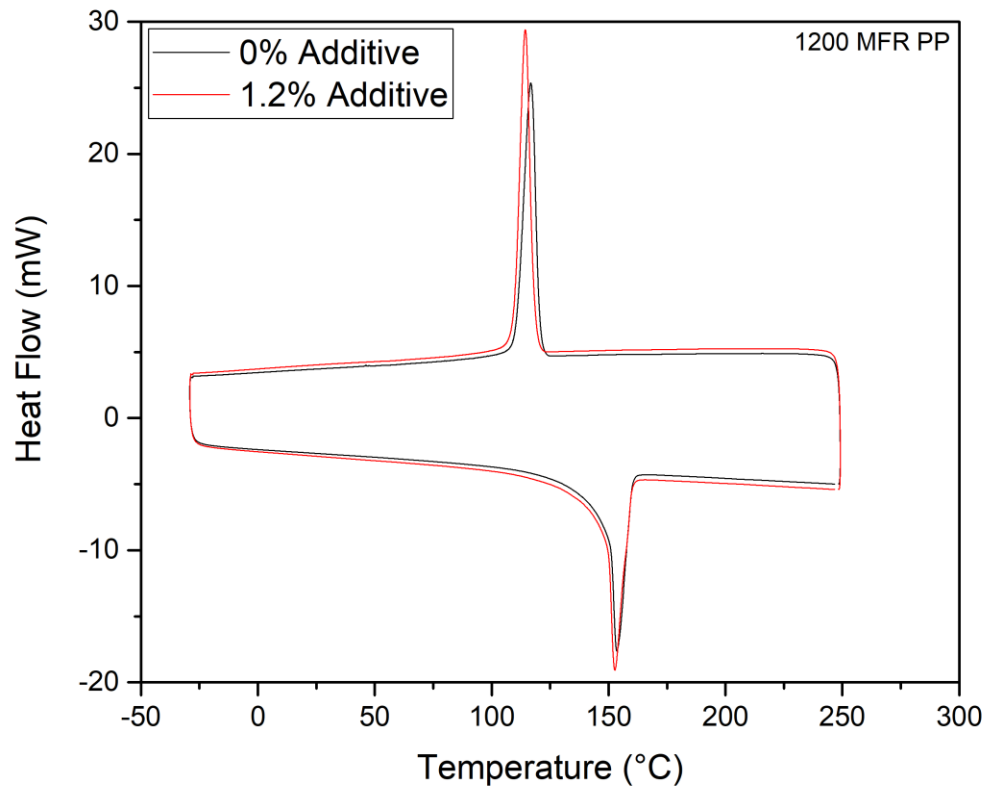


Figure A.2.2: Differential Scanning Calorimetry of neat 1200 MFR PP and additive containing nonwovens.

## APPENDIX B. COMPOSITIONAL ANALYSIS

### B.1 *Fourier Transform Infrared Spectroscopy*

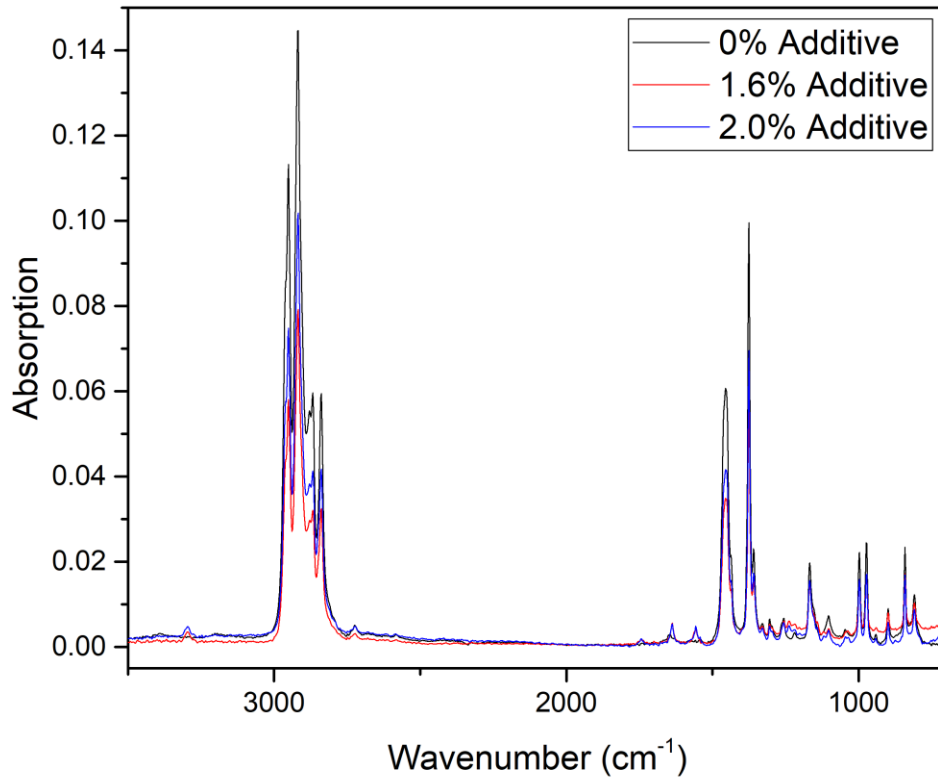


Figure B.1.1: Fourier Transform Infrared Spectroscopy absorption spectra of neat 500 MFR PP and additive containing nonwovens from 700 cm<sup>-1</sup> to 3500 cm<sup>-1</sup>.

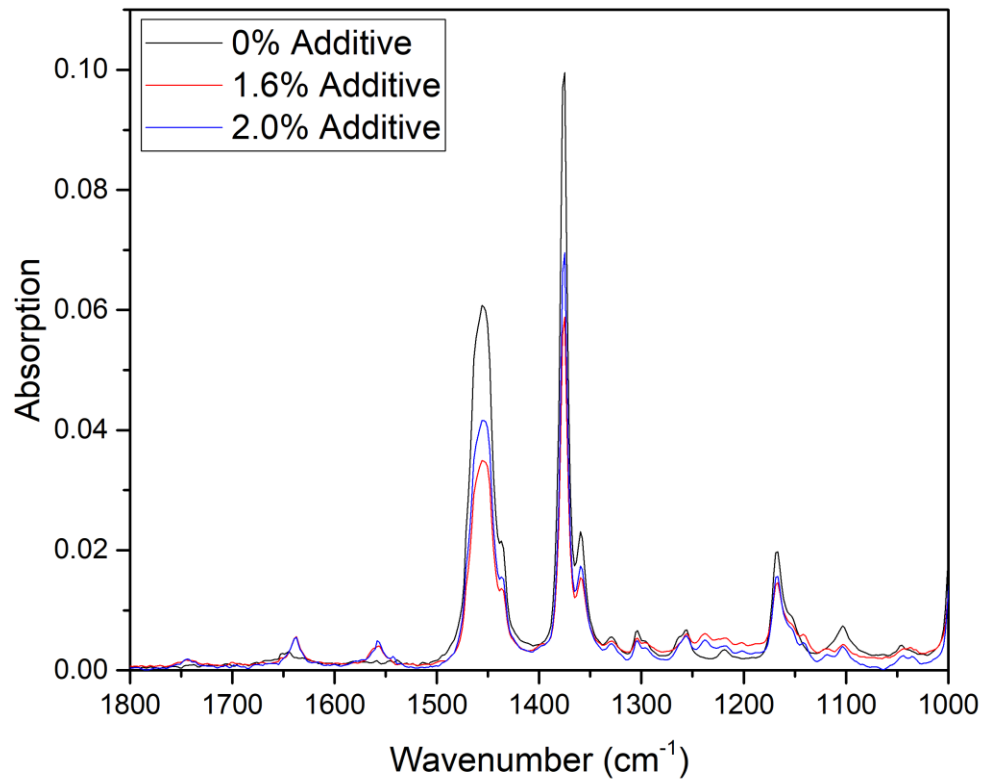


Figure B.1.2: Fourier Transform Infrared Spectroscopy absorption spectra of neat 500 MFR PP and additive containing nonwovens focused upon the fingerprint region from 1000 cm<sup>-1</sup> to 1800 cm<sup>-1</sup>.